Development of a probabilistic method for dike safety assessment based on fragility curves

Author: Lars van den Brand

TU Delft

Witteveen + Bos

Development of a probabilistic method for dike safety assessment based on fragility curves

By

Lars van den Brand

in partial fulfilment of the requirements for the degree of

Master of Science
in Civil Engineering - Trajectory Hydraulic Engineering

at the Delft University of Technology,
to be defended publicly on Friday December 13, 2024 at 10:30 AM.

Thesis committee:	Prof. dr. ir. S.N. Jonkman	TU Delft
	Dr. ir. C. Mai Van	TU Delft
	Prof. dr. C. Jommi	TU Delft
	ir. D.G. Fiolet	Witteveen+Bos

An electronic version of this thesis is available at http://repository.tudelft.nl/.
The cover image is obtained from Van Eyck and Rijkswaterstaat (1995).

TU Delft

Witteveen + Bos

Preface

In this thesis, a probabilistic method for dike safety assessment is developed which is based on fragility curves. The new method is compared to the current Dutch standards for dike safety assessment. This thesis is completed to fulfill the graduation requirements for the Master of Science degree in Civil Engineering at the Delft University of Technology. The research was conducted in collaboration with Witteveen+Bos.

First of all, I would like to thank the members of my thesis committee. I would like to thank Prof. dr. ir. S.N. Jonkman, the chair of the committee, for the valuable feedback during the meetings. I would like to thank Dr. ir. C. Mai Van for his patience in the early stages of the thesis and for his technical insights. I would like to thank Prof. dr. ir. C. Jommi for her contributions with respect to the geotechnical aspects of my thesis. Finally, I want to express my sincere gratitude to Ir. D.G. Fiolet for his guidance the past year. During our weekly progress meetings, I always enjoyed his endless enthusiasm and his professional yet personal attitude.

Furthermore, I want to thank Ir. J. Smid for the weekly assistance. I want to thank him for the pleasant conversations that we had about my thesis, but also for the personal guidance. I also want to thank Ir. A. van der Meer for helping me with all my technical questions about probabilistic dike safety assessment.

Last but not least, I want to thank my family, Hind and my friends for their invaluable support during my studies.

Abstract

Since the start of 2023, Dutch flood risk assessment is performed according to the guidelines of the Assessment and Design Framework (BOI), called the combination protocol. In dike safety assessment, dike failure probabilities of the smallest length scale, the cross section level, are scaled up to the largest length scale, the trajectory level. Consequently, the trajectory failure probability is compared to the norm failure probability. The current Dutch assessment guidelines do not consider correlation; they are related to the theoretical upper and lower bound for combining failure probabilities. By considering correlation, the resulting failure probability ends up in between the upper and the lower bound, improving the failure probability computation.

Advanced probabilistic tools are available to consider correlation in the computation of dike failure probabilities. However, these tools are so complex that they are not suitable for the daily practice of dike assessors. Therefore, this research aims to develop an accessible method to take into account correlation in dike assessment. The method is based on the application of fragility curves. Fragility curves allow the load variables to be separated from the strength variables by plotting the conditional failure probability of a certain structure as a function of the conditional load variables. This way, the correlation of the highly correlated load variables can be regarded independently from the correlation of the weakly correlated strength variables. In this research, the fragility curves are only conditioned on the water level.

The main objective of this research is to compare the newly developed fragility curve method with the current Dutch standards for dike safety assessment. The following research question is answered to achieve this objective: How do the current Dutch standards for dike safety assessment compare to a probabilistic method based on fragility curves?

To find the answer to this question, the research was divided into three parts. First, a literature study was done to learn about the fundamentals of fragility curves and about the current Dutch standards for dike assessment, hereafter referred to as the combination protocol. Then, a fragility-based method for dike assessment was developed. Finally, the combination protocol and the fragility curve method were both applied to two hypothetical sea dike trajectories to make a comparison between the methods. The dike trajectories have a length of 5 kilometers. They are divided into different numbers of dike sections, with a length in the order of 100 meters. The first dike trajectory is rather uniform and consists of dike sections which only vary slightly from each other due to natural variability. The second dike trajectory contains one dominant dike section, which is significantly weaker than the other sections. To make the comparison between the assessment methods, three failure mechanisms are modelled, namely: inner slope stability, overtopping and piping. The failure mechanism models were used to compute the cross section fragility curves of the trajectories, which from the starting point of the assessment.

The main difference between the combination protocol and the fragility curve method is that the combination protocol scales up failure probabilities to go from the cross section level to the dike trajectory level and that the fragility curve method scales up fragility curves. The combination protocol immediately converts the cross section fragility curves into cross section failure probabilities, which are then scaled up to the trajectory failure probability, without considering correlation. Conversely, the fragility curve method first scales up the cross section fragility curves into the trajectory fragility curve and only afterwards converts this trajectory

fragility curve into the trajectory failure probability. In the fragility curve method, the conversion from fragility curve to failure probability occurs as the final step, unlike in the combination protocol, where it is the initial step. The fragility curve method scales up fragility curves by assuming the water level is fully positively correlated and the remaining parameters are independent.

The research question is addressed separately for each level of dike assessment. The fragility curve method is recommended over the combination protocol for the computation of the dike trajectory failure probability of piping. Due to the consideration of the correlation in the water level, the dike trajectory failure probability of piping of the fragility curve method is lower than the one from the combination protocol. The actual reduction of the failure probability depends on the number of dike sections and the value of the dike section failure probabilities.

The fragility curve method is also recommended over the combination protocol for the computation of the dike trajectory failure probability for inner slope stability. The dike trajectory failure probability of inner slope stability is lower for the combination protocol than for the fragility curve method. However, this result is caused by a too low trajectory length effect factor of the combination protocol. The length effect factor is applied to account for the spatial variability of the parameters of inner slope stability. The combination protocol assumes only a very small fraction (3.3%) of the trajectory is responsible for inner slope stability failure. Especially for a rather uniform trajectory, this assumption is too optimistic. Furthermore, the fragility curve method has a clear connection to probability theory. In contrast, the methodology of the combination protocol for inner slope stability lacks the same level of transparency. It relies heavily on a length effect factor, which is highly sensitive to assumptions regarding the fraction of the trajectory contributing to failure. Therefore, the fragility curve method is recommended for inner slope stability.

The combination protocol is recommended for the computation of the dike trajectory failure probability for overtopping. The fragility curve method underestimates the spatial correlation of the overtopping failure mechanism. It is more true to reality to assume a fully positive spatial correlation for overtopping in combination with a length effect factor to account for irregularities in the dike trajectory.

Finally, the fragility curve method is recommended for the computation of the total dike trajectory failure probability. The combination protocol assumes the failure mechanisms are independent. This means the total trajectory failure probability of the combination protocol is approximately equal to the theoretical upper bound. The correlation between failure mechanisms resulting from the fragility curve method has shown to be substantial, causing the total trajectory failure probability of the fragility curve method to lie close to the lower bound. Therefore, the total trajectory failure probability can be reduced by applying the fragility curve method. The exact amount of reduction depends on the difference between the upper and lower bound. The reduction is greatest if the failure mechanisms have comparable trajectory failure probabilities.

Table of Contents

Preface v
Abstract vi
Table of Contents viii
1. Introduction 1
1.1. Problem description 1
1.1.1 Context 1
1.1.2 Problem analysis 3
1.2 Objectives 4
1.3 Outline 4
2. Literature study 5
2.1 Flood risk assessment 5
2.1.1 Dutch history of flood risk assessment 5
2.1.2 Statutory Assessment Framework 2017 (WBI2017) 6
2.1.3 Assessment and Design Framework (BOI) 8
2.1.4 Combination protocol 9
2.2 Reliability theory 10
2.2.1 Reliability methods 10
2.2.2 Numerical integration 11
2.2.3 Monte Carlo analysis 12
2.2.4 First Order Reliability Method 14
2.2.5 Reliability of systems 16
2.2.6 Equivalent planes method 17
2.2.7 Fragility curves 18
2.3 Failure mechanisms 19
2.3.1 Inner slope stability 19
2.3.2 Overtopping 20
2.3.3 Piping 20
3. Methodology 22
3.1 Overview 22
3.2 Base cross section 25
3.3 Failure mechanism models 25
3.3.1 Inner slope stability 26
3.3.2 Overtopping 30
3.3.3 Piping 32

3.4 Cross section fragility curves....35
3.5 Fragility curve method: from cross section to dike section....38
3.6 Fragility curve method: from dike section to trajectory....41
3.6.1 General approach....41
3.6.2 From dike section to trajectory per failure mechanism....41
3.6.3 From dike trajectory per failure mechanism to total trajectory....42
4. Large scale application....44
4.1 Cross section failure probabilities....44
4.2 Fragility curve method: from cross section to dike section....48
4.3 Fragility curve mehtod: from dike section to trajectory....49
4.3.1 From dike section to trajectory per failure mechanism....49
4.3.2 From dike trajectory per failure mechanism to total trajectory....51
4.4 Comparison with the combination protocol....53
4.4.1 From cross section to dike trajectory per failure mechanism....53
4.4.2 From dike trajectory per failure mechanism to total trajectory....55
4.5 Sensitivity analysis....56
4.5.1 Fragility curve method....56
4.5.2 Comparison with the combination protocol....61
5. Discussion....64
5.1 Water level....64
5.2 Failure mechanism models....65
5.3 Fragility curve method....65
6. Conclusions & recommendations....67
6.1 Conclusions....67
6.2 Recommendations....72
References....74
A Parameters cross sections....77
B Fragility curves cross sections of section 3.4....81
C Fragility curves....83
D Cross section failure probabilities....92
E Dike section failure probabilities....95
F Dike trajectory failure probabilities....100
G Python code....103

1. Introduction

1.1. Problem description

1.1.1 Context

Dutch flood defense history

The Netherlands has a long history with flood protection. Due to the low elevation and the large rivers that cross the country, the Netherlands is prone to flooding. This was brutally exposed during the 1953 North Sea flood. The dikes breached at more than 150 locations in the provinces of Zeeland, Zuid-Holland and Noord-Brabant. The flood took the lives of 1836 people and caused economic damage with a current value of approximately 5 billion euros (Rijkswaterstaat, 2024).

The North Sea flood led to the establishment of the Delta commission. Before, the dike height was equal to the highest recorded water level with an added safety margin of fifty centimeters. After the flood, the Delta commission opted for a change in the safety philosophy, which led to the first Dutch safety norm. For every primary water defense structure, this norm prescribed the exceedance probability of the water level that the structure should be able to withstand (Rijkswaterstaat, 2014). In 2017, the safety philosophy changed again due to scientific progress. The safety norm changed to a maximum allowed flooding probability. The Dutch system of primary water defense structures was divided into 234 dike stretches with an average length of 15 kilometers (Slootjes & Van der Most, 2016). These dike stretches are called dike trajectories. The division was made based on the consequences of a flood; along a dike trajectory a flood has similar consequences. Every dike trajectory has its own norm flooding probability. The change in the safety norm naturally led to a change in the design and assessment procedure of primary flood defense structures (Slomp, 2016).

Transition to the BOI (Assessment and Design Framework)

The year 2017 marks the beginning of the first Dutch national dike assessment round, called LBO1, which ran until the 1st of January 2023. The assessment during LBO1 was performed using the instruments from the Statutory Assessment Framework 2017 (WBI2017) (Informatiepunt Leefomgeving, n.d.). The purpose of the WBI2017 is to compute the dike trajectory flooding probability and to compare it with the statutory norm flooding probability. The second national assessment round, called LBO2, runs from 2023-2035. For this period, the assessment instruments have changed from the WBI2017 to the Assessment and Design Framework (BOI) (Ministerie van Infrastructuur en Waterstaat, 2023). One of the largest changes arising from this transition is that the BOI does not use a fixed partitioning of the total dike trajectory failure probability over the failure mechanisms. In the WBI2017, the maximum allowed dike trajectory failure probability could be scaled down to the cross section level by applying the standard partitioning and a length effect factor. The BOI only allows for a bottom up assessment, in which the cross section failure probabilities are combined to obtain the dike trajectory failure probability. Consequently, the dike assessment is completed by comparing the dike trajectory failure probability to the norm (Kanning, 2023). Figure 1.1 defines the different scale levels used in dike assessment.

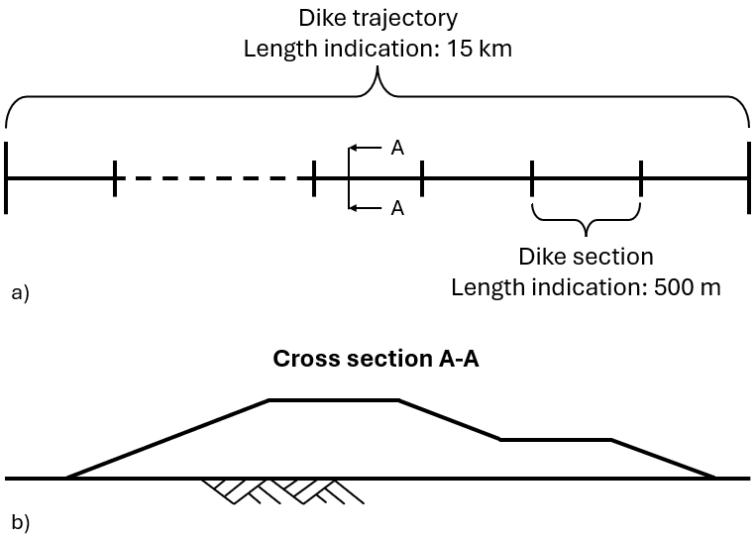

Figure 1.1: Scale levels in dike assessment

Compared to the WBI2017, the BOI opts for a more dike specific assessment procedure. For this procedure, information about the history, geometry and surroundings of the dike is important. The assessment does not blindly consider all failure mechanisms but focuses on the dominant failure paths. A failure path is a sequence of events (or nodes) which leads to an inundation. A failure mechanism comprises all failure paths with the same initial mechanism. A mechanism describes the physics of a change of state and consists of one or more events. As only the dominant failure paths are considered, they can be analyzed in more detail. The BOI describes four ways in which the computation of the failure probability of the dominant failure paths can be improved (Rijkswaterstaat, 2023):

1. Take into account the influence of follow up mechanisms.
2. Work out the initial mechanism in more detail.
3. Take into account the correlation between different failure mechanisms.
4. Take into account the correlation between the same failure mechanism for all the dike sections of a dike trajectory.

The influence of the first option has already been investigated by Remmerswaal (2023). The practice according to the WBI2017 is to assume a dike has failed when an initial mechanism has occurred, like external erosion or an initial slope failure. However, a flood only occurs after a dike breach. By considering the processes that happen in between the initial mechanism and the dike breach, the flooding probability might be reduced. In the report by Remmerswaal (2023), the residual dike strength is assessed after an initial sliding plane due to macro instability, see Figure 1.2. The conclusion of the report is that considering residual dike strength can decrease the probability of flooding by up to 80%.

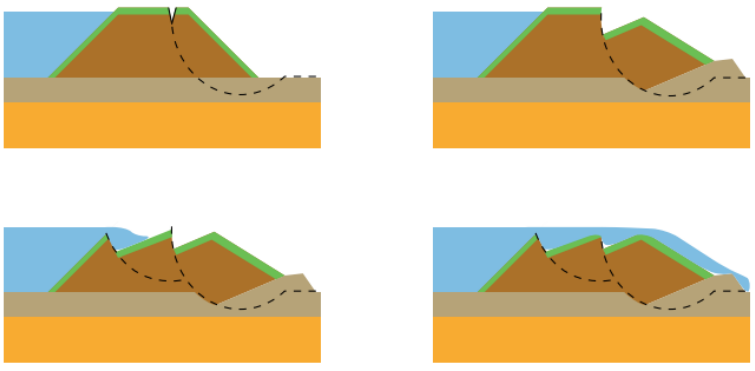

Figure 1.2: The process from initial slope failure to inundation (Remmerswaal, 2023)

1.1.2 Problem analysis

This research focusses on refinement options 3 and 4 from the BOI. Options 3 and 4 are both related to the combination of the cross section failure probabilities to the total dike trajectory failure probability. The WBI2017 and the BOI prescribe the same set of guidelines for dike assessors to perform this combination. The set of guidelines is called the combination protocol. To avoid a complex probabilistic calculation, the combination protocol uses approximations for the combination of dike section failure probabilities per failure mechanism to dike trajectory failure probabilities per failure mechanism and for the combination of the dike trajectory failure probabilities per failure mechanism to the total dike trajectory failure probability (Kanning, 2023). The process of dike combining failure probabilities is illustrated in the fault tree of Figure 1.3. The details of the combination protocol can be found in section 2.1.4.

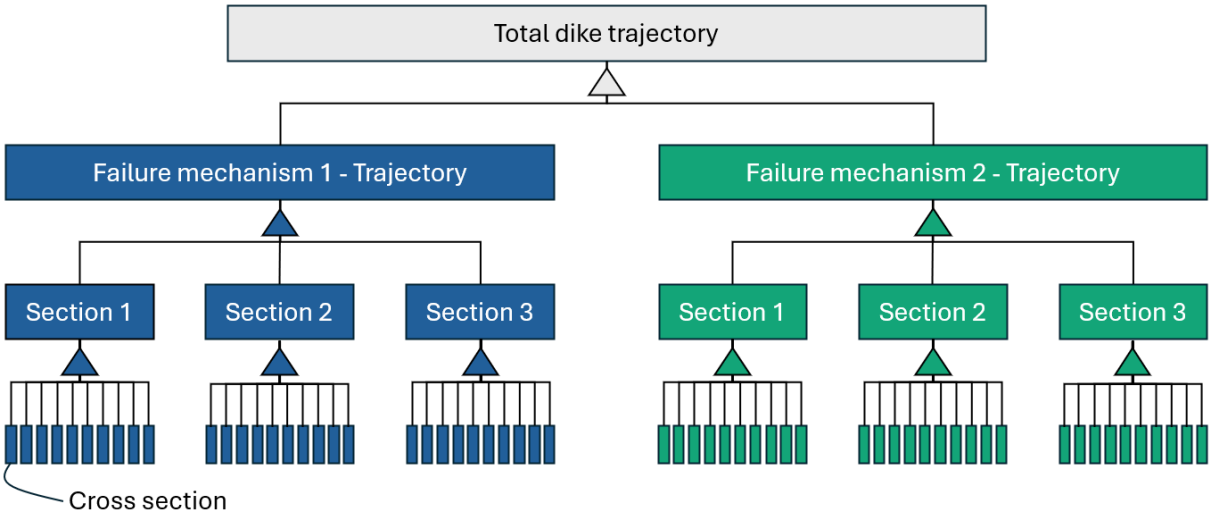

Figure 1.3: Schematization of the upscaling from the cross section level to the dike trajectory level

As can be seen in the figure above, the different scale levels are all connected via so-called OR-gates. An OR-gate indicates a series system. A series system fails if one of the components fails. The approximations of the combination protocol are based on the probabilistic upper and lower bounds of the system failure probability of a series system. For the lower bound, the dike sections and the failure mechanisms are assumed to be fully positively correlated. For the upper bound, the dike sections and failure mechanisms are assumed to be fully negatively correlated. By taking into account the exact value of the correlation in a fully probabilistic analysis, the real dike trajectory failure probability is obtained, which lies somewhere in between the upper and the lower bound. When the failure probability resulting from the probabilistic assessment is lower than the one resulting from the combination protocol, this means the dike trajectory is over designed. When it is higher, the dike trajectory is under designed.

The influence of taking into account the correlation between dike sections and between failure mechanisms has been investigated in (Kanning, 2023) and (Deltares, 2022). These reports found that including correlation could significantly reduce the dike failure probability by up to 24% with respect to the current Dutch assessment method of the BOI. However, both of these studies use advanced probabilistic techniques to combine failure probabilities. These techniques are too complex to be used in the daily practice of dike assessors. This research focusses on the development of a method to combine dike failure probabilities which considers correlation and which is accessible for dike assessors. The method is based on the application of fragility curves.

Fragility curves plot the failure probability of a certain structure or system as a function of one or more load variables. Therefore, fragility-based assessment allows the load variables to be separated from the strength variables, which implies that the correlation of the load variables can also be separated from the correlation of the strength variables. This is the main principle of fragility-based assessment. In dike safety assessment, the loads are generally highly correlated in space whereas the strengths generally have a low spatial correlation. By applying the fragility curve method, one could neglect the correlation of the strengths while still taking into account the correlation of the loads. Neglecting the correlation of the strengths significantly simplifies the computation. Nevertheless, the most important correlation, the correlation of the loads, is still considered. Therefore, it is worth investigating whether fragility-based assessment can also reduce dike failure probabilities with respect to the current Dutch assessment method of the BOI.

1.2 Objectives

The following research question is answered in this report: How do the current Dutch standards for dike safety assessment compare to a probabilistic method based on fragility curves? Four subquestions are posed to answer the research question:

1. How is dike safety assessed according to the current Dutch standards, known as the combination protocol?
2. How can fragility curves be applied to combine dike failure probabilities in a probabilistic way?
3. What is the difference between the assessment of the combination protocol and the fragility-based assessment on the scale of the dike trajectory failure probabilities per failure mechanism and which method is recommended?
4. How does the fragility-based assessment compare to the assessment of the combination protocol on the scale of the total dike trajectory failure probability and which method is preferred?

The objective of the first two subquestions is to obtain a thorough understanding of the methodology that is required to answer the research question. The third and the fourth subquestion are used to quantify the comparison presented in the research question. The third subquestion first provides this quantification on a lower scale, namely for the dike trajectory failure probabilities per failure mechanism. The result of this subquestion is subsequently used in the fourth subquestion to provide the quantification of the comparison on the scale of the total dike trajectory failure probability.

1.3 Outline

The report is constructed in the following way. The literature study is presented in chapter 2. Chapter 3 describes the methodology that is used to answer the research question and the subquestions. In chapter 4, the results of the applied methodology are presented. Chapter 5 contains a discussion of the most important assumptions and limitations of this research. Finally, chapter 6 presents the conclusion with respect to the subquestions and the research question and contains recommendations for future research.

2. Literature study

In this chapter, the literature study is presented. Section 2.1 starts with an overview of the history of Dutch flood risk. Then, the Dutch dike assessment guidelines are dealt with in more detail. Section 2.2 focusses on reliability theory. In the first subsections of section 2.2, different reliability methods are discussed to compute the failure probability of a single element. In the next subsections, the scope shifts from the reliability of a single element to the system reliability. Section 2.2 ends with the explanation of fragility curves in reliability theory. Finally, section 2.3 describes the failure mechanisms inner slope stability, overtopping and piping.

2.1 Flood risk assessment

2.1.1 Dutch history of flood risk assessment

The North Sea flood initiated the Delta plan, which was included in the Delta law of 1958. The Delta law also introduced the first safety norm, known as the Delta height (Rijkswaterstaat, 2024). Before the introduction of the Delta height, the dike height was determined by the highest recorded water level with an added safety margin of 50 centimeters. The Delta height marks a change in the safety philosophy. The new safety norm indicated the exceedance frequency of the water level that dikes should be able to withstand. The Delta height is the water level that belongs to the specified exceedance frequencies. Due to insufficient computer power and insufficient knowledge about dikes, the flood risk could not yet be calculated for the entire country. Therefore, the Delta height was mainly based on the consequences of a flood. The successor of the Delta law is the Wet op de waterkering. This law applied the same safety philosophy. The norm frequencies and the corresponding water heights were only updated according to new insights and the norm frequencies of the river dikes were added. The left side of Figure 2.1 displays the norm frequencies for the Netherlands as established in the Wet op de waterkering (Rijkswaterstaat, 2014).

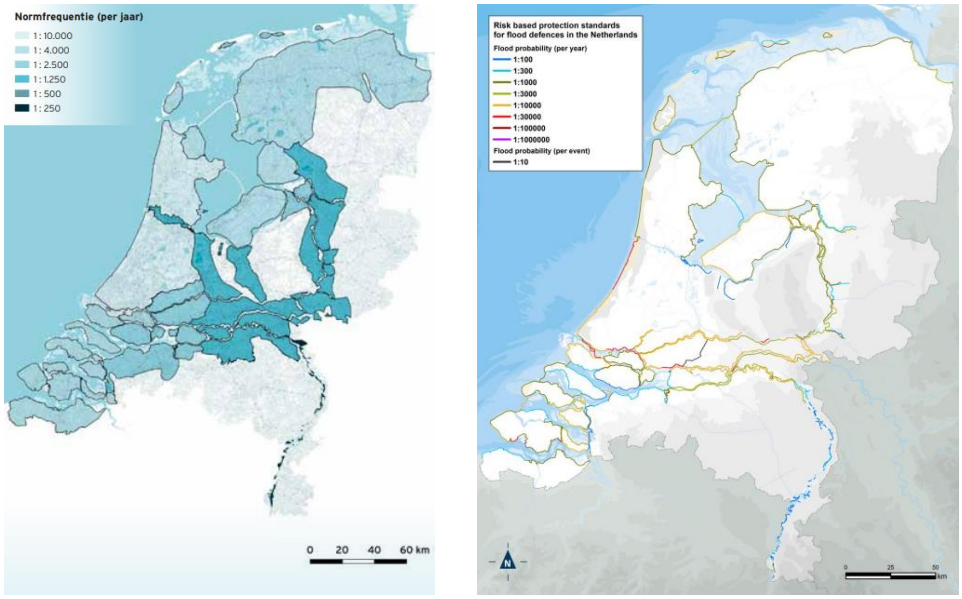

Figure 2.1: First safety norm from the Wet op de waterkering (left) (Rijkswaterstaat, 2014) and the new safety norm from the Waterwet (right) (Slomp, 2016)

The Wet op de waterkering was succeeded by the Waterwet. The Waterwet is an integral water law which combines (parts of) eight older water management laws (Rijkswaterstaat, n.d.). In contrary to the Wet op de Waterkering, the Waterwet describes the legally allowed probability of flooding per dike trajectory, instead of the exceedance probability of the water level that dikes should be able to withstand. The new safety norm is based on an extensive flood risk analysis, which was carried out for the project Veiligheid Nederland in Kaart (VNK2) (Rijkswaterstaat, 2014). The new safety norm is depicted on the right side of Figure 2.1. Risk is the multiplication of the probability of an unwanted event with the consequences. So, by definition, flood risk analysis focuses on the probability of a flood and the corresponding consequences. The VNK2 analysis was used to establish the maximum allowed probability of flooding for every dike trajectory in the Netherlands. The conversion from the risk analysis to a probability is done by considering three different risk criteria. The maximum allowed failure probability should be such that all of the criteria are met. This means the safety standard is equal to the minimum failure probability resulting from this demand. The risk criteria are as follows (Jonkman et al., 2017):

- Individual risk criterion
- Societal risk criterion
- Economic risk criterion

The individual risk criterion is based on the fact that every individual person has the right to have a certain bottom line protection against flooding. The societal risk criterion considers that the societal distress and resentment are larger for floods with higher number of fatalities. For densely populated places this means the societal risk criterion will lead to a stricter flood safety standard than the individual risk criterion. The economic risk criterion opts for the most economical flooding probability.

The changes in the law from a norm exceedance frequency to a norm flooding probability coincided with a drastic change in the design and assessment of primary flood defenses. It changed from an approach which only focused on the design water level and the dike height to an integral approach which considers multiple failure mechanisms. To help the designers and assessors, statutory guidelines were provided in the form of the Design Framework 2014 (OI2014v4) and the Statutory Assessment Framework 2017 (WBI2017), respectively (Smale, 2017). As this report focuses on dike assessment, only the WBI2017 will be discussed.

The WBI2017 was used for the first national assessment round called LBO1. As established in the Waterwet, the safety of the primary water defenses should be assessed every 12 years. The first assessment round was finished on the 1st of January 2023. The second national assessment round will run from 2023-2035. This assessment round will be assisted by a new set of instruments called the Assessment and Design Framework (BOI) (Ministerie van Infrastructuur en Waterstaat, 2023). In the following subsections, the WBI2017 and the BOI are explained in more detail.

2.1.2 Statutory Assessment Framework 2017 (WBI2017)

In the Netherlands, the safeguarding of the water safety is structured around three cycles (Deltares, 2018):

1. The maintenance cycle
2. The assessment cycle
3. The norm-setting cycle

The norm-setting cycle establishes in law the maximum allowed failure probability of the Dutch primary flood defenses. Furthermore, this cycle determines which methods should be used to compute the failure probabilities. The assessment cycle focusses on assessing dike safety in case of a changed norm or assessment procedure. Finally, the maintenance cycle ensures the assessed dikes remain in good condition.

The WBI2017 is specifically designed for the assessment cycle. The WBI2017 consists of two main instruments: the statutory process instrument and a basis instrument. Next to these instruments, the WBI2017 contains additional reports like case studies and research reports. The process instrument prescribes the procedure that has to be followed to assess the safety of primary water defense structures. Furthermore, it prescribes the methods that should be used to determine the hydraulic loads. The basis instrument consists of the required software packages, the basis report and of background reports. The basis report describes the principles on which the WBI2017 is based. The background reports consist of technical reports that describe the failure mechanisms and the methods to quantify their failure probabilities (Deltares, 2018).

The assessment procedure of the WBI2017 consists of a layered procedure. In this procedure, a maximum of three of the following analyses are performed to reach a conclusion:

- Simple check
- Detailed check per dike section
- Detailed check per dike trajectory
- Customized check

In the simple check, decision rules are used to determine whether the contributions of the cross section failure probabilities to the total dike trajectory failure probability are negligible. If this is not the case, the less conservative detailed check per dike section is applied. In this check, probabilistic and semi-probabilistic methods are applied to check whether the cross sections comply with the norm.

If some cross sections still surpass the norm, the WBI2017 prescribes to either perform a detailed check per dike trajectory or to perform a customized check. In the detailed check per trajectory, the results of the detailed check per section are combined to the dike trajectory level. Ideally, the combination is done with methods that consider both spatial correlation and correlation between different failure mechanisms. For the WBI2017, this was not possible yet and the combination was done according to the combination protocol, see section 2.1.4.

The customized check consists of additional location specific analyses. Before carrying out the additional research, a cost-benefit analysis has to be performed to check whether the location specific analyses are worth it (Deltares, 2018). The assessment procedure of the WBI2017 is summarized in Figure 2.2.

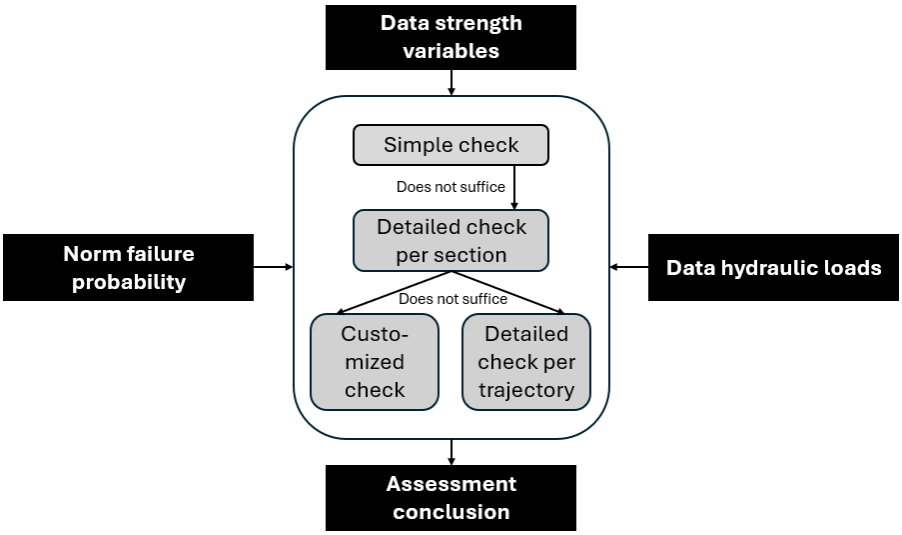

Figure 2.2: Assessment procedure of the WBI2017

2.1.3 Assessment and Design Framework (BOI)

Just like the WBI2017, the BOI consists of two main instruments: the statutory process instrument and a basis instrument. Next to these instruments, the BOI contains additional reports and databases. Contrary to the WBI2017, the BOI contains two process instruments, one for the assessment of primary flood defenses and one for the design. These instruments describe the procedure that should be followed to reach a proper assessment or design, based on flood risk (Rijkswaterstaat, 2023).

The biggest change in the assessment process instrument of the BOI with respect to the process instrument of the WBI2017, is the new approach for determining credible probabilities of flooding. The new approach provides more flexibility for flood defense managers. It focusses on the narrative of the water defense structure, which means that the structure is thoroughly studied. The history, the geometry, the soil and hydraulic parameters and the experience from the flood defense manager are all taken into account. While this increased freedom allows for a more efficient process with fewer mandatory steps, it also requires well-founded decision making and comes with an increased responsibility.

One of the implications of the new flexibility is the shift away from the standard partitioning of the dike trajectory norm failure probability over the different failure mechanisms. The new approach focusses on dominant failure paths and the corresponding failure mechanisms. To support dike assessors with the new approach, workshops are organized in which the dike assessors collaborate with specialists and people from the water board to come to a proper failure probability computation.

Another implication of the increased flexibility is the possibility to immediately apply new knowledge and research insights in new projects. A calendar is developed which maps the progress, impact and release dates of important knowledge advancements.

Finally, the BOI opts for a more realistic failure probability. To realize this, dike assessors should try to estimate parameters with realistic values instead of using very conservative estimates. Another way to come to a more realistic failure probability, is by increasing the level of detail of the failure probability computation. The BOI describes four possibilities to do this (Rijkswaterstaat, 2023):

1. Take into account the influence of follow up mechanisms.
2. Work out the initial mechanisms in more detail.

3. Take into account the correlation between different failure mechanisms.
4. Take into account the correlation between the same failure mechanism for all the dike sections of a dike trajectory.

2.1.4 Combination protocol

As described in section 2.1.2, the combination protocol is used in the WBI2017 to perform the detailed check per dike trajectory. In the BOI, the combination protocol can also be used. The aim of the combination protocol is to combine the assessment results of the cross section level to one final assessment result for the complete dike trajectory. Depending on the failure mechanism, the assessment result is not necessarily the same as a failure probability. For some failure mechanisms no models are available to compute a failure probability. In these cases, the assessment results provide an indication of the distance to the norm. The combination protocol divides the failure probabilities in four categories (Deltares, 2021):

1. Failure mechanisms for which a full probabilistic analysis can be performed.
2. Failure mechanisms for which a semi-probabilistic analysis can be performed. For this category, the resulting safety factor of the semi-probabilistic analysis can be transformed into a failure probability through a calibration study.
3. Failure mechanisms for which a semi-probabilistic analysis can be performed. For this category, no relation is known between the failure probability and the safety factor. Therefore, it is not possible to compute a failure probability for the failure mechanism of this category.
4. Failure mechanisms for which the probabilistic and the semi-probabilistic analyses are both not possible. For this category, only a deterministic analysis is possible. The norm failure probability is used to determine the hydraulic loads.

It is only possible to compute a failure probability for the failure mechanisms of categories 1 and 2. For category 2, the failure probability is computed with a relation between the failure probability and the safety factor from the semi-probabilistic analysis. In this research, the failure mechanisms inner slope stability, overtopping and piping are considered. For these mechanisms, it is possible to compute the failure probability with a fully probabilistic calculation. Therefore, the remainder of this subsection only focusses on the part of the combination protocol that describes the combination of cross section failure probabilities to the total dike trajectory failure probability. This process consists of three steps:

1. First of all, the cross section failure probabilities have to be scaled up to dike section failure probabilities.
2. Then, the dike section failure probabilities per failure mechanism are combined into dike trajectory failure probabilities per failure mechanism.
3. Finally, the dike trajectory failure probabilities per failure mechanism are combined into the total dike trajectory failure probability.

Step 1
For the first step, the combination protocol uses the length effect factor. The length effect factor is used to scale up the cross section failure probability to a failure probability on the dike section or dike trajectory level. For the overtopping failure mechanism, the length effect factor has a fixed value which is specific for every dike trajectory. For inner slope stability and piping the length effect factor depends on the length of the dike section or dike trajectory and can be calculated with equation (2.1).

$$N_{section/trajectory} = 1 + \frac{a_l \cdot L_{section/trajectory}}{b_l} \quad (2.1)$$

In which:

- a_l = The fraction of the dike trajectory that is sensitive to the failure mechanism
- $L_{section/trajectory}$ = The length of either the dike section or the dike trajectory
- b_l = A length that indicates the degree of spatial correlation

Step 2

Step two of the combination protocol, which is the step from the cross section failure probabilities per failure mechanism to the dike trajectory failure probabilities per failure mechanism, is computed as follows:

2.A) Perform the computation under the assumption that the dike sections are independent. Equation (2.2) shows how to compute the system failure probability of a series system of independent components. This gives:

$$p_{trajectory,mech\ i} = 1 - \left(1 - p_{section1,mech\ i}\right) \cdot \left(1 - p_{section2,mech\ i}\right) \cdot \ldots \cdot \left(1 - p_{section\ N,mech\ i}\right) \quad (2.2)$$

2.B) Perform the computation under the assumption that the dike sections are fully correlated. For this step, the maximum cross section failure probability is chosen. Next, multiply this cross section probability with the dike trajectory length effect factor of the failure mechanism, see equation (2.1). This gives:

$$p_{trajectory,mech\ i} = \mathrm{Max}\left(p_{cross\ section,mech\ i}\right) \cdot N_{trajectory,mech\ i} \quad (2.3)$$

2.C) Choose the minimum dike trajectory failure probability per failure mechanism from steps 2A and 2B.

Step 3

For step 3, the step from the dike trajectory failure probabilities per failure mechanism to the total dike trajectory failure probability, the combination protocol assumes the failure mechanisms are independent. This gives the following equation (Deltares, 2021):

$$p_{trajectory} = 1 - \left(1 - p_{trajectory,ISS}\right) \cdot \left(1 - p_{trajectory,Overtopping}\right) \cdot \left(1 - p_{trajectory,Piping}\right) \quad (2.4)$$

2.2 Reliability theory

2.2.1 Reliability methods

Reliability theory is required to assess whether a dike or any other construction is safe enough. In the simplest form, a dike is safe when the resistance is greater than the load. This statement can be mathematically formulated by means of the limit state function, also known as the Z-function (Jonkman et al., 2017):

$$Z = R - S \quad (2.5)$$

The dike fails when the limit state function is smaller than zero, as this means the load is higher than the resistance. Traditionally, the resistance and the load are regarded as deterministic variables. Due to an increase of knowledge and a better understanding of the knowledge gaps, the safety philosophy has shifted to an approach based on probabilistic calculations. Because of this, the load and the resistance can also be represented by stochastic variables, which change in time and space. These variables are modelled by probability distributions. This means that the probability has to be calculated that the limit state function is smaller than zero. In literature, a distinction is made between five different levels of calculating the reliability of a structure. In the following paragraphs, these levels are treated in more detail.

Level IV methods
The level IV methods are risk based. This means both the probability of failure and the corresponding consequences have to be determined. These methods use risk, calculated by the multiplication of the failure probability and the consequences, to assess the reliability.

Level III methods
Level III methods only consider the failure probability and not the consequences of failure. These methods distinguish themselves from the lower level methods by exactly calculating the failure probability. For simple limit state functions, analytical formulations can be used. When limit state functions or the probability distributions of the variables are more complex, numerical integration or Monte Carlo analysis should be applied.

Level II methods
Level II methods approximate the failure probability. To this end, level II methods use the mean values of the stochastic variables and their correlation matrix. The mostly used level II method is the First Order Reliability Method (FORM). This method linearizes the limit state function in the design point. The design point consists of the values of the base variables with the highest probability density, where failure is most likely.

Level I methods
Level I methods are classified as semi-probabilistic. The load and resistance variables are modelled by their design values. The design values are obtained by multiplying the characteristic values with a safety factor. The characteristic values represent a high percentile for the load variables and a low percentile for the resistance variables. Furthermore, the safety factors applied to the loads are larger than one and the ones applied to the resistance variables are smaller than one. The safety factors are deduced from level II methods.

Level 0 methods
Level 0 methods are based on deterministic calculations. The load and resistance variables are represented by deterministic values and a global safety factor is applied.

2.2.2 Numerical integration

Numerical integration is a level III method. The goal of the method is to compute the probability that the limit state function is smaller than zero. In case the limit state function is equal to equation (2.5), the failure probability can be calculated with the following integral (Jonkman et al., 2017):

$$P_f = \iint_{Z<0} f_{R,S}(r,s)dr\,ds \tag{2.6}$$

The joint probability density function $f_{R,S}(r,s)$ is shown in Figure 2.3 below. The left side of the figure shows the marginal probability density functions of the load and the resistance. Furthermore, the left side shows the lines of equal probability of the joint probability density function. The right side depicts the shape of the joint probability density function in three dimensions. The grey volume represents the volume of the joint probability density function which lies in the failure domain $(Z < 0)$. This volume is equal to the integral of equation (2.6).

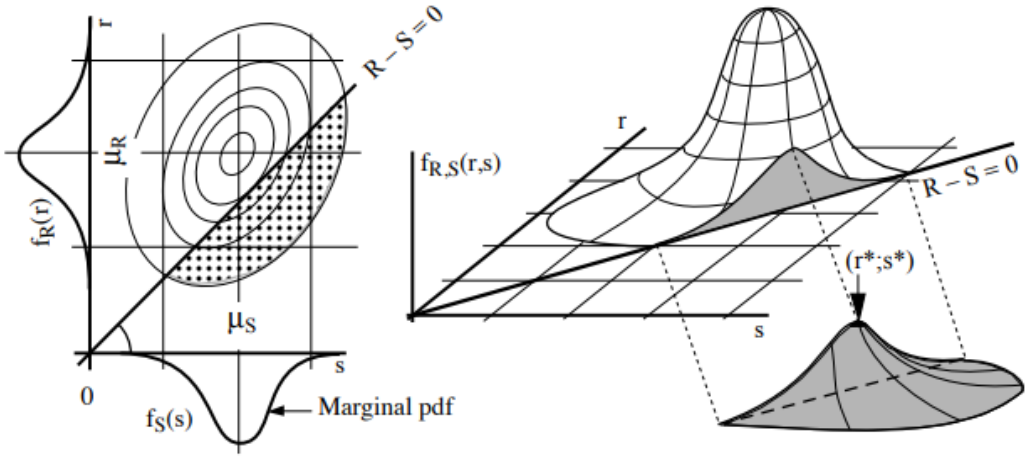

Figure 2.3: Joint probability density function and the design point on the limit state function (Schneider & Vrouwenvelder, 2017)

The level III method numerical integration approximates the integral of equation (2.6) with the following equation:

$$P_f = \sum_i \sum_j f_{R,S}(r_i, s_j)\Delta r \Delta s \tag{2.7}$$

2.2.3 Monte Carlo analysis

The Monte Carlo analysis is a level III method which is based on random sampling and repeated simulations. It consists of three steps. The first step is to generate a random sample for all stochastic variables. To this end, a random number is drawn from a uniform distribution ranging from zero to one for every variable. Then, the random sample of the stochastic variable is computed by taking the inverse of the cumulative distribution function of the stochastic variable for the drawn number from the uniform distribution. This process is illustrated in Figure 2.4 (Jonkman et al., 2017).

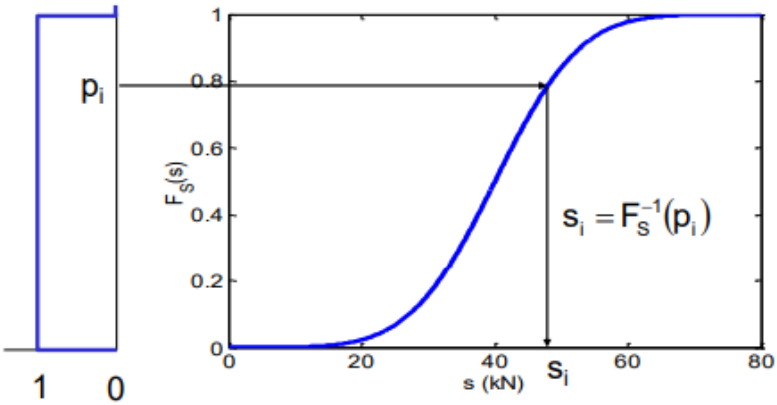

Figure 2.4: Generation of random samples stochastic variables (Jonkman et al., 2017)

The second step of the Monte Carlo analysis is to fill in the random samples of the stochastic variables in the limit state function and to check whether failure occurs ($Z < 0$). The third and final step is to repeat steps one and two thousands of times. The failure probability can now be computed with equation (2.8):

$$P_f = \frac{N_f}{N} = \frac{\sum_1^N I[Z < 0]}{N} \tag{2.8}$$

In which:

- N_f = The number of failures
- N = The total number of samples
- I = The indicator function; if $Z < 0 \rightarrow I = 1$ and if $Z \geq 0 \rightarrow I = 0$

Figure 2.5 shows an example of a Monte Carlo analysis of 200 samples for the simple limit state function of equation (2.5). In this case, the probability of failure is $P_f = \frac{N_f}{N} = \frac{3}{200} = 0.015$. The required number of samples depends on the failure probability, the probability distributions of the stochastic variables and the desired accuracy.

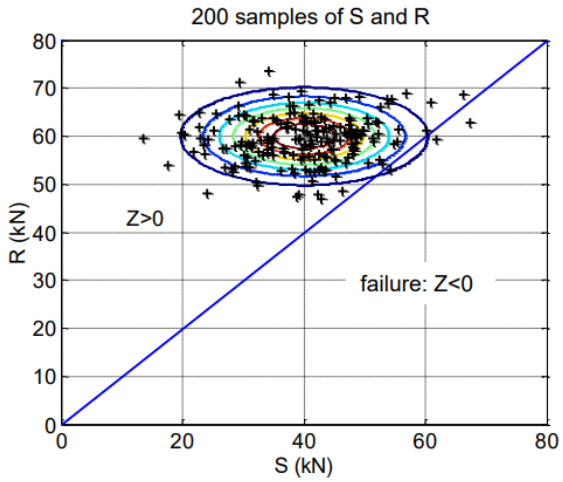

Figure 2.5: Monte Carlo analysis of 200 samples (Jonkman et al., 2017)

Importance sampling

Importance sampling is a special type of Monte Carlo analysis which reduces the required number of samples. For importance sampling, the probability distributions of the stochastic variables are shifted towards the design point. The design point is the point with the highest value of the joint probability density function for which the limit state function is equal to zero. The failure probability can now be calculated with equation (2.9) below.

$$P_f = \frac{\sum_{i=1}^N I[Z < 0] \cdot \left(\frac{f_{R,S}(r_i, s_i)}{h_{R,S}(r_i, s_i)}\right)}{N} \tag{2.9}$$

In which:

- I = The indicator function for the random samples of the shifted stochastic variables
- $f_{R,S}$ = The joint probability density function
- $h_{R,S}$ = The shifter sampling probability density function

In Figure 2.6 importance sampling is applied to the example of the normal Monte Carlo analysis.

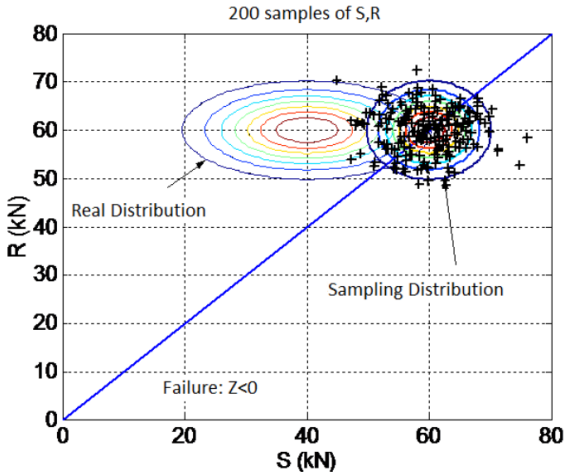

Figure 2.6: Importance sampling (Jonkman et al., 2017)

2.2.4 First Order Reliability Method

The First Order Reliability Method (FORM) is a level II method. FORM is based on the linearization of the limit state function in the design point. By transforming all variables to the stand normal space, the reliability index β is equal to the smallest distance between the (linearized) limit state function and the origin (Hasofer & Lind, 1974). The failure probability is related to the reliability index in the following way:

$$P_f = \Phi(-\beta) \tag{2.10}$$

In which the symbol Φ represents the cumulative distribution function of the standard normal distribution. FORM consists of three steps, which are described below.

Step 1
The first step is to transform the base variables of the limit state function into a set of independent standard normally distributed values by applying the Rosenblatt transformation method. The details of this method can be read in the paper by Rosenblatt (1952).

Step 2
The next step is to linearize the limit state function in the standard normal space in the design point with a first order Taylor series. This leads to the following limit state function:

$$L(\overline{U}) = g(\overline{u}_i^*) + \sum_{i=1}^{N} \frac{\partial g(\overline{U})}{\partial U_i}\bigg|_{\overline{u}^*} (U_i - u_i^*) = \sum_{i=1}^{N} \frac{\partial g(\overline{U})}{\partial U_i}\bigg|_{\overline{u}^*} (U_i - u_i^*)$$
$$= B + \sum_{i=1}^{N} A_i U_i \tag{2.11}$$

In which:

- $L(\overline{U}) =$ The linearized limit state function in the standard normal space
- $g(\overline{U}) =$ The limit state function in the standard normal space
- $\overline{u}^* =$ The design point

As the variables U_i are all independent and standard normally distributed, the linearized limit state function, $L(U)$, is also standard normally distributed. Therefore, the following is true:

$$P(L(U) < 0) = \Phi\left(-\frac{\mu_L}{\sigma_L}\right) \tag{2.12}$$

$$\beta = \frac{\mu_L}{\sigma_L} = \frac{B}{\|\overline{A}\|} = \frac{B}{\sqrt{\sum_{i=1}^{N} A_i^2}} \tag{2.13}$$

The goal of FORM is to compute the probability of failure, $P(Z < 0) \approx P(L(U) < 0)$. Therefore, equation (2.11) can be multiplied with or divided by a constant. Dividing equation (2.11) by the factor $\sigma_L = \|\overline{A}\|$ yields the well-known equation for the linearized limit state function:

$$L(U) = \beta + \sum_{i=1}^{N} \frac{A_i}{\|\overline{A}\|} U_i = \beta + \sum_{i=1}^{N} \alpha_i U_i \tag{2.14}$$

$$L(\bar{u}^*) = 0 \rightarrow \beta + \sum_{i=1}^{N} \alpha_i u_i^* = 0 \rightarrow \beta = -\sum_{i=1}^{N} \alpha_i u_i^* \tag{2.15}$$

$$\left.\begin{matrix} \beta = -\sum_{i=1}^{N} \alpha_i u_i^* \\ \sum_{i=1}^{N} \alpha_i^2 = 1 \end{matrix}\right\} u_i^* = -\alpha_i \beta \tag{2.16}$$

Step 3

Step 2 looks easier than it actually is. The design point is not known upfront. Therefore, step 3 is to iterate until the design point has converged enough. To perform the FORM analysis, a starting point has to be determined for the design point. Often, the origin is used for this. Then, equation (2.15) is used to determine the corresponding value of the reliability index. The equations below show how to perform the iterations to end up with the final reliability index.

$$L(\overline{U}) = g\left(\bar{u}^k\right) + \nabla g\left(\bar{u}^k\right)\left(\overline{U} - \bar{u}^k\right)^T \tag{2.17}$$

Equation (2.17) is almost equal to equation (2.11). In equation (2.17), a guess of the design point is used instead of the actual design point. In the actual design point, the limit state function has a value of zero. Therefore, the new coordinates of the design point are computed by solving the following equation:

$$L\left(\bar{u}^{k+1}\right) = 0 \rightarrow g\left(\bar{u}^k\right) + \nabla g\left(\bar{u}^k\right)\left(\bar{u}^{k+1} - \bar{u}^k\right)^T = 0 \tag{2.18}$$

Rewriting $\bar{u}^k$ with equation (2.16) yields equation (2.19). A similar notation is possible for the new design point $\bar{u}^{k+1}$, see equation (2.20). The reasoning behind this notation is explained in (Du, 2005). Substituting equations (2.19) and (2.20) in equation (2.18) yields equation (2.23):

$$\bar{u}^k = -\beta^k \bar{\alpha}^k \tag{2.19}$$

$$\bar{u}^{k+1} = -\beta^{k+1} \bar{\alpha}^k \tag{2.20}$$

$$g\left(\bar{u}^k\right) + \nabla g\left(\bar{u}^k\right)\left(\bar{\alpha}^k\right)^T\left(\beta^k - \beta^{k+1}\right) = g\left(\bar{u}^k\right) + \left\|\nabla g\left(\bar{u}^k\right)\right\|\left(\beta^k - \beta^{k+1}\right) = 0 \rightarrow \tag{2.21}$$

$$\beta^{k+1} = \beta^k + \frac{g\left(\bar{u}^k\right)}{\|\nabla g(\bar{u}^k)\|} \tag{2.22}$$

$$\bar{u}^{k+1} = -\bar{\alpha}^k \left\{\beta^k + \frac{g\left(\bar{u}^k\right)}{\|\nabla g(\bar{u}^k)\|}\right\} \tag{2.23}$$

The iteration process stops when the convergence criterion is met. A possible convergence criterion could consider the difference between two consecutive reliability indices.

$$\left|\beta^{k+1} - \beta^{k}\right| < \varepsilon \tag{2.24}$$

2.2.5 Reliability of systems

In civil engineering, structures generally consist of multiple elements. A dike trajectory for example is a concatenation of dike sections. Two different types of systems are distinguished: series systems and parallel systems. A series system fails when just one of the elements fails. A parallel system only fails when all elements fail. The distinction between the two types of systems is also reflected in the computation of the failure probability (Jonkman et al., 2017).

Series system

As mentioned before, a series system fails when one of the elements fails. Therefore, the general equation for the failure probability of a series system is as follows:

$$P(F)_{series} = P(F_1 \cup F_2 \cup \ldots \cup F_N) \tag{2.25}$$

The failure probability of a system depends on the correlation between the elements of the system. For a series system, the lower bound of the system failure probability occurs when the elements are fully positively correlated. It is equal to the maximum failure probability of the elements. The upper bound occurs when the elements are fully negatively correlated and is equal to the sum of the failure probabilities of the elements. In case of independent elements, the system failure probability is equal to:

$$P(F)_{series,independent} = 1 - \left(1 - P(F_1)\right) \cdot \left(1 - P(F_2)\right) \cdot \ldots \cdot \left(1 - P(F_n)\right) \tag{2.26}$$

Figure 2.7 shows the system failure probability for a series system of two identical elements as a function of the correlation coefficient, ρ. A value of $\rho = 1$ represents full positive correlation, a value of $\rho = 0$ represents independence and a value of $\rho = -1$ represents full negative correlation.

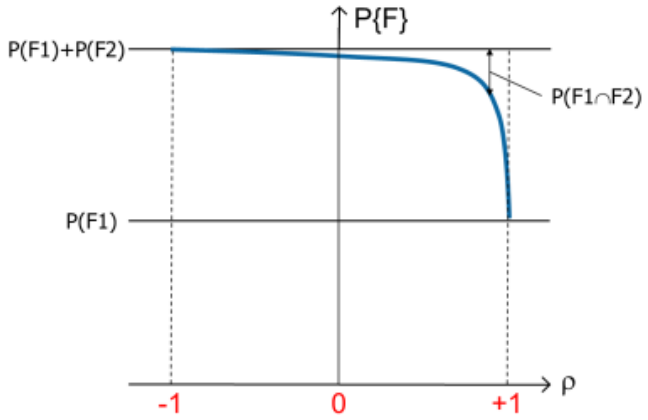

Figure 2.7: System failure probability for a series system of two identical elements as a function of the correlation coefficient (Jonkman et al., 2017)

Parallel system

A parallel system fails when all elements fail. Therefore, the general equation for the failure probability of a parallel system is as follows:

$$P(F)_{parallel} = P(F_1 \cap F_2 \cap \ldots \cap F_N) \tag{2.27}$$

For a parallel system, the lower bound of the system failure probability occurs when the elements are fully negatively correlated and is equal to zero. The upper bound occurs when the elements are fully positively correlated and is equal to the minimum failure probability of the elements. In case of independent elements, the system failure probability is equal to:

$$P(F)_{parallel,independent} = P(F_1) \cdot P(F_2) \cdot \ldots \cdot P(F_N) \tag{2.28}$$

2.2.6 Equivalent planes method

Combining elements

If the elements of a system are correlated, the system failure probability lies somewhere between the upper and the lower bound. The equivalent planes method can be used to compute the system failure probability in an accurate and efficient manner. At the most basic level, the equivalent planes method describes a way to compute the failure probability that one limit state functions fails provided that another limit state function also fails (Roscoe et al., 2015). In formula form this gives:

$$P(Z_2 < 0 | Z_1 < 0) = P(F_2|F_1) \tag{2.29}$$

Being able to compute this conditional failure probability is essential for the computation of the system failure probability. Imagine a series system of two components. The system failure probability is presented in equation (2.25). The intersection of the failure of the elements can be rewritten, see equation (2.31). Substitution of equation (2.31) in equation (2.30) yields equation (2.32).

$$P(F)_{1,2} = P(F_1 \cup F_2) = P(F_1) + P(F_2) - P(F_1 \cap F_2) \tag{2.30}$$

$$P(F_1 \cap F_2) = P(F_1) \cdot P(F_2|F_1) \tag{2.31}$$

$$P(F)_{1,2} = P(F_1) + P(F_2) - P(F_1 \cap F_2) = P(F_1) + P(F_2) - P(F_1) \cdot P(F_2|F_1) \tag{2.32}$$

As can be seen, the only remaining unknown in the system failure probability is the probability that element 2 fails provided that element 1 fails. The other probabilities in the system failure probability are marginal failure probabilities, which can be calculated with the reliability methods discussed in the previous subsections. The conditional failure probability can be computed with the equivalent planes method. The equivalent planes method can also be used to compute the failure probability of a system consisting of more than two elements. This is explained below:

$$\begin{aligned} P(F)_{system} &= P(F_1 \cup F_2 \cup \ldots \cup F_N) = P\left(F_{1,2} \cup F_3 \cup \ldots \cup F_N\right) \\ &= P\left(F_{1,2,3} \cup F_4 \cup \ldots \cup F_N\right) \end{aligned} \tag{2.33}$$

$$\begin{aligned} P(F)_{system} &= P\left(F_{1,2,\ldots,N-1} \cup F_N\right) \\ &= P\left(F_{1,2,\ldots,N-1}\right) + P(F_N) - P\left(F_{1,2,\ldots,N-1}\right) \cdot P\left(F_N|F_{1,2,\ldots,N-1}\right) \end{aligned} \tag{2.34}$$

Equation (2.32) can be used to combine two limit state functions. This is done $N-1$ times, until the system failure probability is reduced to equation (2.34). The first part of this subsection has proven that the system failure probability can be computed for a system consisting of N elements if the probability $P(Z_2 < 0|Z_1 < 0)$ can be computed. Below, it is explained how the equivalent planes method computes this conditional failure probability.

Conditional failure probability

Using the notation of equation (2.11), the limit state functions Z_1 and Z_2 can be written as:

$$Z_1 = \beta_1 + \sum_{i=1}^{N} \alpha_{1,i} U_{1,i} = \beta_1 - w_1 \tag{2.35}$$

$$Z_2 = \beta_2 + \sum_{i=1}^{N} \alpha_{2,i} U_{2,i} = \beta_2 - w_2 \tag{2.36}$$

The correlation between limit state functions Z_1 and Z_2 is computed with equation (2.37).

$$\rho(Z_1, Z_2) = \sum_{i=1}^{N} \alpha_{1,i} \cdot \alpha_{2,i} \cdot \rho_{12,i} \tag{2.37}$$

The variable $\rho_{12,i}$ represents the autocorrelation between variables $U_{1,i}$ and $U_{2,i}$. In equations (2.35) and (2.36) the reliability index is a constant. Therefore, the correlation between Z_1 and Z_2 equals the correlation between w_1 and w_2. Hence, variable w_2 can be expressed as a function of w_1 and an independent standard normally distributed variable, w_2^*.

$$w_2 = \rho \cdot w_1 + \sqrt{1 - \rho^2} \cdot w_2^* \tag{2.38}$$

$$Z_2 = \beta_2 - w_2 = \beta_2 - \left(\rho \cdot w_1 + \sqrt{1 - \rho^2} \cdot w_2^*\right) \tag{2.39}$$

$$Z_1 < 0 \rightarrow \beta_1 - w_1 < 0 \rightarrow w_1 > \beta_1 \tag{2.40}$$

The conditional failure probability $P(Z_2 < 0 | Z_1 < 0)$ can now be calculated by replacing variable w_1 with variable w_1', which represents the tail of the probability density function of w_1 for the values $w_1 > \beta_1$.

$$P(Z_2 < 0 | Z_1 < 0) = P(Z_2' < 0) \tag{2.41}$$

$$Z_2' = \beta_2 - \left(\rho \cdot w_1' + \sqrt{1 - \rho^2} \cdot w_2^*\right) \tag{2.42}$$

Equations (2.41) and (2.42) reduce the conditional failure probability $P(Z_2 < 0 | Z_1 < 0)$ to the marginal failure probability $P(Z_2' < 0)$, which can be solved with level II and III reliability methods. The equivalent planes method is also referred to as the Hohenbichler-Rackwitz method (Roscoe et al., 2015).

2.2.7 Fragility curves

A fragility curve plots the conditional failure probability of a certain structure as a function of the load (Schweckendiek et al., 2017). In hydraulic engineering, the load is often the water level. To generate a fragility curve, the conditional failure probability is computed for multiple fixed water levels. These values provide the basis of the fragility curve. Next, interpolation is applied to draw a line through these points. Figure 2.8 shows the fragility curve of a dike cross section for the failure mechanism overtopping.

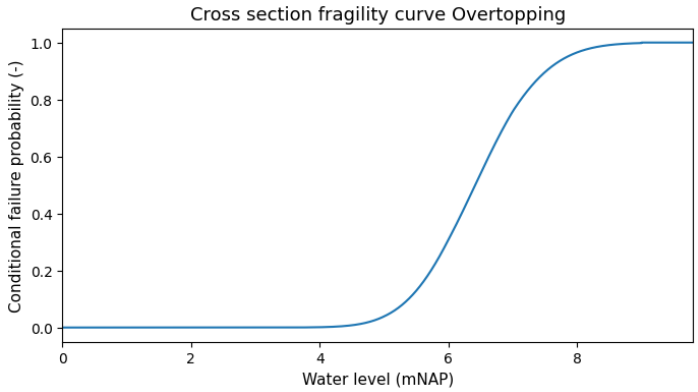

Figure 2.8: Fragility curve of a dike cross section for overtopping

The failure probability can be computed by integrating the product of the fragility curve and the probability density function of the load variable, see equation (2.43) (Schweckendiek et al., 2017). For the fragility curve of Figure 2.8, this means that the probability distribution of the water level is required. Often, an extreme value distribution is used for the load variable. As the extreme value distribution describes the yearly maximum of the load variable, the failure probability resulting from equation (2.43) has the unit $[year^{-1}]$.

$$P_f = \int_{-\infty}^{\infty} P(Z < 0|s) f_S(s) ds \tag{2.43}$$

2.3 Failure mechanisms

As stated in the subsection on the combination protocol, only a handful of failure mechanisms can be computed either in a full probabilistic or semi-probabilistic way. From this list of mechanisms, only four of them are applicable to the dike trajectory that is modelled in this research. For example, the reliability of the closure of a structure is not applicable as there is no structure that can open and close. Furthermore, the stone stability is not applicable as the dike contains grass revetments. The only failure mechanism which is left out but could have been included, is the erosion of the outer slope. In this research, slope erosion is modelled with the critical mean overtopping equation. This equation is only applicable for the inner slope erosion failure mechanism, also known as overtopping. Next to overtopping, the two remaining failure mechanisms which are included in this research are inner slope stability and piping. This section provides a description of the failure mechanisms. The software packages and equations that are used to model the failure mechanisms are described in section 3.3.

2.3.1 Inner slope stability

A typical inner slope failure is schematized in Figure 2.9. Failure takes place if the driving force along the slip plane is greater than the resisting force. Usually, dikes are perfectly stable during dry conditions. However, a lot of rain or a long lasting high outside water level lead to infiltration of water in the dike body. This leads to increased pore water pressures and causes a low effective soil stress and thus a low shear resistance. The reduced shear resistance could lead to a slope failure and eventually to the collapse of the dike (Jonkman et al., 2021).

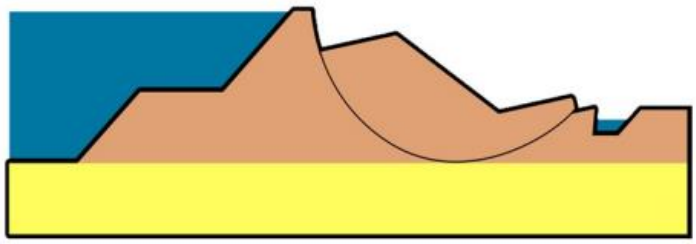

Figure 2.9: Schematization of an inner slope failure (Jonkman et al., 2021)

2.3.2 Overtopping

When a wave breaks on a dike or just in front of it, the water runs up the slope the dike. The height to which the water runs up is called the run-up level. Even when the top of the wave is below the crest level of the dike, the water may still surpass the crest due to the run up. When the run-up level exceeds the crest level, the water flows across the crest and down the inner slope of the dike. This process is called overflow. When large volumes of water run down the inner slope, the erosion increases and eventually leads to instability of the inner slope. Consequently, this leads to dike failure.

Overflow takes place when the design water level exceeds the crest level of the dike. This failure mechanism is different from overtopping. In this research, overflow is integrated in the models of all failure mechanisms. The failure mechanisms are modelled with fragility curves. Overflow is included by increasing the conditional probability of failure to one when the water level exceeds the crest height (Jonkman et al., 2021).

2.3.3 Piping

Piping is the general term for a chain of processes, see Figure 2.10 (Jonkman et al., 2021).

a) Uplift: due to the high water level on the outer side of the dike, the pore pressures in the aquifer rise. The pore pressure is omnidirectional, meaning it also results in an upward pressure. When the weight of the aquitard is surpassed by the pore pressure, the aquitard ruptures and lifts up.
b) Seepage: Groundwater can now flow through the opening in the damaged aquitard.
c) Heave: The location where the groundwater flows out is called the exit point. Sand particles are taken along with the water flow if the gradient at the exit point surpasses the so-called heave gradient.
d) Upstream erosion: As more sand particles are eroded, a channel starts to form below the dike which runs from the land side to the outer side. The channel is called a pipe.
e) Continuous pipe: When the erosion channel reaches the water body on the outer side of the dike, the hydraulic resistance drops and the flow is increased.
f) Collapse: The foundation of the dike is compromised, leading to its collapse.

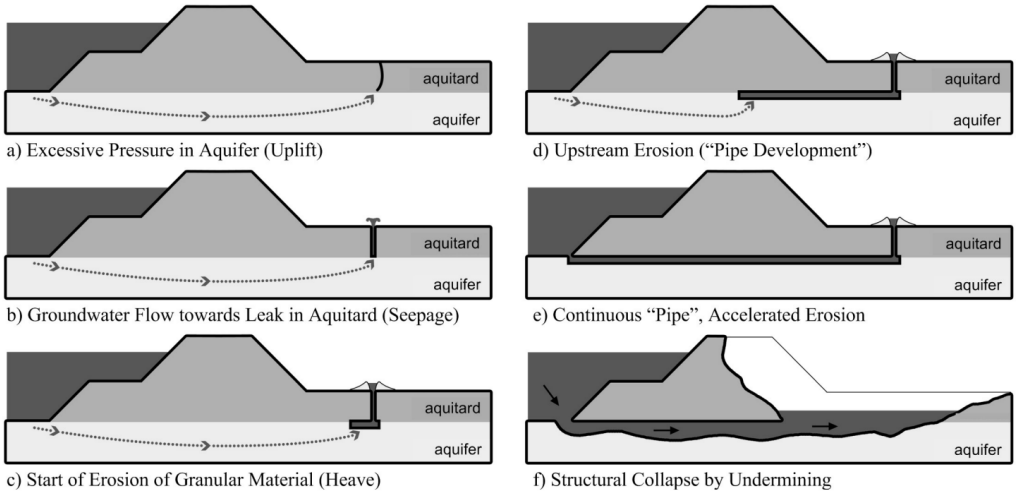

Figure 2.10: Stages of piping (Jonkman et al., 2021)

3. Methodology

Chapter three starts with an overview of the methodology. In this overview, the methodology is divided into 8 steps. Furthermore, the dike trajectory that is modelled in this research is introduced. In section 3.2 the geometry of the dike trajectory is presented in more detail. Section 3.3 describes the failure mechanisms and the models that are used to compute the fragility curves. In section 3.4 one fragility curve is computed for every failure mechanism for every representative cross section of the dike trajectories. The fragility curve method is explained in sections 3.5 and 3.6. Section 3.5 demonstrates how the cross section fragility curves should be scaled up to dike section fragility curves. Section 3.6 first explains how the fragility curve method scales up the dike section fragility curves per failure mechanism to the total dike trajectory fragility curve. Then, section 3.6 shows how to compute the dike trajectory failure probability from the probability distribution of the water level and the dike trajectory fragility curve.

3.1 Overview

The aim of this research is to develop an accessible method for dike safety assessment which considers correlation. The new method is called the fragility curve method, as it is based on the combination of fragility curves. This method is compared with the current Dutch practice for combining dike failure probabilities, prescribed by the combination protocol. Both dike assessment methods are applied to a hypothetical sea dike. The details of the hypothetical sea dike are presented in section 3.2. Figure 3.1 presents a general overview of the methodology followed in this research. The aim of the first five steps is to provide the starting point for the application of the fragility curve method and the combination protocol. The starting point consists of the fragility curves of the representative cross sections. Every dike section is modelled by one representative cross section.

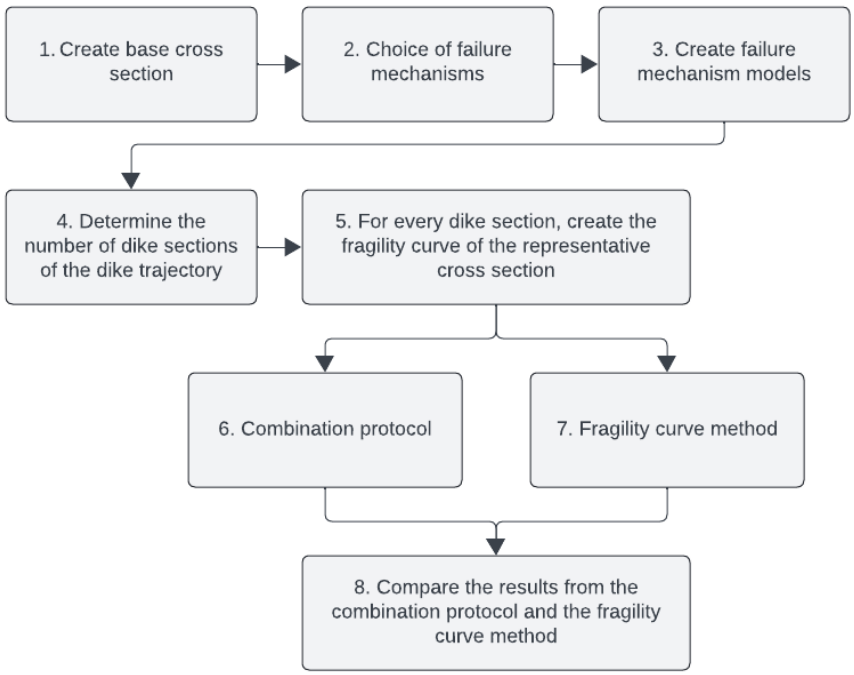

Figure 3.1: General flow chart of the methodology

In steps 6 and 7, the combination protocol and the fragility curve method are applied to compute the total dike trajectory failure probability from the cross section fragility curves. The main difference between the combination protocol and the fragility curve method is that the combination protocol scales up failure probabilities to go from the cross section level to the dike trajectory level and that the fragility curve method scales up fragility curves. The combination protocol immediately converts the cross section fragility curves into cross section failure probabilities with equation (2.43). Then, the combination protocol scales up the cross section failure probabilities into the dike trajectory failure probability. On the other hand, the fragility curve method scales up the cross section fragility curves into the dike trajectory fragility curve. Then, it converts the dike trajectory fragility curve into the dike trajectory failure probability. For the fragility curve method, the conversion from fragility curve to failure probability is the last step instead of the first step, as is the case for the combination protocol. The fragility curve method is worked out in more detail in sections 3.5 and 3.6. The flow chart of Figure 3.2 introduces the fragility curve method. The combination protocol is explained in subsection 2.1.4 of the literature study. The methodology of the combination protocol is summarized in the flow chart of Figure 3.3.

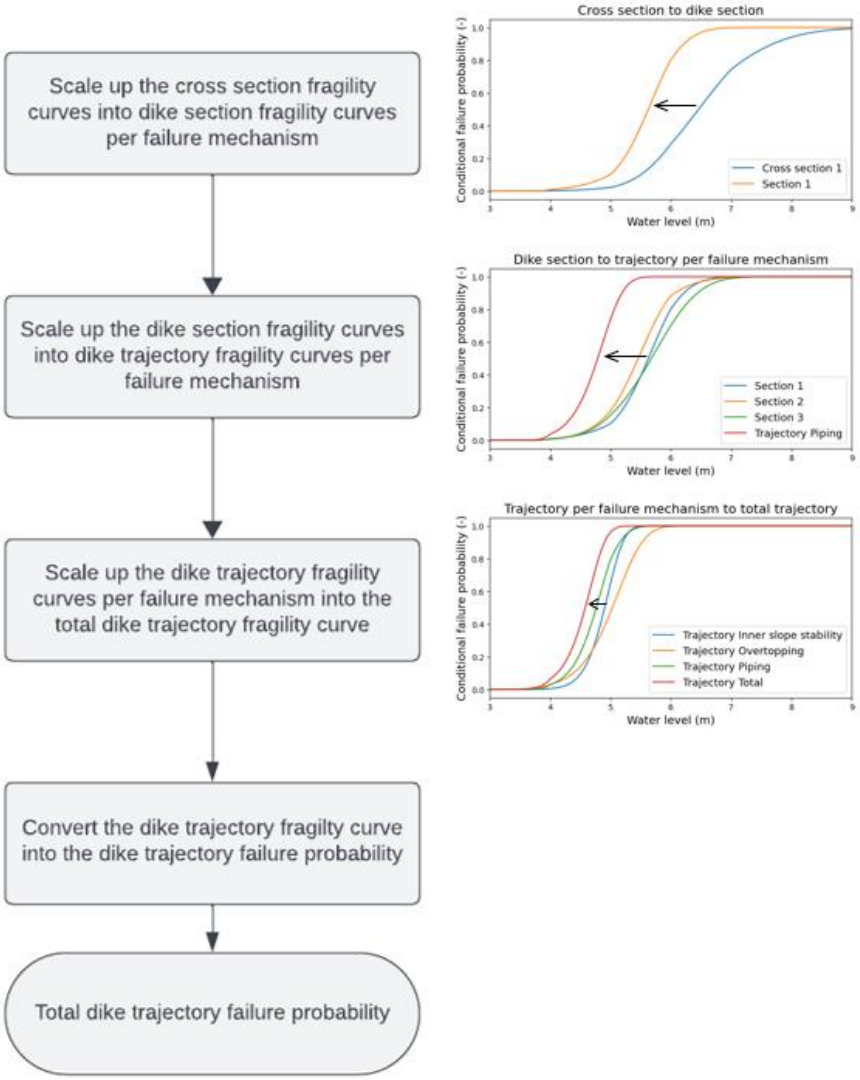

Figure 3.2: Flow chart fragility curve method

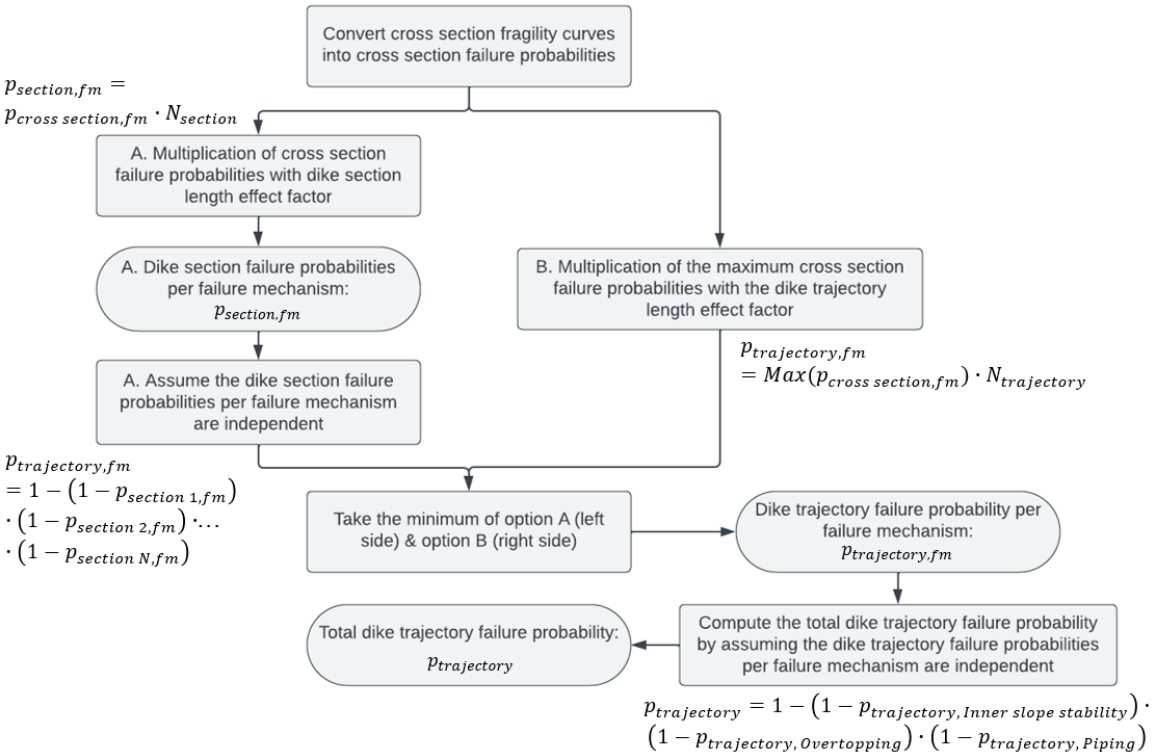

Figure 3.3: Flow chart combination protocol

To be able to make a proper comparison between the dike safety assessment of the combination protocol and the fragility curve method, both methods are applied to six different dike trajectories, see Table 3.1. These trajectories can be subdivided into two groups. The dike trajectories of the first group contain dike sections which only vary slightly with respect to each other due to natural variability. Therefore, the corresponding section failure probabilities are all in the same order of magnitude. For the dike trajectories of the second group, one of the dike sections is significantly weaker than the other ones for all failure mechanisms. The remaining dike sections exhibit only minor natural variations in comparison to one another, just like the dike sections of the first group. As a result, the failure probabilities of the dominant dike section are one order of magnitude higher than the failure probabilities of the other dike sections.

The only difference between the dike trajectories within a group is the number of dike sections, which varies between 5, 10 and 15. The length of all dike trajectories is the same and measures 5 kilometers. This implies that the length of the dike sections varies between the different trajectories. The more dike sections a trajectory contains, the shorter the length of each section. For every dike trajectory, the length of the dike sections is the same for all failure mechanisms. Finally, the length effect is not neglected, see subsection 2.1.4. A length effect factor is applied to take into account the spatial variability when scaling up from the cross section level to the dike section level. In the remainder of this chapter, the steps of the methodology of Figure 3.1 are explained in more detail.

Table 3.1: Description of the dike trajectories

	Dike sections	Number of dike sections
Trajectory 1.1	Small natural variability	5
Trajectory 1.2	Small natural variability	10
Trajectory 1.3	Small natural variability	15
Trajectory 2.1	One dominant section	5
Trajectory 2.2	One dominant section	10
Trajectory 2.3	One dominant section	15

3.2 Base cross section

In this section, the geometry of the base cross section is presented. The dike trajectories that are schematized are all representative of a Dutch sea dike and have a length of 5 kilometers. The base cross section is present in all trajectories and provides an indication of what the hypothetical sea dike looks like. It consists of a sand core with a cover layer of organic clay. The dike is built on an aquitard of organic clay, which lies on top of a sand aquifer. Below the sand aquifer lies a layer of deep clay. The last layer is a layer of sand, which extents until a great depth. The ground level is assumed to be at $0\ mNAP$. The details of the geometry of the base cross section are presented in Table 3.2.

Table 3.2: Geometry base cross section

Parameter	Unit	CS1
Crest height	$mNAP$	9.0
Width levee	m	19
Length foreshore	m	10
Thickness cover layer	m	1.5
Inner slope gradient	-	1/4
Outer slope gradient	-	1/4
Inner berm length	m	16
Inner berm height	m	4
Thickness aquitard	m	5
Thickness aquifer	m	8
Thickness deep clay layer	m	5
Thickness deep sand layer	m	>10

The base cross section is depicted in Figure 3.4 below. The other parameters that are required to perform the failure probability computations are mentioned in section 3.3.

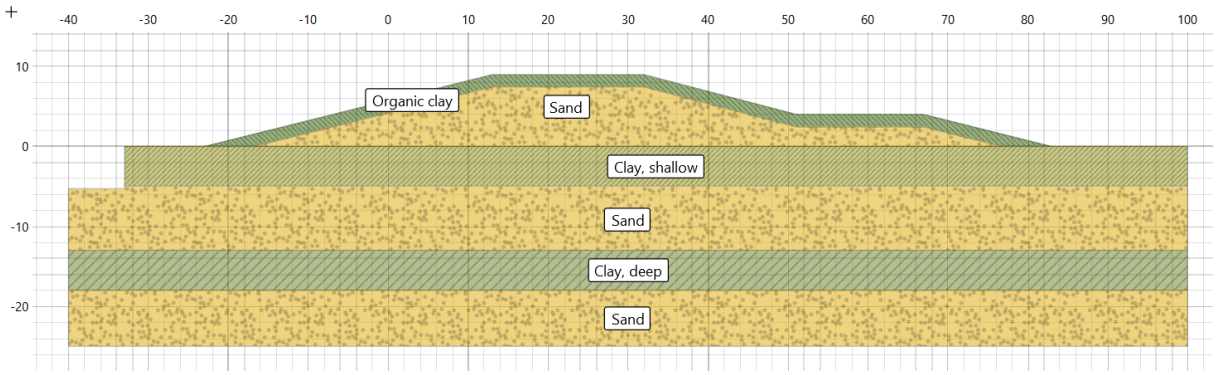

Figure 3.4: Base cross section

3.3 Failure mechanism models

Not all failure mechanisms can be computed with a full probabilistic or semi-probabilistic method. From the failure mechanisms for which such a method does exist, only four of them are applicable to the fictional dike trajectory of this research. For example, stone stability is not applicable as the dike contains grass revetments. The only failure mechanism which is left out but could have been included, is the erosion of the outer slope. In this research, slope erosion is modelled with the critical mean overtopping equation. This equation is only applicable for the inner slope erosion failure mechanism, also known as overtopping (OT). Next to

overtopping, the two remaining failure mechanisms which are modelled are inner slope stability (ISS) and piping (PP). This section describes the equations and software packages that are used to model the failure mechanisms.

3.3.1 Inner slope stability

Method

To be able to include correlation in the combination of failure probabilities from the cross section to the dike trajectory level, the failure probabilities on the cross section level have to be calculated in a full probabilistic way. To this end, the application D-Stability is used. D-Stability is a software product from Deltares that is designed to assess slip planes. It can perform deterministic, semi-probabilistic as well as fully probabilistic assessments. The fully probabilistic analysis can either be done with a FORM analysis or by Mone Carlo Importance Sampling (MCIS). The FORM analysis uses a given slip plane whereas the MCIS method is used when the slip plane is determined by a search algorithm. Due to the extra slip plane search, the run time of the MCIS method is in the order of hours whereas the run time of the FORM analysis is in the order of minutes. Therefore, the FORM analysis is chosen.

As mentioned before, the FORM analysis of a slip plane requires a previously determined slip plane as input. The input slip plane is found by performing a semi-probabilistic slip plane calculation with the design values of the soil parameters. This slip plane is consequently imported into the FORM analysis, which uses the probability distributions of the soil parameters to compute the probability of failure.

The semi-probabilistic calculation to determine the representative slip plane is performed with the Uplift-Van method in combination with a search algorithm. The FORM analysis is also performed with the Uplift-Van method. The Uplift-Van model is the most suitable limit equilibrium model for the fictional dike, as the dike has a clear distinction between the aquifer and the aquitard. At this distinction, the increased pore water pressures due to a high outside water level cause a reduction in the effective stress, which leads to a reduction of the shear stress. The slip circle of the Uplift-Van method is able to run along this distinction as it consists of an active circle, a horizontal part and a passive circle (Deltares, 2023).

As mentioned in section 3.1, the fragility curve method uses fragility curves to combine dike failure probabilities. Therefore, the process of determining a representative slip plane and consequently performing a FORM analysis for this slip plane is done several times for different outside water levels. The D-Stability model is run for the following water levels: $h = 0mNAP$, $h = 2mNAP$, $h = 4mNAP$, $h = 6mNAP$ and $h = 8mNAP$. For every water level, the model computes the failure probability conditional to the water level. The fragility curve of the cross section that was put into the model consists of the collection of all conditional failure probabilities.

Soil parameters

The geometry of the base cross section has already been presented in section 3.2. These values are all deterministic. The remaining parameters required to perform the stability assessment of the inner slope are presented in Table 3.3, along with their corresponding mean value and standard deviation. These values belong to the base cross section. If a certain parameter does not have a value for the standard deviation, this means the parameter is deterministic. All other soil parameters are lognormally distributed. This is the only option provided by D-Stability. However, it is a logical option, as these soil parameters cannot have a value lower than zero (Deltares, 2023).

Table 3.3: Soil parameters of the base cross section for the stability assessment of the inner slope

Parameter	Unit	Mean	Standard Deviation
Organic clay			
Unit weight above phreatic level	kn/m^3	13.9	-
Unit weight below phreatic level	kn/m^3	13.9	-
Shear strength ratio	-	0.24	0.01
Strength increase exponent	-	0.85	0.05
Shallow clay			
Unit weight above phreatic level	kn/m^3	14.8	-
Unit weight below phreatic level	kn/m^3	14.8	-
Shear strength ratio	-	0.235	0.01
Strength increase exponent	-	0.9	0.05
Deep clay			
Unit weight above phreatic level	kn/m^3	15.6	-
Unit weight below phreatic level	kn/m^3	15.6	-
Shear strength ratio	-	0.23	0.01
Strength increase exponent	-	0.9	0.05
Sand			
Unit weight above phreatic level	kn/m^3	18	-
Unit weight below phreatic level	kn/m^3	20	-
Cohesion	kn/m^2	0	-
Frictional angle	deg	30	1
Dilatancy angle	deg	0	-

The Default shear strength models are used from D-Stability. This means that for the clay layers the SHANSHEP model is used for undrained shear stresses. For the sand layer the advanced Mohr-Coulomb model is used for drained shear stresses.

Hydraulic head

To perform the slip plane computations, D-Stability requires information on the hydraulic head. First of all, the phreatic line has to be determined. On the outer side of the dike, the phreatic level is equal to the outside water level. The phreatic level of the hinterland is assumed to be equal to the ground level of the hinterland. The phreatic level along the core of the dike is computed with the guidelines form the Technical Advisory committee for Water defenses (TAW). The fictional dike trajectory consists of a sand core with a clay cover layer of 1.5 m. For such a dike, the guidelines prescribe the following (TAW, 2004):

1. Start at the point where the outside water level meets the outer slope of the dike.
2. The phreatic level drops with a value of $0.5 \cdot \mathrm{h}$. The new point is located at the boundary of the sand core and the clay cover layer.
3. The phreatic level at the inner slope of the dike has a value of $0.25 \cdot \mathrm{h}$. Draw a straight line from the point form step 2 to this point on the inner slope.
4. Follow the line of the inner slope until the toe of the dike.

To clarify this procedure, an example is presented in Figure 3.5. The phreatic line should actually follow the red dotted line. However, D-Stability does not allow the phreatic line to have two values at the same location. The blue dotted line is the actual line used in D-Stability. As can be seen, this is only a small adjustment. Furthermore, the approximation does not have an effect on the phreatic line of a possible slip plane of the inner slope.

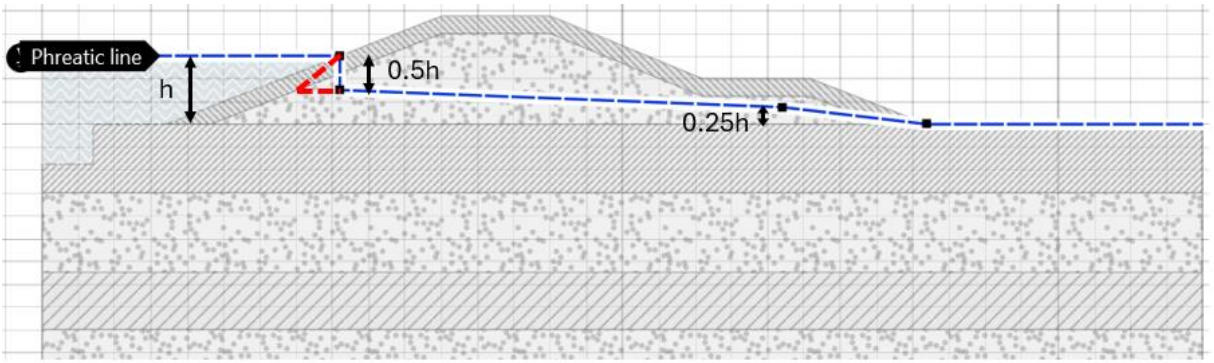

Figure 3.5: Example phreatic line

Next to the phreatic line, the piezometric head at the boundary of the clay aquitard and the sand aquifer has to be determined as well. Due to the high permeability of the first sand layer, high outside water levels cause a high piezometric head in the aquifer at the inner side of the dike. The reduction of the piezometric head from the inflow point at the outer side of the dike can be approximated with the following equations:

$$\varphi_{exit} = h_p + \lambda \cdot (h - h_p) \tag{3.1}$$

$$\lambda = 100 \cdot \frac{\lambda_h}{L_f + B + \lambda_h} \cdot e^{\frac{\left(\frac{B}{2} - x_{exit}\right)}{\lambda_h}}, x_{exit} > B/2 \tag{3.2}$$

$$\lambda_h = \sqrt{kDd/k_h} \tag{3.3}$$

In which:

- φ_{exit} = The piezometric head at the specified location inland of the dike $[mNAP]$
- h_p = The phreatic level of the hinterland $[mNAP]$
- h = The water level on the outer side of the dike $[mNAP]$
- $100 - \lambda$ = The piezometric head reduction factor $[\%]$
- L_f = The foreshore length $[m]$
- B = The width of the dike $[m]$
- λ_h = The leakage factor $[m]$
- x_{exit} = The distance from the center of the dike to the specified inland location $[m]$
- k = The hydraulic conductivity of the aquifer $[m/s]$
- k_h = The hydraulic conductivity of the aquitard $[m/s]$
- D = The thickness of the aquifer $[m]$
- d = The thickness of the aquitard $[m]$

For the base cross section, the effective foreshore length equals $L_f = 10\,m$. The hydraulic conductivity of the aquifer is $k = 1.2 \cdot 10^{-3}\,m/s$ and the hydraulic conductivity of the aquitard is $k_h = 2.4 \cdot 10^{-6}\,m/s$ (De Vree, n.d.). The thickness of the aquifer and aquitard and the width of the dike follow from Table 3.2. For the exit point, a location two meters inland of the inner toe is chosen. For the base cross section this gives a head reduction factor of $100 - \lambda = 45.8\%$. With the head reduction factor, the piezometric head at the exit point can be calculated for the different outside water levels. To complete the head line representing the piezometric head at the top of the aquifer, a straight line is drawn through the outside water level at the inflow point and the computed water level at the exit point. This procedure is illustrated in Figure 3.6.

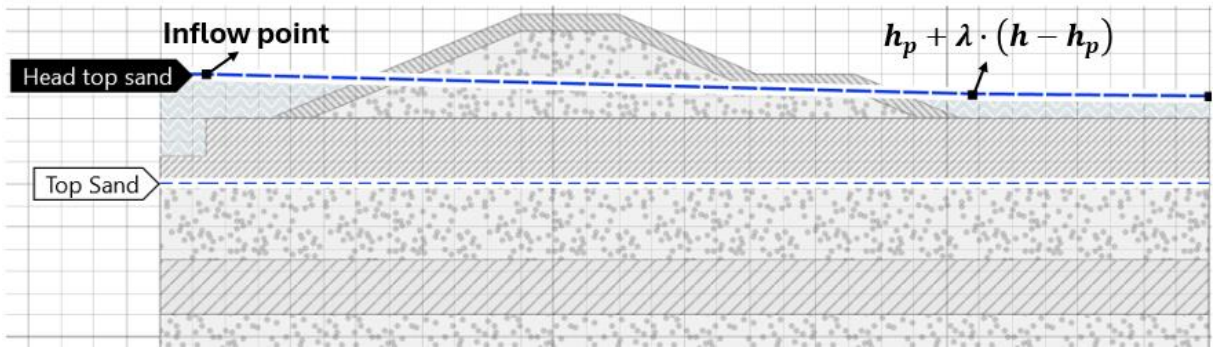

Figure 3.6: Piezometric head top of aquifer in case of no uplift

The next step is to check if the piezometric head at the top of the aquifer does not exceed the uplift potential. Uplift takes place if the pore pressure at the top of the aquifer exceeds the pressure from the weight of the soil above. In formula form this gives:

$$No\ uplift\ if: \gamma_{water} \cdot \varphi_{aquifer} + \gamma_{water} \cdot d < d \cdot \gamma_{aquitard} \tag{3.4}$$

$$h_p + \lambda \cdot (h - h_p) < \frac{d \cdot (\gamma_{aquitard} - \gamma_{water})}{\gamma_{water}}, \quad h_p = 0 \rightarrow$$

$$h < \frac{d \cdot (\gamma_{aquitard} - \gamma_{water})}{\lambda \cdot \gamma_{water}} \tag{3.5}$$

For the base cross section this gives $h < 4.69\ m$, which means that the piezometric head at the top of the aquifer needs to be limited for the water levels $h > 4.69\ m$. The limit at the location of the toe of the inner slope can be calculated with the following formula:

$$\varphi_{aquifer,toe} < \frac{d \cdot (\gamma_{aquitard} - \gamma_{water})}{\gamma_{water}} \tag{3.6}$$

For the base cross section this gives $\varphi_{aquifer,toe} < 2.54\ mNAP$. According to the guidelines from the TAW (2004), the uplift zone has a length of $L_{uplift} = 2 \cdot d$. After the uplift zone, the piezometric head must decrease with a gradient of $1/50$. Figure 3.7 shows the piezometric head at the top of the aquifer for an outside water level of $h = 8\ mNAP$.

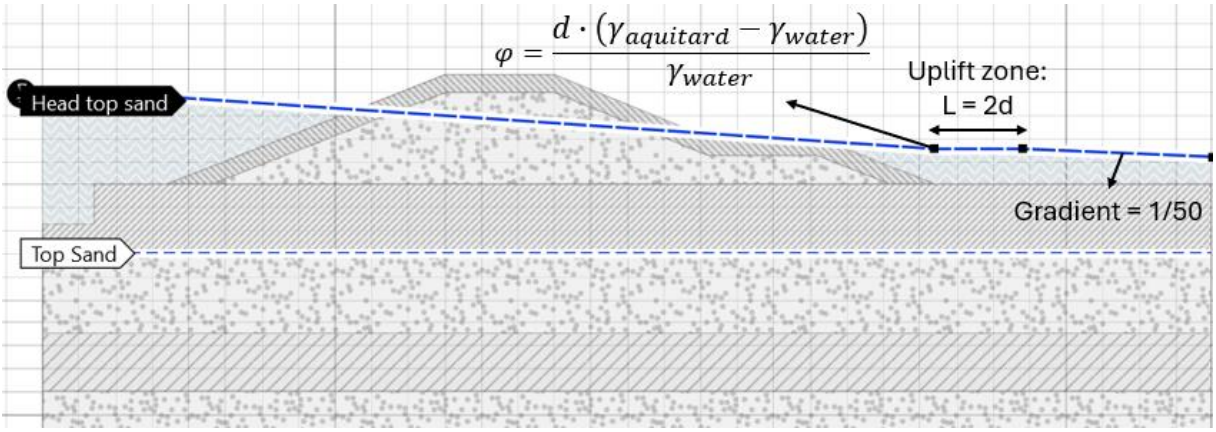

Figure 3.7: Piezometric head top of aquifer for an outside water level of $h = 8\ m$

The last step is to determine the pore water pressure in the aquitard. At the top of the aquitard, the pore water pressure is hydrostatic. At the bottom of the aquitard, the pore water pressure is equal to the computed pore water pressure at the top of the aquifer, which is larger than the

hydrostatic water pressure. The intrusion length is assumed to be three meters. The pore water pressure is hydrostatic until the top of the intrusion layer. From there, the pore water pressure is connected in a straight line with the increased pore water pressure at the bottom of the aquitard, see Figure 3.8. An intrusion length of three meters is chosen, as the fictional dike is a sea dike, which is influenced by the tide.

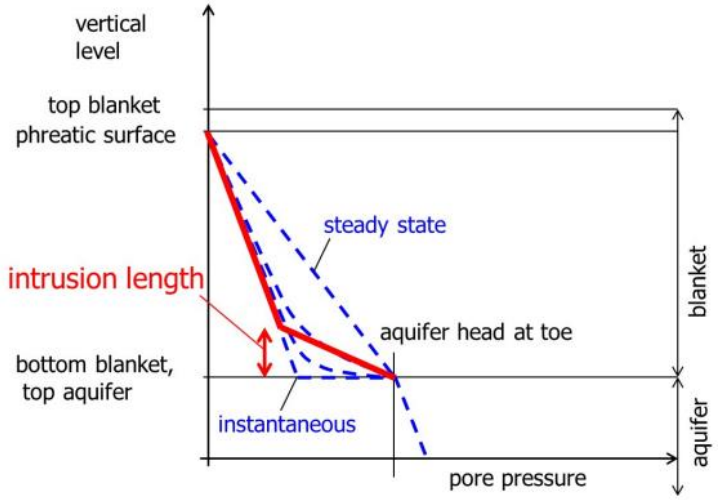

Figure 3.8: Intrusion length

Fragility curve base cross section

As all parameters are known, D-Stability is used to create the fragility curve of the base cross section for the failure mechanism inner slope stability, see Figure 3.9 below. In this figure, the conditional failure probability is plot on the y-axis instead of the reliability index.

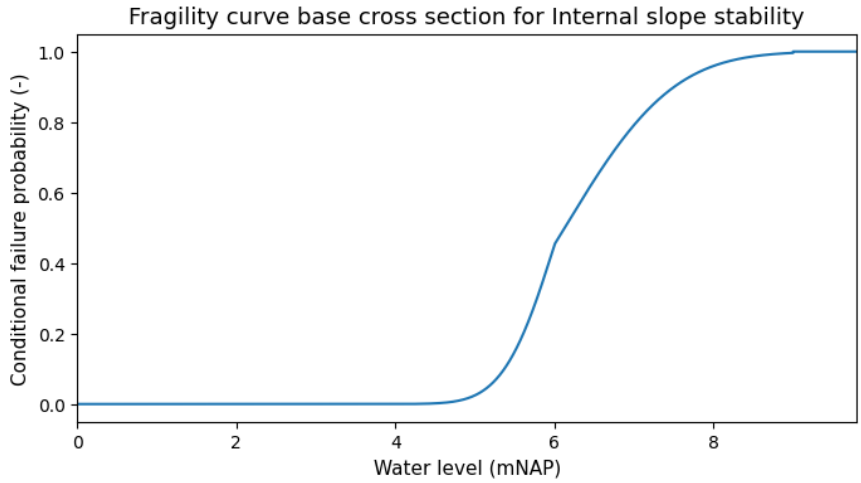

Figure 3.9: Fragility curve of the base cross section for inner slope stability

3.3.2 Overtopping

Method

The cross section failure probabilities of overtopping also have to be calculated in a probabilistic way. As mentioned in section 3.1, the fragility curve method is based on the combination of fragility curves. These fragility curves consist of the conditional cross section failure probabilities. The Probabilistic Toolkit application is used to compute the cross section fragility curves for the failure mechanism overtopping. The Probabilistic Toolkit is a software product from Deltares designed to analyze the effect of uncertainty on a model. The conditional

failure probabilities are computed for the following outside water levels: $h = 0mNAP,\ h = 1mNAP,\ h = 2mNAP,\ h = 3mNAP,\ h = 4mNAP,\ h = 5mNAP,\ h = 6mNAP,\ h = 7mNAP$ and $h = 8mNAP$. For every water level, a directional Monte Carlo analysis is performed consisting of 25,000 realizations.

The Probabilistic Toolkit requires a limit state function to compute the conditional failure probabilities. The limit state function is presented in equation (*3.7*).

$$Z_{Overtopping} = q_c - MIN(q, q_{max}) \tag{3.7}$$

In which:

- q_c = The critical overtopping rate $[m^3/s/m]$
- q = The actual overtopping rate $[m^3/s/m]$
- q_{max} = The upper limit of the actual overtopping rate $[m^3/s/m]$

The critical overtopping rate follows a lognormal distribution. The values of the mean and the standard deviation depend on the quality of the grass layer of the inner slope and the wave height class. The grass layer is classified as medium dense turf. Three options are available for the wave height class, namely: $0-1\ m\ (I), 1-2\ m\ (II) \& 2-3\ m\ (III)$. By analyzing the wave heights along the Dutch coast with the Hydra-NL software, wave height class III is chosen for the fictional dike trajectory. Hydra-NL is a probabilistic model which calculates the hydraulic loads required for the design and assessment of the Dutch primary flood defenses. The medium dense turf and wave height class III result in a mean value of the critical overtopping rate of $\mu_{q_c} = 0.040\ m^3/s/m$ and a standard deviation of $\sigma_{q_c} = 0.050\ m^3/s/m$ (Rijkswaterstaat, 2022).

Actual overtopping rate

The actual overtopping rate is calculated with the formulas from (TAW, 2002). The spectral wave height and wave period are determined with the Bretschneider equations (Bretschneider, 1957).

$$\frac{q}{\sqrt{g \cdot H_{mo}^3}} = \frac{A}{\sqrt{\tan(\alpha)}} \cdot \xi_{m-1,0} \cdot \gamma_b \cdot \exp\left(-B \cdot \frac{R_c}{\gamma_b \cdot \gamma_f \cdot \gamma_\beta \cdot \gamma_v \cdot \xi_{m-1,0} \cdot H_{mo}}\right) \tag{3.8}$$

$$\frac{q_{max}}{\sqrt{g \cdot H_{mo}^3}} = C \cdot \exp\left(-D \cdot \frac{R_c}{\gamma_f \cdot \gamma_\beta \cdot H_{mo}}\right) \tag{3.9}$$

In which:

$$\xi_{m-1,0} = \frac{\tan(\alpha)}{\sqrt{\frac{H_{mo}}{gT_{m-1,0}^2/2\pi}}} \tag{3.10}$$

$$R_c = CrestHeight - h \tag{3.11}$$

$$H_{mo} \approx H_s = \frac{u_{10}^2}{g} \cdot 0.283 \tanh\left(0.530\left(\frac{dg}{u_{10}^2}\right)^{0.75}\right) \tanh\left(\frac{0.0125\left(\frac{Fg}{u_{10}^2}\right)^{0.42}}{tanh\left(0.530\left(\frac{dg}{u_{10}^2}\right)^{0.75}\right)}\right) \tag{3.12}$$

$$T_s = \frac{u_{10}}{g} \cdot 2.4 \cdot \pi \cdot \tanh\left(0.833\left(\frac{dg}{u_{10}^2}\right)^{0.375}\right)\tanh\left(\frac{0.077\left(\frac{Fg}{u_{10}^2}\right)^{0.25}}{tanh\left(0.833\left(\frac{dg}{u_{10}^2}\right)^{0.375}\right)}\right) \quad (3.13)$$

$$T_{m-1,o} = \frac{T_p}{1.1} = \frac{1.08}{1.1} \cdot T_s \quad (3.14)$$

Table 3.4 below contains all the parameters and their distributions required to compute the fragility curve for the base cross section. The gamma (γ) factors in equations (3.8) and (3.9) are reduction factors. These are all assumed to be equal to one.

Table 3.4: Parameters base cross section for the overtopping model

Parameter	Unit	Symbol	Distribution	Mean	St. Dev.
Foreshore water depth	m	d_1	Normal	5.3	0.2
Fetch	km	F_1	Normal	75	3
Wind speed 10 $\boldsymbol{m}$ above surface	m/s	u_{10}	Weibull	25	5
Gravitational constant	m/s^2	g	Deterministic	9.81	-
Empirical parameter	-	A	Deterministic	0.067	-
Empirical parameter	-	B	Normal	4.75	0.5
Empirical parameter	-	C	Deterministic	0.2	-
Empirical parameter	-	D	Normal	2.6	0.35
Critical overtopping rate	m^2/s	q_c	Lognormal	0.040	0.050

Fragility curve of the base cross section

As all parameters are known, the Probabilistic Toolkit model is used to compute the fragility curve of the base cross section. The fragility curve is presented in Figure 3.10 below.

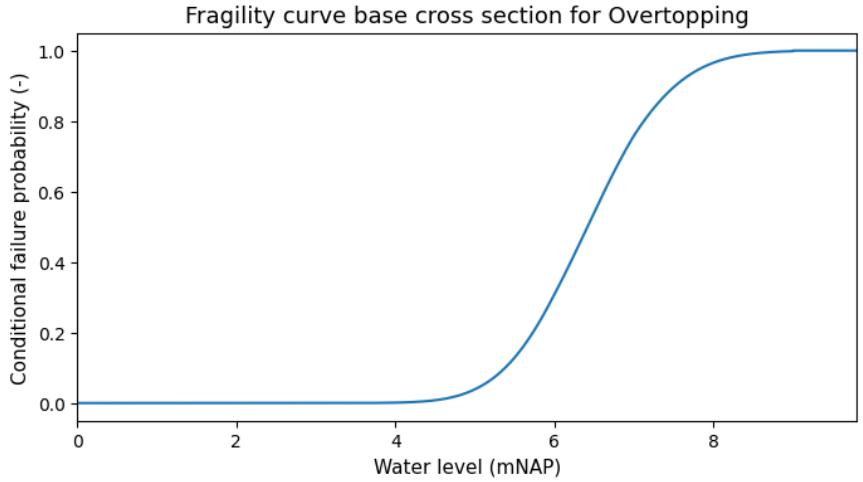

Figure 3.10: Fragility curve of the base cross section for overtopping

3.3.3 Piping

Method

To be able to include correlation, the cross section failure probabilities of overtopping are calculated in a probabilistic way. As for the other failure mechanisms, fragility curves are computed which consist of the conditional cross section failure probabilities. The Probabilistic Toolkit application is used to compute the fragility curves for the failure mechanism piping. The

conditional failure probabilities are computed for the following outside water levels: $h = 0mNAP,\ h = 1mNAP,\ h = 2mNAP,\ h = 3mNAP,\ h = 4mNAP,\ h = 5mNAP,\ h = 6mNAP,\ h = 7mNAP$ and $h = 8mNAP$. For every water level, a directional Monte Carlo analysis is performed consisting of 25,000 realizations.

As mentioned in section 2.3, piping is the general term for a chain of processes. Therefore, it cannot be described by one limit state function. Piping is modelled as a parallel system of the three main processes, namely: uplift, heave and backward erosion. The limit stare functions for these processes are presented in the formulas below. The equation for backward erosion is called the Sellmeijer equation (Sellmeijer et al., 2011).

Uplift:

$$Z_u = m_u \cdot \Delta\varphi_{c,u} - \Delta\varphi \tag{3.15}$$

$$\Delta\varphi_{c,u} = d \cdot \frac{\gamma_{sat} - \gamma_w}{\gamma_w} \tag{3.16}$$

$$\Delta\varphi = \varphi_{exit} - h_p \tag{3.17}$$

In which:

- m_u = Model factor for uplift $[-]$
- $\Delta\varphi_{c,u}$ = Critical head difference $[m]$
- γ_{sat} = Saturated volumetric weight of the blanket layer $[kN/m^3]$
- $\Delta\varphi$ = Actual head difference at the exit point $[m]$

Heave:

$$Z_h = i_{c,h} - i \tag{3.18}$$

$$i = \frac{\varphi_{exit} - h_p}{d} \tag{3.19}$$

In which:

- $i_{c,h}$ = Critical heave gradient $[-]$
- i = Actual heave gradient at the exit point $[-]$

Backward erosion:

$$Z_p = m_p \cdot H_c - H = m_p \cdot H_c - \left(h - h_p - 0.3d\right) \tag{3.20}$$

$$H_c = F_1 \cdot F_2 \cdot F_3 \cdot L \tag{3.21}$$

$$F_1 = \eta \cdot \left(\frac{\gamma_s}{\gamma_w} - 1\right) \cdot tan(\theta) \tag{3.22}$$

$$F_2 = \frac{d_{70m}}{\sqrt[3]{\frac{\nu \cdot k \cdot L}{g}}} \cdot \left(\frac{d_{70}}{d_{70m}}\right)^{0.4} \tag{3.23}$$

$$F_3 = 0.91 \cdot (D/L)^{\frac{0.28}{(D/L)^{2.8}-1}+0.04} \tag{3.24}$$

In which:

- m_p = Model factor for backward erosion $[-]$
- H_c = Critical head difference $[m]$

- H = Actual head difference at the exit point $[m]$
- η = Drag factor coefficient $[-]$
- γ_s = Volumetric weight of sand grains = $26.5\ kN/m^3$
- θ = Bedding angle [°]
- d_{70} = 70%-quantile of the grain size distribution $[m]$
- d_{70m} = Reference value for d_{70} in small scale tests $[m]$
- ν = Kinematic viscosity of water = $1.33 \cdot 10^{-6}\ m^2/s$
- L = Seepage length $[m]$

The individual models for the submechanisms have now been specified. Piping failure only occurs if all three submechanisms take place at the same time. In the Probabilistic Toolkit, the limit state functions of the submechanisms are modelled with probabilistic AND-gates for a parallel system. The system failure probability is computed with the equivalent planes method, see subsection 2.2.6.

Parameters

Table 3.5 contains all the parameters and their distributions that are required to compute the fragility curve of the base cross section. The probabilistic distributions of the critical heave gradient and the model factors for backward erosion and uplift follow from (Deltares, 2016). These parameters are lognormally distributed.

To have a probability of failure of piping which is comparable with the failure probabilities of the other two failure mechanisms, the aquifer needs to have a high hydraulic conductivity. If the hydraulic conductivity of the aquifer is low, heave and uplift will have a relatively high failure probability, but the system failure probability of piping will be very low due to the low failure probability of backward erosion. For heave and uplift only the ratio of the hydraulic conductivities of the aquifer and aquitard is important. Therefore, the hydraulic conductivity of the aquifer is on the high end of the spectrum for sand (De Vree, n.d.).

Table 3.5: Parameters base cross section for the piping model

				CS Base	
Parameter	**Unit**	**Symbol**	**PD**	**Mean**	**SD**
Hydraulic conductivity aquifer	m/s	k	L	0.0012	$6{\cdot}10^{-4}$
Hydraulic conductivity aquitard	m/s	k_h	L	$2.4{\cdot}10^{-6}$	$1.2{\cdot}10^{-6}$
Exit location (w.r.t. center of levee)	m	x_{exit}	D	2	-
Volumetric weight water	kn/m^3	γ_w	D	10	-
Saturated volumetric weight aquitard	kn/m^3	$\gamma_{sat,a}$	D	14.8	-
Model factor uplift	-	m_u	L	1.0	0.1
Critical heave gradient	-	$i_{c,h}$	L	0.5	0.1
Phreatic level exit point	$mNAP$	h_p	N	0	0.1
Seepage length	m	$L_{seepage}$	D	55	-
Volumetric weight sand grains	kn/m^3	γ_s	D	26.5	-
Bedding angle	°	θ	D	37	-
Drag factor coefficient	-	η	D	0.25	-
Kinematic viscosity water	m^2/s	ν	D	$1.33{\cdot}10^{-6}$	-
70%-fractile grain size distribution aquifer	u	d_{70}	L	$1.5{\cdot}10^{-4}$	$1.8{\cdot}10^{-5}$
Reference value d70	m	d_{70m}	D	$2.08{\cdot}10^{-4}$	-
Model factor piping	-	m_p	L	1.0	0.12

Fragility curve of the base cross section

As all parameters are known, the Probabilistic Toolkit model is used to create the fragility curve of the base cross section. The fragility curve is presented in Figure 3.11 below. The graph contains a discontinuity for a water level of $h = 9\ mNAP$. This can be explained by the applied procedure. Conditional failure probabilities are computed for water levels up to $h = 8\ mNAP$. Above this water level, extrapolation is applied to obtain the conditional failure probabilities in between $8\ mNAP \leq h \geq 9\ mNAP$. For the water levels $h > 9\ mNAP$ the conditional failure probability is set equal to one as the crest height is then exceeded by the water level.

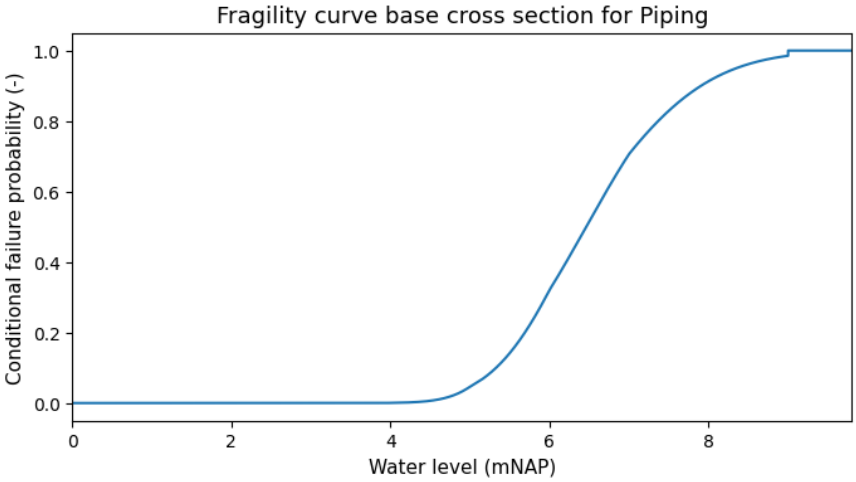

Figure 3.11: Fragility curve of the base cross section for piping

3.4 Cross section fragility curves

This section deals with steps 4 and 5 from the flowchart of Figure 3.1. Step 4 is to determine the number of dike sections. As can be seen in Table 3.1, the number of dike sections varies between 5, 10 and 15. In this research, the dike sections are assumed to be uniform. Therefore, only one representative cross section is required for every dike section. Step 5 is to compute the fragility curves of the representative cross sections for each dike trajectory. For each cross section, three fragility curves need to be computed: one for the failure mechanism inner slope stability, one for overtopping and one for piping.

The most obvious approach would be to design a new set of cross sections for every dike trajectory. This approach is very time consuming. First of all, the design of the cross sections is a labour intensive process. Furthermore, after the design of the cross sections, the three failure mechanism models should be run for every cross section. To save time, a more efficient approach is used.

In short, the method is based on two cross sections: the base cross section and a cross section of which the parameters are slightly altered with respect to the parameters of the base cross section. The slight changes are the effect of natural variability. For both cross sections, the fragility curves are computed with the failure mechanism models of section 3.3. The difference between the fragility curves of the cross sections provides an indication of the effect of natural variability in the dike parameters. This difference is used to model the fragility curves of new cross sections, without actually designing the cross sections. The exact procedure is explained below step by step.

Step 1: Design three cross sections
Design three cross sections: a base cross section, a cross section that represents small natural variability with respect to the base cross section and a dominant cross section. For all failure mechanisms, the failure probabilities of the dominant cross section are significantly higher than the failure probabilities of the base cross section. The failure probabilities of the cross section which represents small natural variability are in the same order of magnitude as the failure probabilities of the base cross section. The parameters of the base cross section are shown in Tables 3.2 until 3.5. The parameters of the cross section with small natural variability and the parameters of the dominant cross section are presented in Appendix A. The schematisations of the cross sections are presented in Figure 3.12 and Figure 3.13.

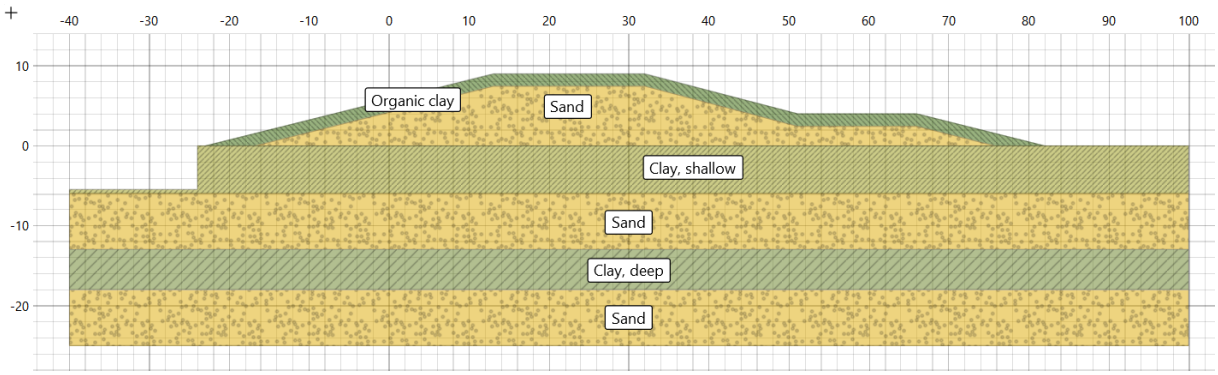

Figure 3.12: Cross section with small natural variability

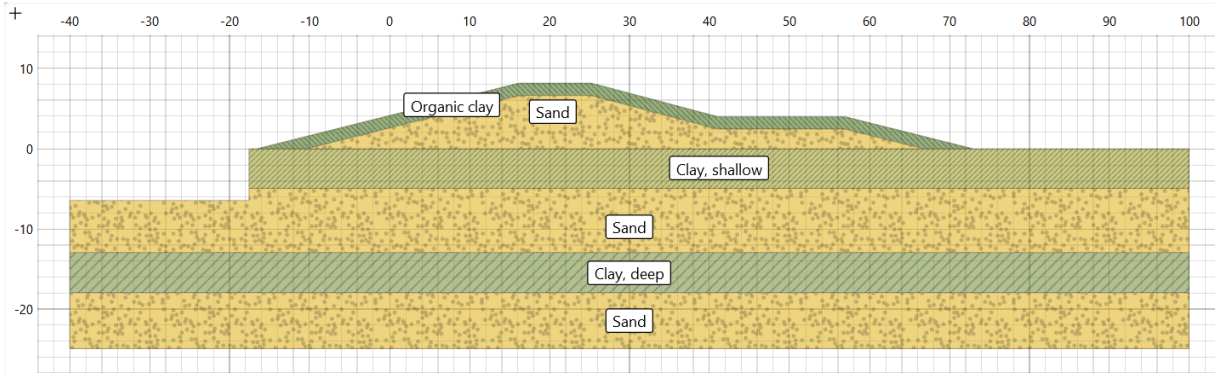

Figure 3.13: Dominant cross section

Step 2: Run the failure mechanism models
For every failure mechanism, construct the fragility curves of the cross sections designed in step 1 by running the failure mechanism models. The fragility curves are presented in Appendix B.

Step 3: Average absolute difference
Now, the fragility curves of the base cross section and the cross section with natural variability are known. These fragility curves are used to create the fragility curves of new cross sections. To do this, the first step is to compute the average absolute difference between the fragility curves of the base cross section and the fragility curves of the cross section with the natural variability. To clarify this step, the fragility curves and the difference between them are presented in Table 3.6 and Figure 3.14 for the failure mechanism piping.

Table 3.6: Difference base fragility curve and natural variability fragility curve for piping

Water level ($mNAP$)	**0**	**1**	**2**	**3**	**4**	**5**	**6**	**7**	**8**
β base cross section (-)	∞	∞	9.8	5.76	3.30	1.68	0.46	-0.54	-1.36
β natural variability cross section (-)	∞	∞	11.0	6.30	3.44	1.49	0.12	-0.89	-1.67
Difference ($diff_{h,i}$) (-)	0.0	0.0	-1.2	-0.54	-0.14	0.19	0.35	0.35	0.31

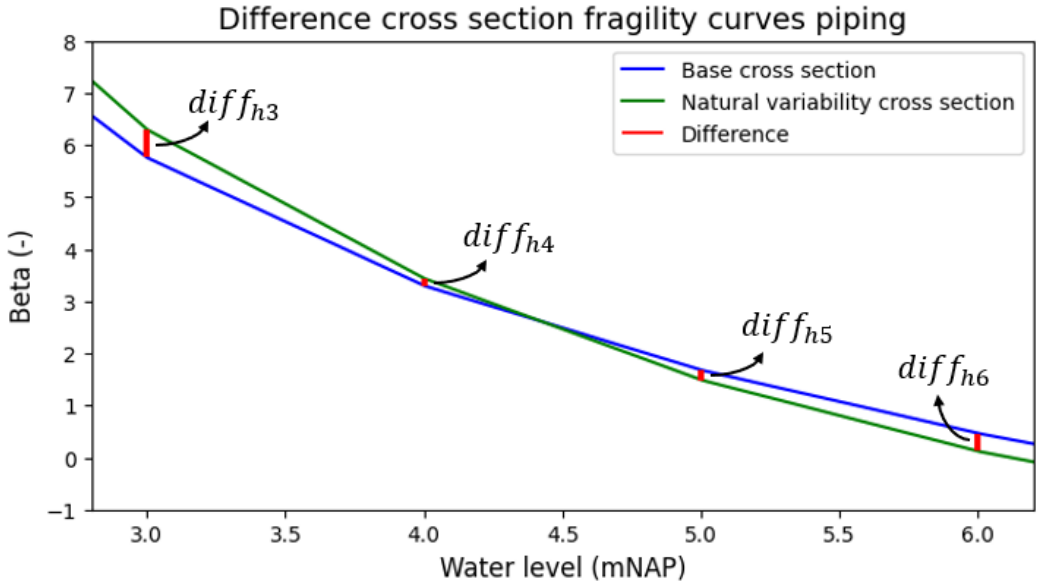

Figure 3.14: Difference base fragility curve and natural variability fragility curve for piping

The average absolute difference is computed as follows:

$$\mu_{piping} = \frac{(|diff_{h0}|+|diff_{h1}| + |diff_{h2}|+\cdots+|diff_{h8}|)}{8} = \frac{0+0+1.2+0.54+0.14+0.19+0.35+0.35+0.31}{8} = 0.34 \quad (3.25)$$

Step 4: Fragility curves new cross section

The fragility curves of a new cross section are created by taking the fragility curves of the base cross section and by adding a certain number to every point of the base fragility curves. The number that is added is a random draw from the uniform distribution with range $[-2\mu_{fm}; 2\mu_{fm}]$. Here, μ_{fm} represents the average absolute difference between the base cross section and the cross section with natural variability for one of the failure mechanisms, see equation (3.25). This way, the absolute average of the uniform distribution equals μ_{fm}. The process described above is demonstrated in Table 3.7 and Figure 3.15 for the failure mechanism piping.

Table 3.7: The method to create the fragility curve of a new cross section for piping

Water level ($mNAP$)	**0**	**1**	**2**	**3**	**4**	**5**	**6**	**7**	**8**
β base cross section (-)	∞	∞	9.80	5.76	3.30	1.68	0.46	-0.54	-1.36
Random draw uniform distribution with range $[-2\mu_{fm}; 2\mu_{fm}]$ (-)	-0.02	-0.11	0.26	-0.28	0.20	0.65	0.37	-0.67	0.06
β new cross section (-)	∞	∞	10.06	5.48	3.50	2.33	0.83	-1.21	-1.30

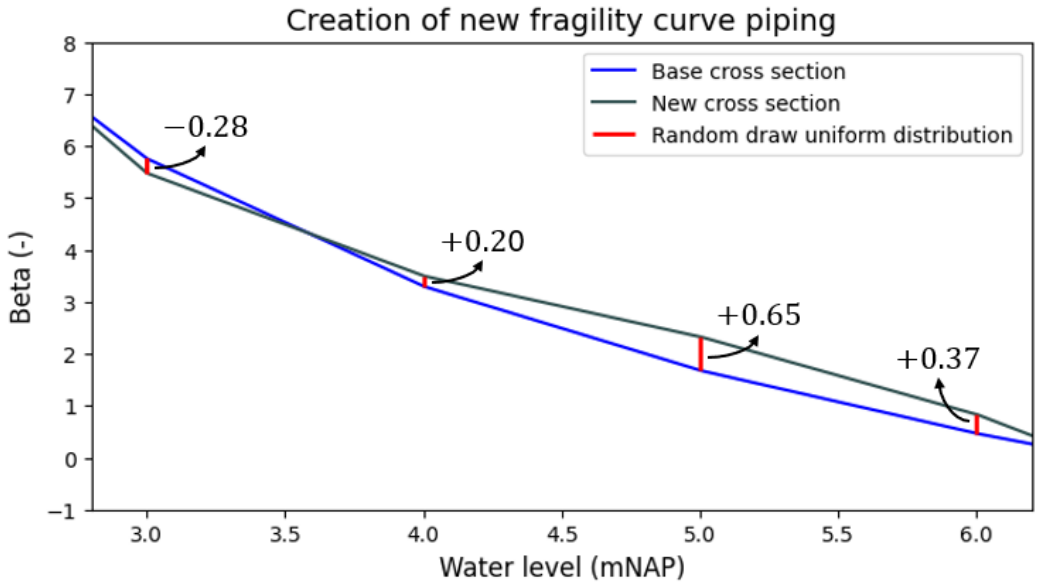

Figure 3.15: Creation of the piping fragility curve of a new cross section

Step 5: Creating the remaining fragility curves
For dike trajectories 1.1, 1.2 and 1.3 the base cross section forms the first cross section. The remaining cross sections of these trajectories are all modelled by doing step 4 for all three failure mechanisms. For every new cross section, this results in three new fragility curves: one for inner slope stability, one for overtopping and one for piping.

For dike trajectories 2.1, 2.2 and 2.3 the base cross section also forms the first cross section. The dominant cross section forms the second cross section. The fragility curves of the remaining cross sections are computed with step 4.

The method presented above yields one fragility curve per failure mechanism for all cross sections of the dike trajectory. The alternative is to design all cross sections by hand. Then, to obtain the fragility curves, the three failure mechanism models should be run for every cross section. With the more efficient method, the number of dike sections can be quickly adjusted without having to design new dike sections and without running any models. For this study it does not matter that the cross section fragility curves cannot be directly linked to a dike profile. The aim of this study is to investigate the influence of correlation in the combination of dike failure probabilities. The aim is not to model the individual failure mechanisms as accurately as possible.

3.5 Fragility curve method: from cross section to dike section

The next step is to scale up the cross section fragility curves to dike section fragility curves per failure mechanism. Due to the spatial variation of resistance parameters, the failure probability of a dike section is higher than the failure probability of one specific cross section. The longer the dike section, the higher the probability that the load exceeds the resistance at a certain location along the section. To account for this effect, the length effect factor is applied when scaling up from the cross section level to the dike section level.

It is assumed that the dike trajectory is divided into dike sections in such a way that the dike sections are uniform. Equation (2.1) computes the length effect factor according to the rules from the combination protocol of the BOI. The equation contains the factor a_l, which implies that only a part of the dike section is relevant for the failure mechanism. The equation

is designed to scale up from the cross section level to the dike trajectory level. Across the borders of a dike section, uniformity is not guaranteed. For example, it is possible that one dike section is dominant for a certain failure mechanism in a dike trajectory consisting of twenty dike sections. Then, it makes sense to apply the reduction factor a_l and equation (2.1) is applicable. However, due to the uniformity within a dike section, a different equation is used in this research to scale up from the cross section level to the dike section level. The equation is presented below (Deltares, 2021).

$$N_s = \frac{1-(1-p_{cs})^{L_{section}/b_l}}{p_{cs}} \tag{3.26}$$

In which:

- N_s = The length effect to scale up from the cross section to the dike section
- p_{cs} = The cross section failure probability
- $L_{section}$ = The length of a dike section
- b_l = A length that indicates the degree of spatial correlation

In principle, this equation divides the dike section in a number of independent parts. This number is equal to $L_{section}/b_l$. The factor b_l is a measure of the correlation length of the failure mechanism. The correlation length represents the distance over which the correlation between a certain variable has significantly reduced. Therefore, to a good approximation, the factor b_l describes the distance over which a failure mechanism can be regarded as independent. The ratio $L_{section}/b_l$ thus describes how many independent length scales fit into the dike section. Now, an independent series system is created. The equation to calculate the failure probability of a series system of n independent components is presented below.

$$P(F_{system}) = P(F_1 \cup F_2 \cup \ldots \cup F_n) = 1-(1-P(F_1))\cdot(1-P(F_2))\cdot\ldots\cdot(1-P(F_n)) \tag{3.27}$$

Filling in equation (3.27) with $n = L_{section}/b_l$ and $P(F_1) = P(F_2) = \cdots = P(F_n) = p_{cs}$ yields the top of equation (3.26). For inner slope stability the factor b_l has a value of $b_{l,ISS} = 50\ m$ and for piping the factor has a value of $b_{l,Piping} = 300\ m$. With a dike section length of $L_{section} = 500\ m$, this means the section is divided into $n_{ISS} = 10$ independent parts for inner slope stability and into $n_{Piping} = 1.67$ independent parts for piping. To apply the dike section length effect factor, the fragility curves are first converted into conditional failure probabilities. Then the length effect factor is applied to every single conditional failure probability of the fragility curves. This procedure is demonstrated for a simple dike trajectory consisting of only three dike sections. Table 3.8 contains the cross section fragility curves for the failure mechanism piping. The fragility curves are plotted in Figure 3.16.

Table 3.8: Cross section fragility curves for piping example

Water level ($mNAP$)	**0**	**1**	**2**	**3**	**4**	**5**	**6**	**7**	**8**
$p_{Cross\ section\ 1}\|h$	0.0	0.0	0.0	0.0	0.0005	0.0465	0.3210	0.7064	0.9131
$p_{Cross\ section\ 2}\|h$	0.0	0.0	0.0	0.0	0.0020	0.0222	0.2878	0.7427	0.9405
$p_{Cross\ section\ 3}\|h$	0.0	0.0	0.0	0.0	0.0015	0.0270	0.1818	0.5444	0.8954

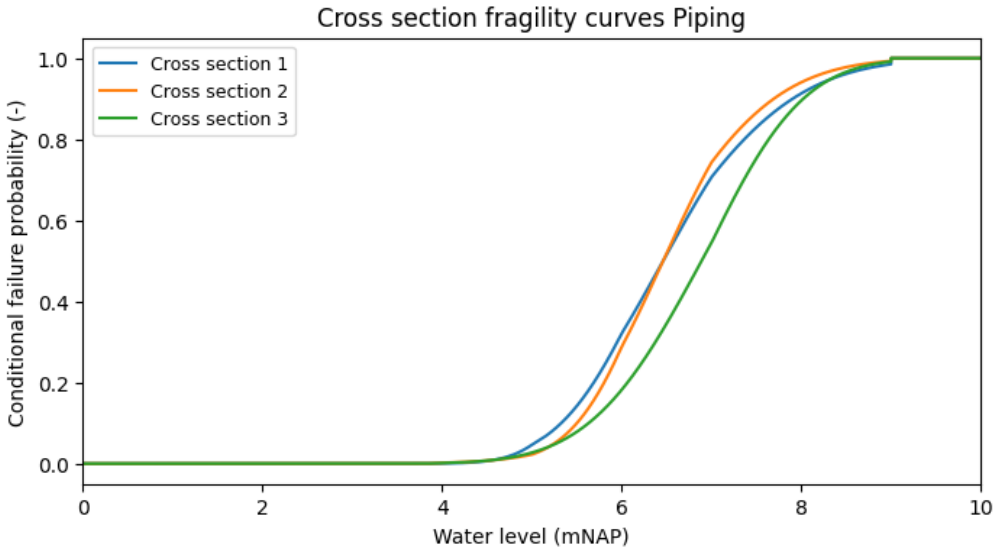

Figure 3.16: Cross section fragility curves for piping example

Table 3.9 and Figure 3.17 show how the length effect factor is applied. In this example the length of the dike section is $L_{section} = 1000\ m$. For piping the factor b_l has a value of $b_{l,Piping} = 300\ m$. For clarity reasons, the upscaling is only shown for dike section 1 in Figure 3.17.

Table 3.9: Dike section fragility curves for piping example

Water level ($mNAP$)	**0**	**1**	**2**	**3**	**4**	**5**	**6**	**7**	**8**
$\boldsymbol{p_{Section\ 1}\|h}$	$p_{s1} = N \cdot p_{cs1}\|h_0 = 1-(1-p_{cs1}\|h_0)^{L_{section}/b_l} = 1-(1-0.0)^{3.33} = 0$	0.0	0.0	0.0	0.0016	0.1467	0.7248	0.9832	0.9997
$\boldsymbol{p_{Section\ 2}\|h}$	$p_{s2} = N \cdot p_{cs2}\|h_0 = 1-(1-p_{cs2}\|h_0)^{L_{section}/b_l} = 1-(1-0.0)^{3.33} = 0$	0.0	0.0	0.0	0.0066	0.0720	0.6774	0.9892	0.9999
$\boldsymbol{p_{Section\ 3}\|h}$	$p_{s3} = N \cdot p_{cs3}\|h_0 = 1-(1-p_{cs3}\|h_0)^{L_{section}/b_l} = 1-(1-0.0)^{3.33} = 0$	0.0	0.0	0.0	0.0051	0.0873	0.4877	0.9272	0.9995

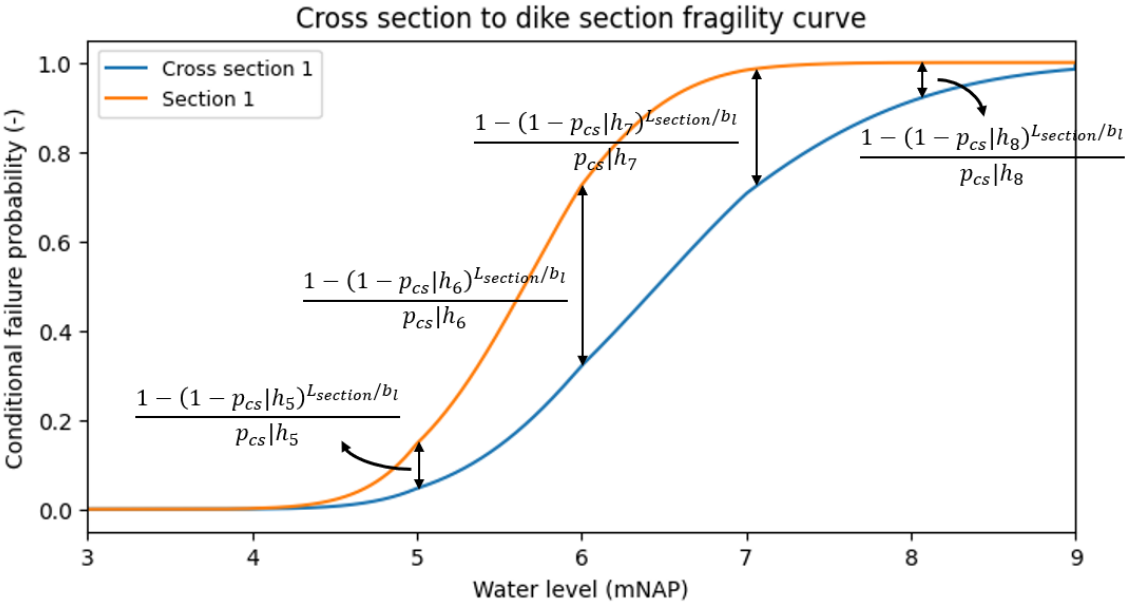

Figure 3.17: Application of length effect factor to cross section fragility curve

3.6 Fragility curve method: from dike section to trajectory

3.6.1 General approach

The goal of the fragility curve method is to obtain the total dike trajectory failure probability. This still requires three steps. The first step is to combine the dike section fragility curves per failure mechanism into the dike trajectory fragility curves per failure mechanism. The second step consists of combining the dike trajectory fragility curves per failure mechanism into the total dike trajectory fragility curve. In the last step, the total dike trajectory fragility curve and the probability distribution of the water level are used to compute the dike trajectory failure probability.

The fragility curve method considers correlation in the computation of the dike trajectory failure probability through the combination of fragility curves. As explained in sections 3.4 and 3.5, three fragility curves are computed for every dike section. For all fragility curves, the conditional parameter is the water level. The water level is assumed to be the same along the entire dike trajectory. Furthermore, it is assumed that the water level lasts long enough to infiltrate in the dike body and lead to the phreatic line presented in Figure 3.5. Finally, the time dependency of piping is neglected. Because of these assumptions, the water level is the same for all dike sections and for all failure mechanisms. Therefore, the water level is assumed to be fully correlated. All other parameters are assumed to be independent. This assumption of independence can be justified. Take the inner slope stability failure mechanism for example. Except for the water level, the only stochastic variables are soil parameters. Soil parameters have a high spatial variability and can therefore be assumed to be independent on the scale of dike sections. In the next part of this section it is explained how fragility curves are combined in the fragility curve method.

3.6.2 From dike section to trajectory per failure mechanism

By taking the water level as the conditional variable, the water level becomes a deterministic variable in the computation of the conditional failure probabilities of the fragility curves. As mentioned before, the remaining stochastic variables are assumed independent between dike sections. This has consequences for the combination of dike section fragility curves into the dike trajectory fragility curves per failure mechanism. For every water level, the associated conditional failure probabilities of the dike sections can be seen as a series system of independent components. So, for every water level, the conditional dike trajectory failure probability per failure mechanism is computed with equation (*3.27*). This gives the following equation:

$$P\left(F_{track,fm\,i}|h\right) = 1 - \left(1 - P\left(F_{s1,i}|h\right)\right) \cdot \left(1 - P\left(F_{s2,i}|h\right)\right) \cdot \ldots \cdot \left(1 - P\left(F_{sn,i}|h\right)\right) \qquad (3.28)$$

In which:

- $P\left(F_{track,fm\,i}|h\right)$ = Conditional dike trajectory failure probability for failure mechanism i
- $P\left(F_{sj,i}|h\right)$ = Conditional failure probability for dike section j and failure mechanism i

The above procedure is illustrated in Table 3.10 and Figure 3.18 for the piping example of the previous section.

Table 3.10: The step from dike section fragility curves to the dike trajectory fragility curve for piping

Water level (m)	0	1	2	3	4	5	6	7	8
Section 1	0.0	0.0	0.0	0.0	0.0016	0.1467	0.7248	0.9832	0.9997
Section 2	0.0	0.0	0.0	0.0	0.0066	0.0720	0.6774	0.9892	0.9999
Section 3	0.0	0.0	0.0	0.0	0.0051	0.0873	0.4877	0.9272	0.9995
Trajectory	$1-(1-p_{s1}\|h_0)\cdot(1-p_{s2}\|h_0)\cdot(1-p_{s3}\|h_0) = 1-(1-0.0)\cdot(1-0.0)\cdot(1-0.0) = 0.0$	0.0	0.0	0.0	0.0132	0.2773	0.9545	1.000	1.000

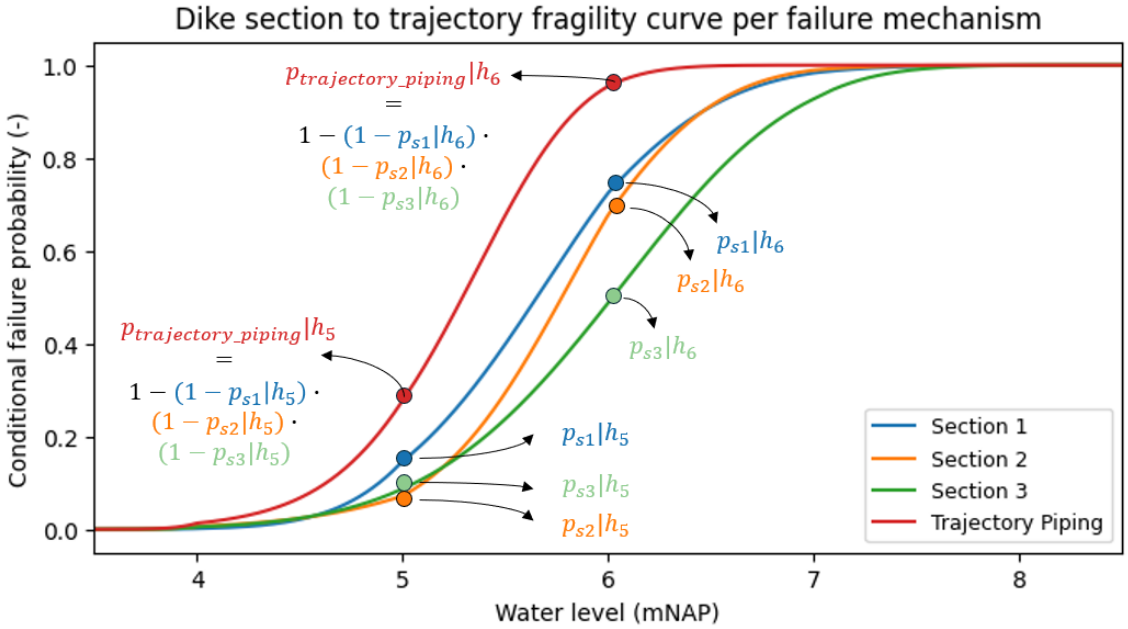

Figure 3.18: The step from dike section fragility curves to the dike trajectory fragility curve for piping

3.6.3 From dike trajectory per failure mechanism to total trajectory

All variables of the failure mechanism models except for the water level are also assumed independent between different failure mechanisms. Therefore, the same procedure can be applied that is used for the combination of the dike section fragility curves into the dike trajectory fragility curves per failure mechanism. This gives the following equation:

$$P(F_{track}|h) = 1-\left(1-P\left(F_{track,fm1}|h\right)\right)\cdot\left(1-P\left(F_{track,fm2}|h\right)\right)\cdot\ldots \cdot\left(1-P\left(F_{track,fm\,n}|h\right)\right) \tag{3.29}$$

In which:

- $P(F_{track}|h)$ = Conditional dike trajectory failure probability

The final step is to use the total dike trajectory fragility curve to compute the failure probabilty. Equation (2.43) is used for this computation. So, the failure probability is computed by multiplying the probability density function of the water level with the conditional failure probabilities from the fragility curve and by consequently integrating over the water level. To obtain the yearly failure probability, the water level distribution should represent the probability of occurrence of the yearly maxima. Therefore, the water level is modelled with a Gumbel distribution. When two water levels and the corresponding return periods are known, the parameters of the Gumbel distribution can be deduced. Hydra-NL is used to obtain the 10-year

and 30-year return water levels at the coast of the Dutch city Vlissingen. The probability density function of the Gumbel distribution is presented below in equation (3.30).

$$f(h) = \frac{1}{\beta} e^{-(z+e^{-z})}, \quad z = \frac{h-\mu}{\beta} \tag{3.30}$$

A 10-year return water level of $3.841\ mNAP$ and a 30-year return water level of $4.113\ mNAP$ result in $\mu = 2.32$ and $\beta = 0.5$. The application of equation (2.43) is visualised in Figure 3.19. Figure 3.19a) shows the conditional failure probability of the dike trajectory. The probability distribution of the water level is plotted in Figure 3.19b). Figure 3.19c) shows the product of the conditional failure probability of the dike trajectory and the probability distribution of the water level. Integrating this grapgh yields the total dike trajectory failure probability.

This procedure can also be applied to other fragility curves. For example, if the cross section fragility curve for piping is used, the result of the computation is the cross section failure probability for piping.

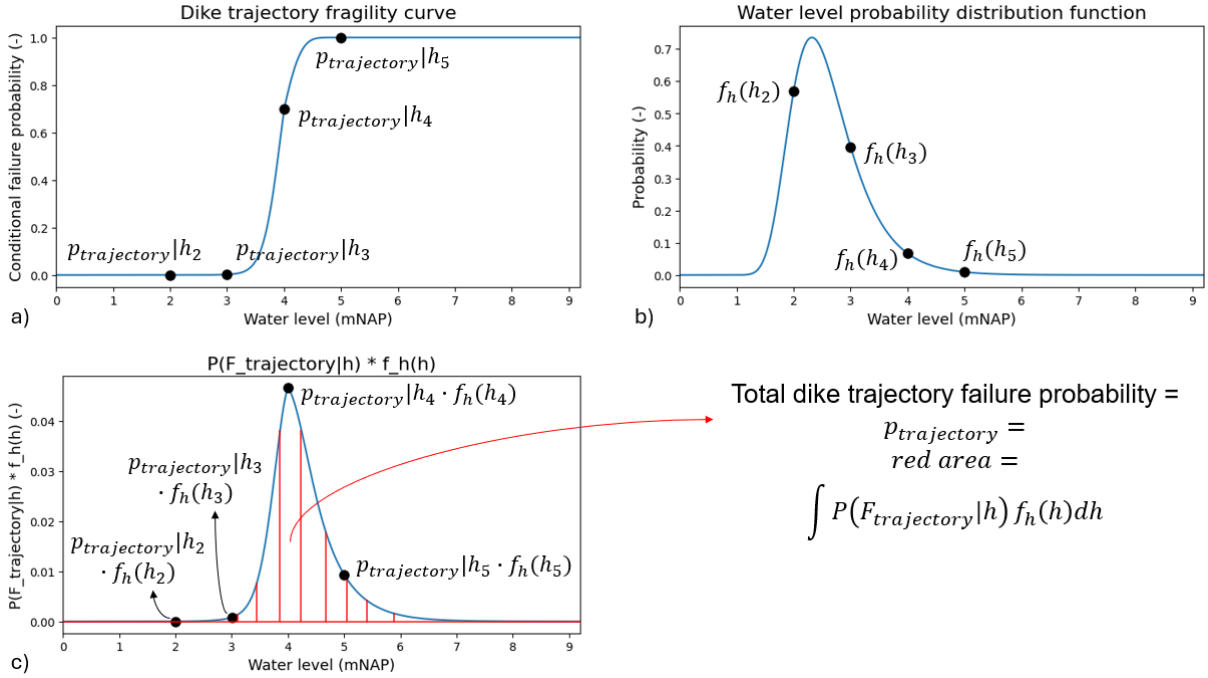

Figure 3.19: The computation of the total dike trajectory failure probability from the dike trajectory fragility curve

4. Large scale application

In chapter 3, the methodology of this research is explained. The goal of the research is to compare the dike safety assessment of the fragility curve method with the assessment from the combination protocol of the BOI. To this end, six different dike trajectories are modelled, see Table 3.1. The dike safety assessment methods are both applied to all of these dike trajectories to test how they perform under different circumstances. The dike sections of dike trajectories 1.1, 1.2 and 1.3 only vary slightly with respect to each other. The difference between these trajectories is the number of uniform dike sections. Dike trajectories 2.1, 2.2 and 2.3 have in common that one of the dike sections of these trajectories is significantly weaker than the other dike sections for all failure mechanisms. Again, the difference between these dike trajectories is that they consist of different numbers of dike sections.

In this chapter, the results are presented of the methodology of chapter 3. First of all, in section 4.1 the cross section fragility curves are presented along with the corresponding cross section failure probabilities. Sections 4.2 and 4.3 focus on the results of the fragility curve method. Section 4.2 deals with the upscaling from the cross section fragility curves to the dike section fragility curves. In section 4.3, the dike section fragility curves per failure mechanism are scaled up to the total dike trajectory fragility curve. Consequently, this fragility curve is used to compute the total trajectory failure probability. In section 4.4, the results of the combination protocol are presented and compared with the results of the fragility curve method. Section 4.5 provides a sensitivity analysis to get a deeper understanding of the fragility curve method and how it compares to the combination protocol.

4.1 Cross section failure probabilities

As mentioned before, the dike sections are assumed to be uniform. Therefore, every dike section can be modelled with one representative cross section. In this section, the fragility curves are presented of the representative cross sections for the failure mechanisms inner slope stability, overtopping and piping.

Instead of designing every cross section of the different dike trajectories by hand, a more efficient method is applied. Two cross sections are designed, the base cross section and a cross section of which the parameters are slightly different due to natural variation. These cross sections are put into the failure mechanism models to obtain the cross section fragility curves. The difference between the fragility curves of the base cross section and the fragility curves of the cross section with natural variability is used to compute the fragility curves of new cross sections.

Results

The cross section fragility curves of dike trajectories 1.1 and 2.1 are presented in Figures 4.1 until 4.6. These figures also contain the dike section and dike trajectory fragility curves per failure mechanism. The cross section fragility curves of the other trajectories are added to Appendix C. Furthermore, equation (2.43) is applied to compute the cross section failure probabilities from the cross section fragility curves. For dike trajectories 1.1 and 2.1 the cross section failure probabilities are presented in Table 4.1 and Table 4.2, respectively. The cross section failure probabilities of the remaining trajectories are added to Appendix D.

Trajectory 1.1: Rather uniform trajectory consisting of 5 dike sections

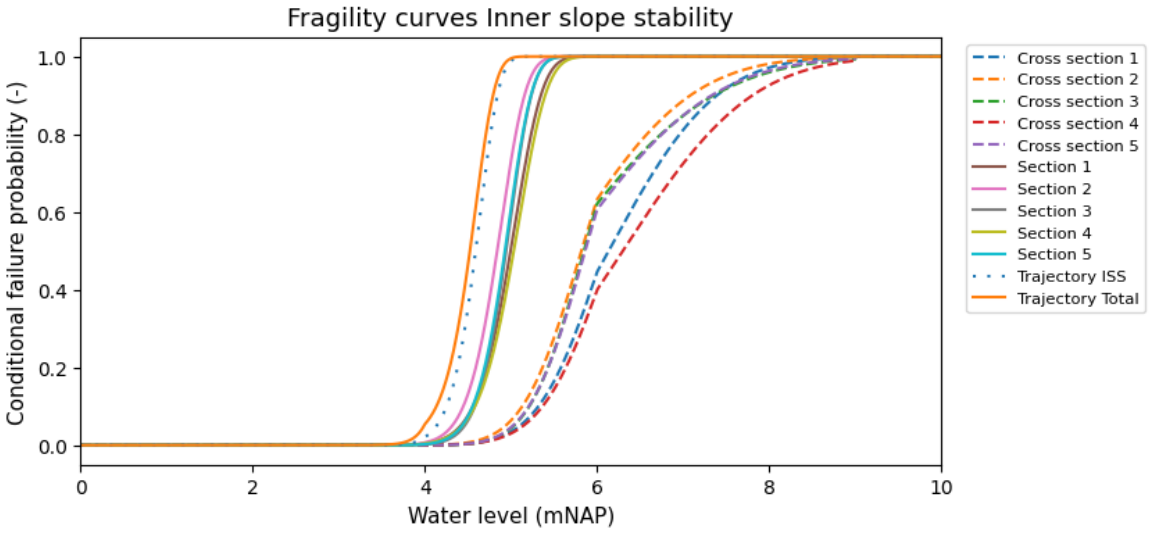

Figure 4.1: Fragility curves inner slope stability dike trajectory 1.1

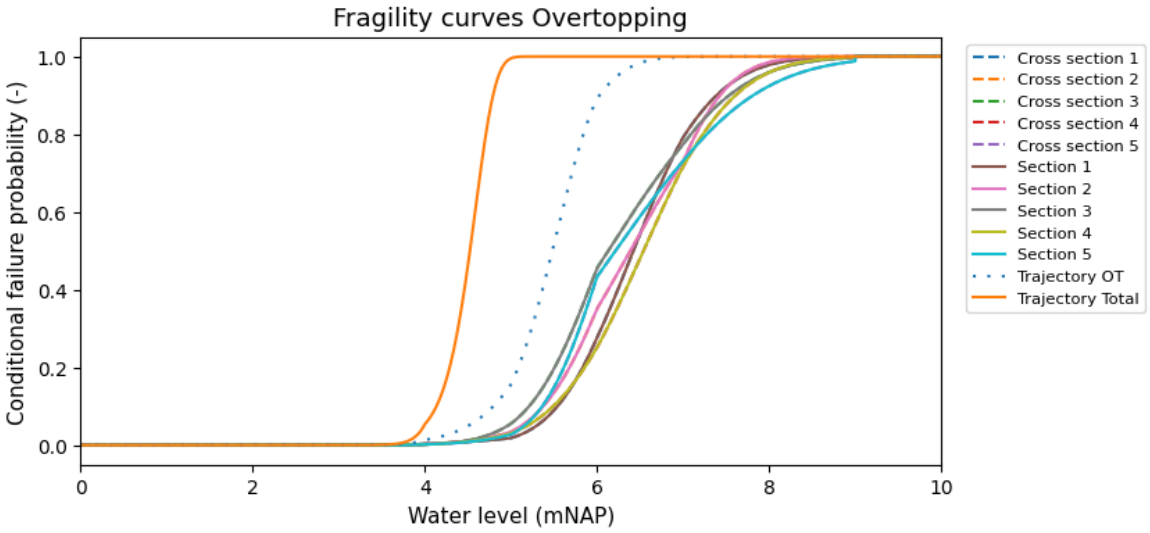

Figure 4.2: Fragility curves overtopping dike trajectory 1.1

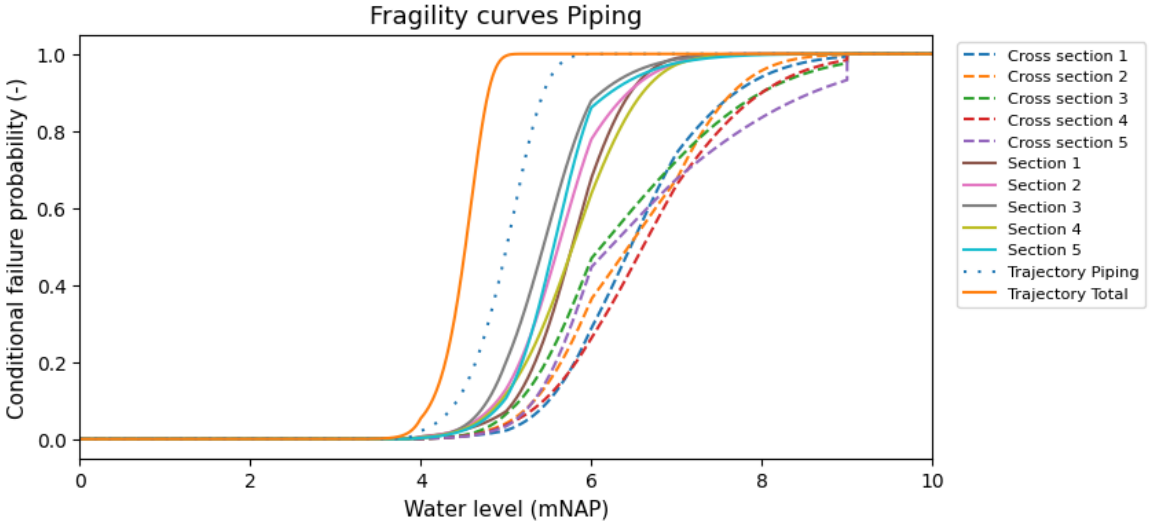

Figure 4.3: Fragility curves piping dike trajectory 1.1

Table 4.1: Cross section failure probabilities dike trajectory 1.1

	Inner slope stability	Overtopping	Piping
Cross section 1	0.0011	0.0009	0.0008
Cross section 2	0.0016	0.0011	0.0011
Cross section 3	0.0013	0.0014	0.0014
Cross section 4	0.0009	0.0009	0.0009
Cross section 5	0.0014	0.0011	0.0011

Figures 4.1 until 4.3 present the fragility curves for a rather uniform dike trajectory which consists of 5 dike sections. As you can see, the dike section fragility curves lie left of the cross section fragility curves for the failure mechanisms inner slope stability and piping due to the application of the dike section length effect factor. For overtopping, the cross section fragility curves are equal to the dike section fragility curves, as the dike section length effect factor of overtopping is equal to 1. The figures also show the combination of the dike section fragility curves into the dike trajectory fragility curve per failure mechanism. Again, this step results in a shift to the left and makes the fragility curve steeper.

An interesting difference between the failure mechanisms is the distance between the dike section fragility curves and the dike trajectory fragility curve. For inner slope stability, the dike trajectory fragility curve lies the closest to the dike section fragility curves, then for piping and then for overtopping. The closer the dike trajectory fragility curve lies to the maximum dike section fragility curve, the higher the correlation. This is further explained in section 4.3, in which the correlation is also quantified.

Trajectory 2.1: Trajectory consisting of 5 dike sections of which one is dominant

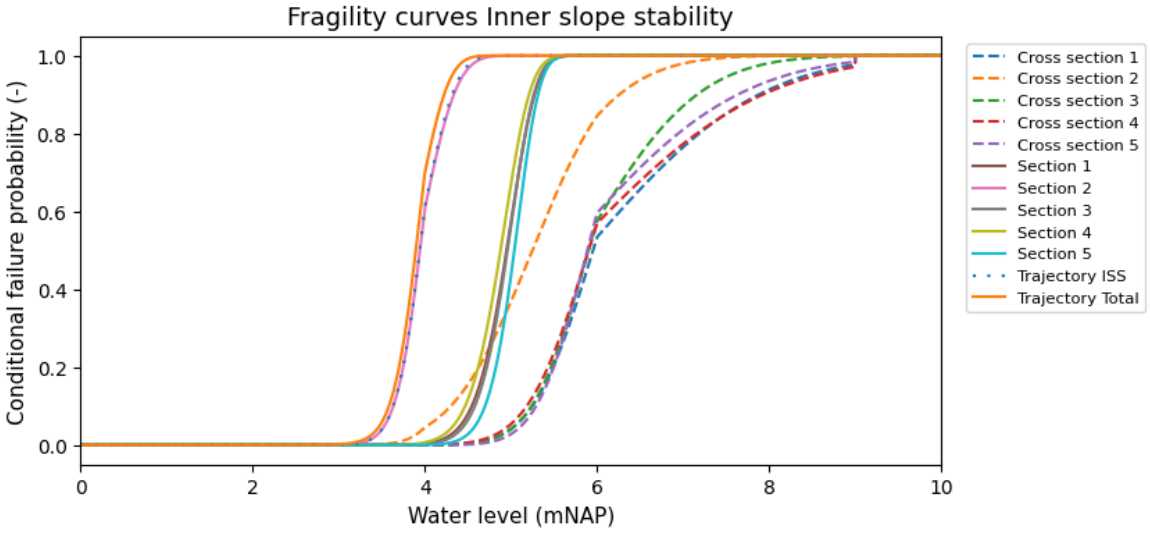

Figure 4.4: Fragility curves inner slope stability dike trajectory 2.1

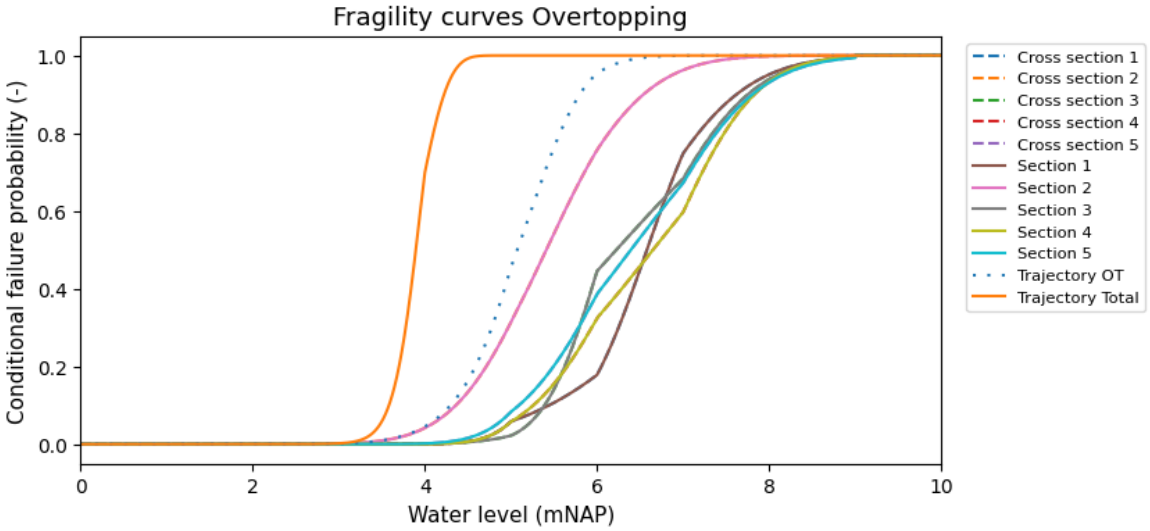

Figure 4.5: Fragility curves overtopping dike trajectory 2.1

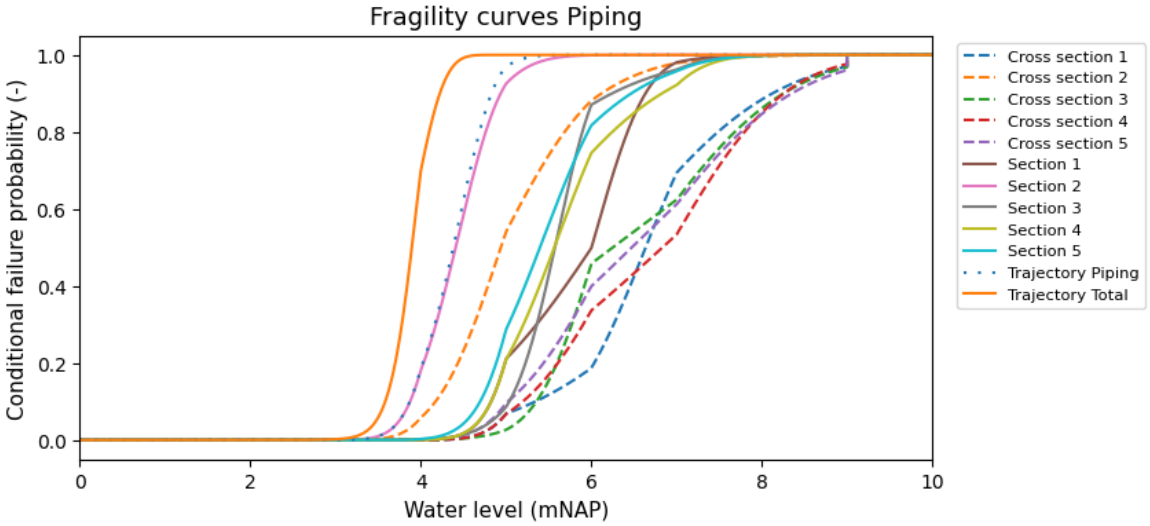

Figure 4.6: Fragility curves piping dike trajectory 2.1

Table 4.2: Cross section failure probabilities dike trajectory 2.1

	Inner slope stability	Overtopping	Piping
Cross section 1	0.0012	0.0009	0.0009
Cross section 2	0.0072	0.0074	0.0097
Cross section 3	0.0013	0.0010	0.0010
Cross section 4	0.0014	0.0010	0.0011
Cross section 5	0.0011	0.0015	0.0015

Figures 4.4 until 4.6 present the fragility curves for a dike trajectory which consists of 5 dike sections of which one section is dominant. For every failure mechanism, the dominant cross section and dike section fragility curve clearly lie further to the left of the other cross section and dike section fragility curves, respectively.

For every failure mechanism, the distance between the dike section fragility curves and the dike trajectory fragility curve has decreased with respect to the uniform dike trajectory. This means that the correlation between the dike sections is higher for the dike trajectory with a dominant dike section.

4.2 Fragility curve method: from cross section to dike section

In this section the cross section fragility curves are scaled up to dike section fragility curves per failure mechanism. Due to the spatial variation of both load and resistance parameters, the failure probability of a dike section is higher than the failure probability of one specific cross section. To account for this, a length effect factor is applied when scaling up from the cross section level to the dike section level.

Due to the uniformity of the dike sections, the length effect factor of equation (3.26) is used. This length effect factor divides the dike sections in smaller parts that can be regarded as independent with respect to each other. The length scale of the smaller parts depends on the spatial correlation of the failure mechanism.

Results

The dike section fragility curves of dike trajectories 1.1 and 2.1 are plotted in Figures 4.1 until 4.6. The dike section fragility curves of the remaining trajectories are added to Appendix C. In these figures, one can clearly observe the shift between the cross section and dike section fragility curves for the failure mechanisms inner slope stability and piping. The dike section failure probabilities of dike trajectories 1.1 and 1.2 are presented in Table 4.3 and Table 4.4, respectively. The dike section failure probabilities of the remaining trajectories are added to Appendix E.

Table 4.3: Dike section failure probabilities for dike trajectory 1.1

	Inner slope stability	Overtopping	Piping
Section 1	0.0062	0.0009	0.0021
Section 2	0.0080	0.0011	0.0027
Section 3	0.0063	0.0014	0.0033
Section 4	0.0058	0.0009	0.0023
Section 5	0.0066	0.0011	0.0025

Table 4.4: Dike section failure probabilities for dike trajectory 2.1

	Inner slope stability	Overtopping	Piping
Section 1	0.0065	0.0009	0.0023
Section 2	0.0420	0.0074	0.0210
Section 3	0.0062	0.0010	0.0023
Section 4	0.0076	0.0010	0.0027
Section 5	0.0051	0.0015	0.0037

For the failure mechanisms inner slope stability and piping, the dike section failure probabilities have increaed with respect to the cross section failure probabilities. For overtopping, the dike section failure probabilities are equal to the cross section failure probabilities. Again, this can be explained by the dike section length effect factor. For example, for section 1 the dike section length effect factor for inner slope stability is $N_{s,ISS} = 19.8$ and for piping it is $N_{s,Piping} = 3.3$. These length effect factors are computed with equation (3.26). As overtopping is fully correlated in space and the dike sections are uniform, the dike section length effect factor for overtopping is equal to $N_{s,OT} = 1$.

Inner slope stability has the highest failure probability, then piping and then overtopping. Another observation from the tables above is that the failure probabilities of the dominant dike

section are almost one order of magnitude higher than the failure probabilities of the other dike sections.

4.3 Fragility curve mehtod: from dike section to trajectory

4.3.1 From dike section to trajectory per failure mechanism

In this subsection, the dike section fragility curves per failure mechanism are combined into the dike trajectory per failure mechanism. The fragility curve method assumes that the water level is fully correlated between dike sections and that the other parameters are independent. Therefore, for every water level, the conditional dike section failure probabilities can be regarded as an independent series system. The results of the combination of the dike section fragility curves are presented below. Next to the dike section failure probabilities and the dike trajectory failure probabilities per failure mechanism, the tables of this subsection also contain three rows named 'Lower bound, 'Upper bound' and 'Correlation scale'. The 'Upper bound' row presents the sum of the dike section failure probabilities per failure mechanism and the 'Lower bound' row presents the maximum of these probabilities.

According to probability theory, the system failure probability of a series system is bounded by the maximum and the sum of the component failure probabilities. The maximum component failure probability forms the lower bound of the system failure probability and occurs if the components are fully positively correlated. The sum of the components forms the upper bound and occurs if the components are fully negatively correlated. For any correlation in between full positive or full negative correlation, the system failure probability lies somewhere in between the upper and the lower bound.

The correlation scale is a linear scale that indicates where the system failure probability lies with respect to the lower and upper bound. Since the lower bound represents full positive correlation, the correlation scale is higher if the computed system failure probabilities lie closer to the lower bound. The equation for the correlation scale is presented below. The numerator and denominator of equation (4.1) are visualized in Figure 4.7.

$$Correlation\ scale = \frac{Upper\ bound - p_{fragility\ curve\ method}}{Upper\ bound - Lower\ bound} \cdot 100\% = \frac{Sum - p_{fragility\ curve\ method}}{Sum - Max} \cdot 100\% \quad (4.1)$$

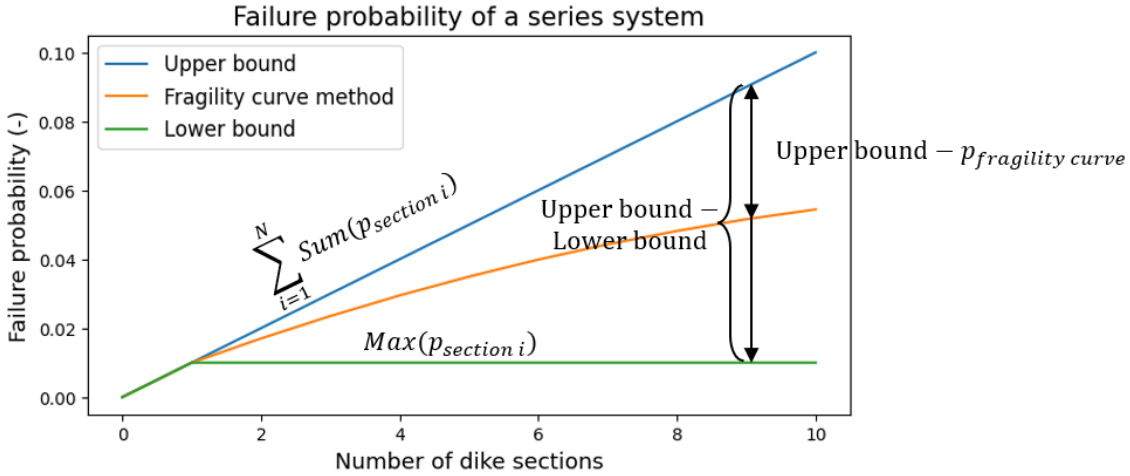

Figure 4.7: Visualization of the elements of the correlation scale

For the step from the dike section level to the dike trajectory level per failure mechanism, the system is the dike trajectory per failure mechanism and the components are the dike sections per failure mechanism. Since the correlation in the water level is taken into account, the dike trajectory failure probabilities per failure mechanism are expected to lie somewhere in between the upper and the lower bound.

Results

For dike trajectories 1.1 and 2.1 the dike section fragility curves per failure mechanisms and the resulting dike trajectory fragility curves per failure mechanism are presented in Figures 4.1 until 4.6 of section 4.1. The corresponding failure probabilities are shown in Table 4.5 and Table 4.6. For the remaining trajectories, the fragility curves are added to Appendix C and the corresponding failure probabilities are presented in the tables of Appendix E.

Table 4.5: Combination of dike section failure probabilities for dike trajectory 1.1

	Inner slope stability	Overtopping	Piping
Section 1	0.0062	0.0009	0.0021
Section 2	0.0080	0.0011	0.0027
Section 3	0.0063	0.0014	0.0033
Section 4	0.0058	0.0009	0.0023
Section 5	0.0066	0.0011	0.0025
Dike trajectory - Fragility curve method	0.0126	0.0037	0.0071
Upper bound (Sum)	0.0329	0.0054	0.0129
Lower bound (Max)	0.0080	0.0014	0.0033
Correlation scale	81.69	42.66	60.24

Table 4.6: Combination of dike section failure probabilities for dike trajectory 2.1

	Inner slope stability	Overtopping	Piping
Section 1	0.0065	0.0009	0.0023
Section 2	0.0420	0.0074	0.0210
Section 3	0.0062	0.0010	0.0023
Section 4	0.0076	0.0010	0.0027
Section 5	0.0051	0.0015	0.0037
Dike trajectory - Fragility curve method	0.0423	0.0091	0.0219
Upper bound (Sum)	0.0675	0.0118	0.0321
Lower bound (Max)	0.0420	0.0074	0.0210
Correlation scale	98.76	60.96	92.46

The above tables quantify what is already observed in the fragility curves of section 4.1. As can be seen, all dike trajectory failure probabilities lie well in between the theoretical upper and lower bound, resulting in relatively high values of the correlation scale. The correlation scale is highest for inner slope stability, then for piping and then for overtopping. Due to the high spatial correlation of overtopping, one would expect the correlation scale of overtopping to be the highest. However, this is not the case, as the fragility curve only considers the correlation in the water level. The correlation between other important parameters for overtopping, like the wind speed, is neglected. In the D-Stability model, the water level has a high influence on the failure probability, leading to high values of the correlation scale for inner slope stability.

Besides the failure mechanism models, the dike section length effect factor also contributes to the fact that the correlation scale is the highest for inner slope stability, then for piping and then

for overtopping. Inner slope stability has the highest length effect factor. This factor shifts the fragility curve to the left and makes it steeper, see Figure 3.17. When steep fragility curves are combined with the method explained in Figure 3.18, the new fragility curve lies closer to the original fragility curves than when fragility curves are combined with a gentle slope, see Figure 4.8. Therefore, the correlation scale is higher for the combination of steep fragility curves.

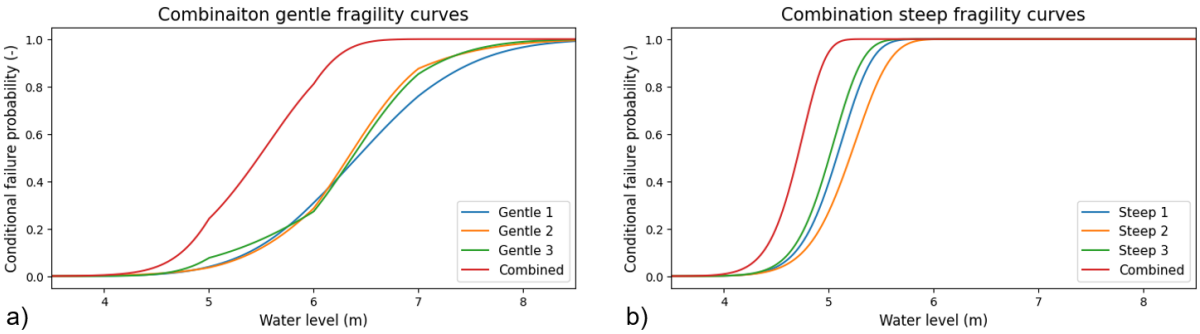

Figure 4.8: Comparison of the combination of a) gentle and b) steep fragility curves

For the dike trajectories with a dominant dike section, the correlation scale between the dike sections reaches values of more than 90% for inner slope stability and piping. This means the dike sections are almost regarded as fully correlated and the resulting dike trajectory failure probabilities for inner slope stability and piping are almost equal to the maximum dike section failure probabilities.

For all failure mechanisms, the correlation scale is higher for the dike trajectory with a dominant dike section. In other words, the presence of the dominant dike section increases the correlation.

4.3.2 From dike trajectory per failure mechanism to total trajectory

In this subsection the dike trajectory fragility curves per failure mechanism are combined into the total dike trajectory fragility curve. Consequently, the total dike trajectory failure probability is computed from the total dike trajectory fragility curve and the probability distribution of the water level. The fragility curve method assumes that the water level is fully correlated between the failure mechanisms and that all other parameters are independent. Hence, for every water level, the conditional dike trajectory failure probabilities per failure mechanism can be regarded as an independent series system. The results of the combination of the dike trajectory fragility curves per failure mechanism are presented below.

Results

For dike trajectories 1.1 and 2.1 the dike trajectory fragility curves per failure mechanism and the total dike trajectory fragility curve are plotted in Figure 4.9 and Figure 4.10, respectively. For the remaining trajectories, the fragility curves are presented in Appendix C.

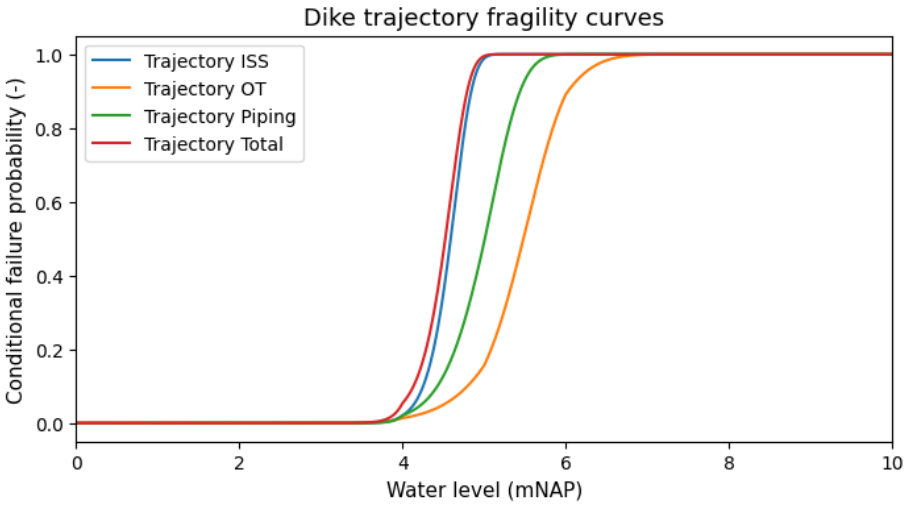

Figure 4.9: Dike trajectory fragility curves dike trajectory 1.1

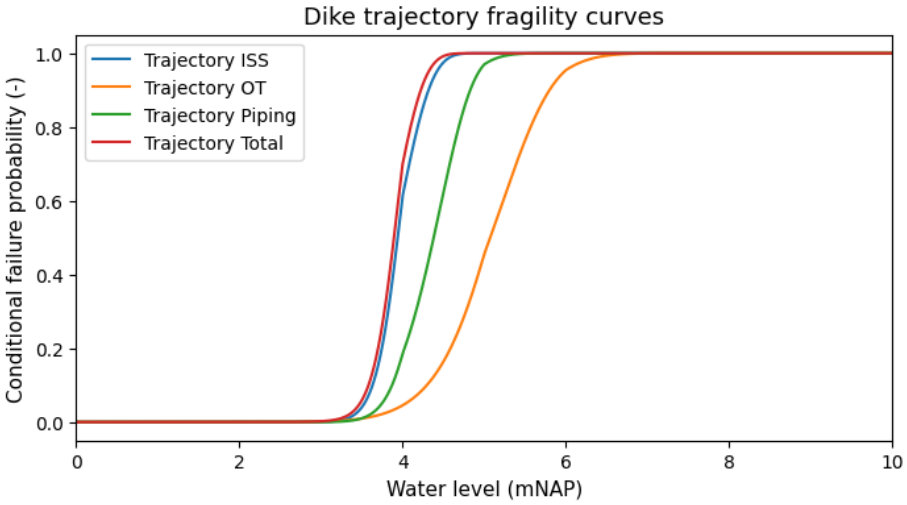

Figure 4.10: Dike trajectory fragility curves dike trajectory 2.1

For the rather uniform dike trajectory and for the trajectory with a dominant dike section, the final fragility curve of the dike trajectory lies really close to the dike trajectory fragility curve for inner slope stability. Therefore, the dike trajectory failure probability lies close to the maximum component failure probability, which implies that the correlation between the failure mechanisms is relatively high. The correlation is quantified in Tables 4.7 and 4.8.

For dike trajectories 1.1 and 2.1, the step from the dike trajectory failure probabilities per failure mechanism to the total dike trajectory failure probability is presented in Table 4.7 and Table 4.8, respectively. For the remaining trajectories, this step is shown in the tables of Appendix F.

Table 4.7: Combination of dike trajectory failure probabilities per failure mechanism for trajectory 1.1

	Failure probability
Trajectory failure probability for inner slope stability	0.0126
Trajectory failure probability for overtopping	0.0037
Trajectory failure probability for piping	0.0071
Total trajectory failure probability - Fragility curve method	0.0150
Upper bound (Sum)	0.0233
Lower bound (Max)	0.0126
Correlation scale	77.66

Table 4.8: Combination of dike trajectory failure probabilities per failure mechanism for trajectory 2.1

	Failure probability
Trajectory failure probability for inner slope stability	0.0423
Trajectory failure probability for overtopping	0.0091
Trajectory failure probability for piping	0.0219
Total trajectory failure probability - Fragility curve method	0.0475
Upper bound (Sum)	0.0733
Lower bound (Max)	0.0423
Correlation scale	83.21

These tables provide a numerical presentation of what is already shown in the fragility curves of Figures 4.9 and 4.10. The total dike trajectory fragility curve lies very close to the dike trajectory fragility curve for inner slope stability. This means the total trajectory failure probability lies relatively close to the theoretical lower bound, resulting in a correlation scale of around 80%.

In case of a dominant dike section, the trajectory failure probabilities per failure mechanism and the total dike trajectory failure probability are significantly higher (approximately three times as high). However, the correlation scale, indicating the correlation between the failure mechanisms, is only 6% higher for the trajectory with a dominant dike section.

This can be explained by the fact that all dike trajectory failure probabilities per failure mechanism are approximately equally higher for the dike trajectory with a dominant dike section, compared to the more uniform trajectory. Therefore, the dike trajectory fragility curves per failure mechanism all shift to the left by almost the same amount. The combination of these fragility curves into the total dike trajectory fragility curve therefore does not result in a significant change of the correlation scale.

4.4 Comparison with the combination protocol

For the BOI and the WBI2017 cross section failure probabilities are scaled up the total dike trajectory failure probability by applying the guidelines of the combination protocol. In this section, the combination protocol is applied to the cross section failure probabilities of the six dike trajectories of Table 3.1 and the results are compared with the fragility curve method.

4.4.1 From cross section to dike trajectory per failure mechanism

As a starting point, the combination protocol requires the cross section failure per failure mechanism. The cross section failure probabilities are computed by applying equation (2.43) to the cross section fragility curves of section 4.1. The combination protocol is schematized in the flow chart of Figure 3.3. To compute the dike trajectory failure probability per failure mechanism, the combination protocol applies the following steps:

1. First compute the dike section failure probabilities by multiplying the cross section failure probabilities with the dike section length effect factor. Then, compute the dike trajectory failure probabilities per failure mechanism by assuming the dike section failure probabilities are independent.
2. Multiply the maximum cross section failure probability per failure mechanism with the dike trajectory length effect factor.
3. Take the minimum dike trajectory failure probability per failure mechanism resulting from the two options presented above.

The dike trajectory length effect factor is computed with equation (2.1) and the dike section length effect factor is computed with equation (3.26). These equations are applicable to the failure mechanisms inner slope stability and piping. The corresponding a_l- and b_l-parameters for equation (2.1) are shown in Table 4.9 below (Deltares, 2021).

The dike section length effect factor of overtopping is assumed to be equal to one, as the dike sections are uniform. However, the entire dike trajectory is not uniform. The dike trajectory length effect factor of overtopping has a fixed value which is specific for every dike trajectory and can very between the values $N_{trajectory} = 1, 2\ or\ 3$. The dike trajectories of this research are all assumed to have three different orientations. Therefore, the length effect factor for overtopping is equal to $N_{trajectory} = 3$ for all trajectories.

Table 4.9: Value of a_l- and b_l-parameters

Failure mechanism	$\boldsymbol{a_l}\ (-)$	$\boldsymbol{b_l}\ (\boldsymbol{m})$
Inner slope stability	0.033	50
Piping	0.4	300

Results

Table 4.10 and Table 4.11 compare the computed dike trajectory failure probability per failure mechanism from the combination protocol with the one from the fragility curve method. The row ‘Combination protocol - option 1’ refers to the option of the combination protocol that assumes the dike sections are independent. The row 'Combination protocol - option 2’ refers to the option of the combination protocol that multiplies the maximum cross section failure probability with the dike trajectory length effect factor. The row ‘Combination protocol - final’ refers to the minimum of options 1 and 2 of the combination protocol.

Table 4.10: Comparison of dike trajectory failure probability per failure mechanism between the combination protocol and the fragility curve method for dike trajectory 1.1

	Inner slope stability	**Overtopping**	**Piping**
Section 1	0.0062	0.0009	0.0021
Section 2	0.0080	0.0011	0.0027
Section 3	0.0063	0.0014	0.0033
Section 4	0.0058	0.0009	0.0023
Section 5	0.0066	0.0011	0.0025
Trajectory length effect factor	4.30	3.00	7.67
Combination protocol - option 1	0.0329	0.0054	0.0129
Combination protocol - option 2	0.0068	0.0041	0.0104
Combination protocol - final	0.0068	0.0041	0.0104
Fragility curve method	0.0126	0.0037	0.0071

Table 4.11: Comparison of dike trajectory failure probability per failure mechanism between the combination protocol and the fragility curve method for dike trajectory 2.1

	Inner slope stability	Overtopping	Piping
Section 1	0.0065	0.0009	0.0023
Section 2	0.0420	0.0074	0.0210
Section 3	0.0062	0.0010	0.0023
Section 4	0.0076	0.0010	0.0027
Section 5	0.0051	0.0015	0.0037
Trajectory length effect factor	4.30	3.00	7.67
Combination protocol - option 1	0.0675	0.0118	0.0321
Combination protocol - option 2	0.0311	0.0223	0.0744
Combination protocol - final	0.0311	0.0118	0.0321
Fragility curve method	0.0423	0.0091	0.0219

The most important rows from the tables above are the rows that present the dike trajectory failure probabilities per failure mechanism from the combination protocol and from the fragility curve method. For inner slope stability, the trajectory failure probability from the fragility curve method is higher than the one from the combination protocol, in case of a uniform dike trajectory and in case of a dike trajectory with a dominant dike section. For piping and overtopping, the fragility curve method is lower than the combination protocol for both dike trajectories. These observations are elucidated in the sensitivity study of subsection 4.5.2.

4.4.2 From dike trajectory per failure mechanism to total trajectory

The next step is to combine the dike trajectory failure probabilities per failure mechanism to the total dike trajectory failure probability. To do this, the combination protocol assumes the failure mechanisms are independent. In Table 4.12 and Table 4.13 the combination of the dike trajectory failure probabilities per failure mechanism to the total dike trajectory failure probability is compared for the combination protocol and the fragility curve method.

Table 4.12: Comparison of total dike trajectory failure probability between the combination protocol and the fragility curve method for dike trajectory 1.1

	Failure probability
Trajectory failure probability for inner slope stability	0.0126
Trajectory failure probability for overtopping	0.0037
Trajectory failure probability for piping	0.0071
Total trajectory failure probability - Fragility curve method	0.0150
Total trajectory failure probability - Combination protocol (Combination protocol probabilities per failure mechanism)	0.0213
Total trajectory failure probability- Combination protocol (Fragility curve method probabilities per failure mechanism)	0.0233

Table 4.13: Comparison of total dike trajectory failure probability between the combination protocol and the fragility curve method for dike trajectory 2.1

	Failure probability
Trajectory failure probability for inner slope stability	0.0423
Trajectory failure probability for overtopping	0.0091
Trajectory failure probability for piping	0.0219
Total trajectory failure probability - Fragility curve method	0.0475
Total trajectory failure probability - Combination protocol (Combination protocol probabilities per failure mechanism)	0.0750
Total trajectory failure probability- Combination protocol (Fragility curve method probabilities per failure mechanism)	0.0733

The total trajectory failure probability of the fragility curve method is lower than the one from the combination protocol. The combination protocol assumes the failure mechanisms are independent. This results in a dike trajectory failure probability which is almost exactly equal to the upper bound. By including the correlation in the water level, the correlation scale computed by the fragility curve method varies around a value of 75%. Therefore, the computed dike trajectory failure probability lies closer to the lower bound than to the upper bound. As the failure mechanisms all have comparable dike trajectory failure probabilities, the upper and the lower bound lie relatively far apart. Because of this, the fragility curve method is significantly lower than the combination protocol with respect to the total dike trajectory failure probability.

4.5 Sensitivity analysis

4.5.1 Fragility curve method

Correlation dike sections

As explained in section 4.3, the failure probability of an independent series system is bounded by the maximum failure probability and the sum of the failure probabilities of the components. By taking correlation into account between the components, the system failure probability ends up somewhere in between the bounds. However, taking into account correlation increases the complexity of the computation. A good first indication of whether the increased computation time is worth it, can be obtained by looking at the difference between the upper and the lower bound. The closer they lie together, the lower the possible influence of the correlation.

Figures 4.11 until 4.13 are created to illustrate the effect of including the spatial correlation of the water level. These figures plot the dike trajectory failure probability per failure mechanism as a function of the number of dike sections. In these plots, the length of the dike sections remains the same as the number of dike sections increases, which implies that the length of the dike trajectory is not fixed. The theoretical upper and lower bound are plotted as well. The dike sections of the plots on the left side of figures 4.11 until 4.13 are not the same. They contain small natural variations with respect to each other. The plots on the right side also contain one dominant dike section with a failure probability that is one order of magnitude higher. The dominant dike section is section number 5, which explains the jump in the dike trajectory failure probabilities at this section.

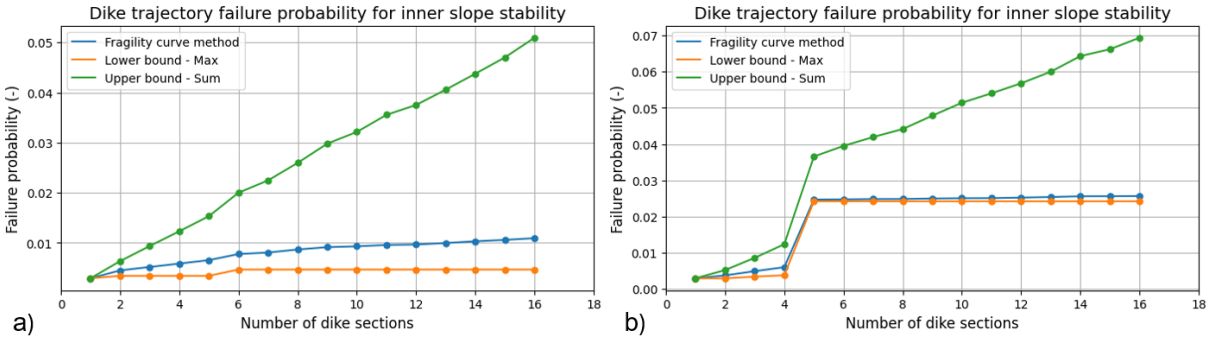

Figure 4.11: The dike trajectory failure probability for inner slope stability as a function of the number of dike sections for a) dike sections with ± equal failure probabilities and for b) one dominant dike section

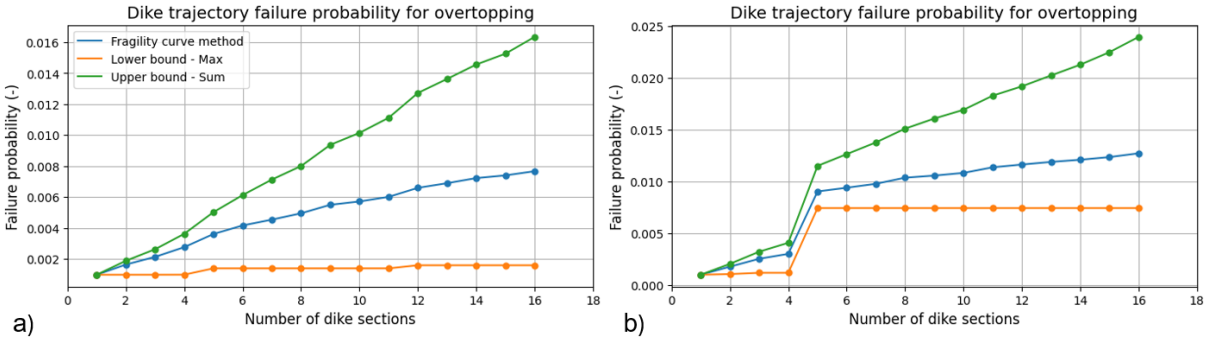

Figure 4.12: The dike trajectory failure probability for overtopping as a function of the number of dike sections for a) dike sections with ± equal failure probabilities and for b) one dominant dike section

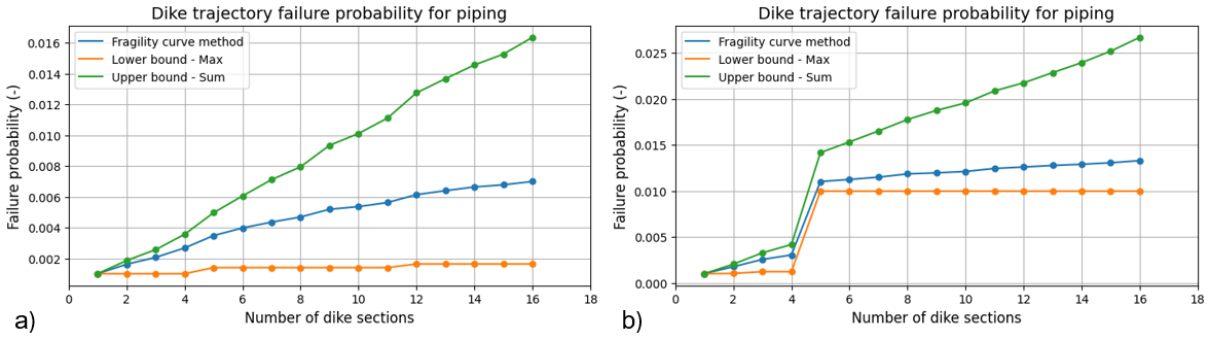

Figure 4.13: The dike trajectory failure probability for piping as a function of the number of dike sections for a) dike sections with approximately equal failure probabilities and for b) one dominant dike section

The dike trajectory failure probabilities form the fragility curve method lie closer to the lower bound for the plots with a dominant dike section. The lower bound represents full positive correlation. Therefore, the presence of the dominant dike section increases the correlation.

Furthermore, these plots also confirm that the correlation between the dike sections is the highest for the failure mechanism inner slope stability. Another observation worth mentioning is that the upper and the lower bound get further apart as the number of dike sections increases. This means that the net effect of including the correlation on the dike trajectory failure probability increases as the dike trajectory becomes longer.

Correlation failure mechanisms

For all dike trajectories, both with and without a dominant dike section, the correlation between the dike sections is relatively high for all failure mechanisms. For the rather uniform dike trajectories, the correlation scale has a value around 75%. For the trajectories with a dominant

dike section, the correlation scale is slightly higher with a value of around 80%. The correlation between the failure mechanisms slightly reduces for a higher number of dike sections.

Figure 4.14 illustrates the effect of including the correlation of the water level between the failure mechanisms. In this figure, the total dike trajectory failure probability is plot as a function of the number of dike sections. Just like in plots 4.11 until 4.13, the length of the dike trajectory increases for a higher number of dike sections. The right side of Figure 4.14 shows the result in case one dike section is dominant. For the left plot, all dike sections have equal failure probabilities.

As the total dike trajectory failure probability from the fragility curve method lies relatively close to the lower bound, Figure 4.14 confirms that including the correlation in the water level between the failure mechanisms can have a significant impact on the total dike trajectory failure probability. Furthermore, Figure 4.14 confirms that the presence of the dominant dike section increases the correlation between the failure mechanisms.

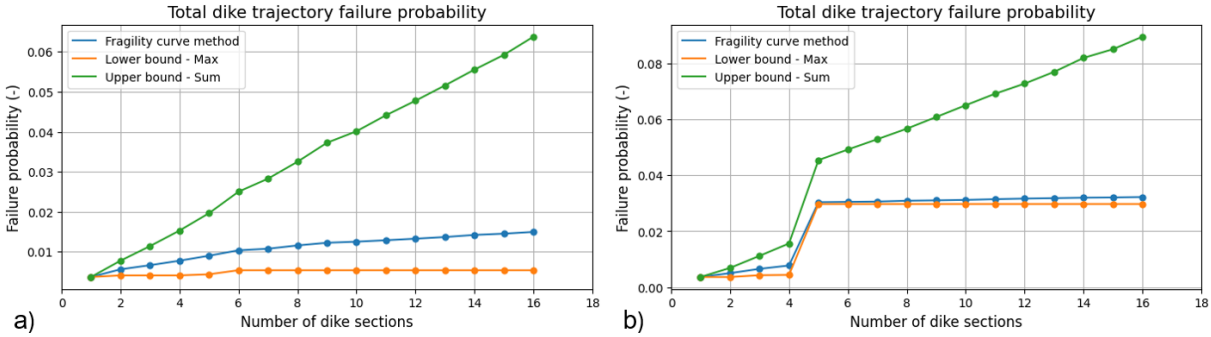

Figure 4.14: The total dike trajectory failure probability as a function of the number of dike sections for a) dike sections with approximately equal failure probabilities and for b) one dominant dike section

Effect number of dike sections

All dike trajectories have a fixed length of 5 kilometres. If the dike trajectory length remains the same, a greater number of dike sections results in shorter dike sections. This leads to a lower length effect factor for the conversion from the cross section failure probabilities to the dike section failure probabilities. On the other hand, a larger number of dike sections means the upper and lower bound of the dike trajectory failure probabilities per failure mechanism lie further apart. For the same value of the correlation scale, this would lead to a higher failure probability.

For the rather uniform dike trajectories, the parameters only vary slightly along the trajectory. The only difference between these trajectories is the number of dike sections. Therefore, these dike trajectories can be interpreted as different schematizations of the same dike trajectory. Dike trajectory 1.3 consists of 15 dike sections, whereas dike trajectory 1.1 consists of just 5 dike sections. To go from 15 to 5 dike sections, the 15 dike sections are divided into 5 groups of 3 dike sections. From every group, the most dominant dike section is picked as one of the dike sections of dike trajectory 1.1. Since the dike trajectories with a varying number of dike sections are all schematisations of the same dike trajectory, the dike trajectory failure probability should remain the same. The dike trajectory failure probability is plot as a function of the number of dike sections in Figure 4.15. An important difference with respect to Figures 4.11 until 4.14 is that the length of the dike trajectory is now fixed instead of the length of the dike sections. The length of the dike sections decreases for a higher number of dike sections. Figure 4.15 shows the dike trajectory failure probabilities for a trajectory that consists of dike sections of which the failure probabilities are all of the same order of magnitude.

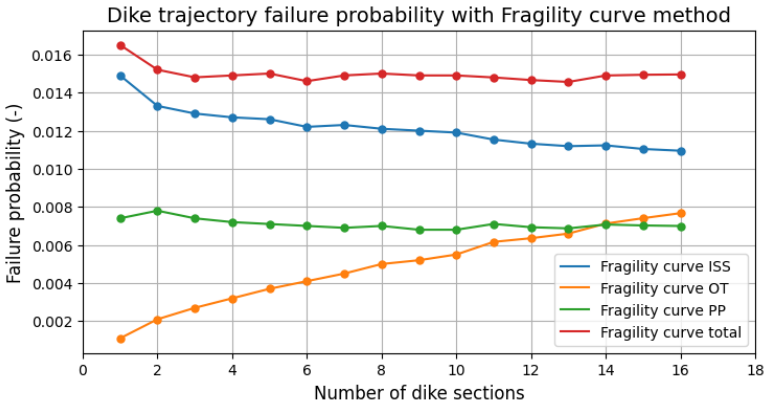

Figure 4.15: Dike trajectory failure probability computed with the fragility curve method for dike sections with approximately equal failure probabilities

For the dike trajectories with equal dike section failure probabilities, the correlation between the dike sections slightly increases as the number of dike sections increases for all failure mechanisms. However, due to the fact that the upper and the lower bound get further apart, the net effect for the failure mechanism overtopping is that the dike trajectory failure probability for overtopping increases.

For inner slope stability and piping, the length effect factor also plays a role. The length effect factor decreases due to smaller dike sections as the number of dike sections increases. For piping, this causes the dike trajectory failure probability to be approximately constant with respect to the number of dike sections. The dike trajectory failure probability of inner slope stability slightly reduces as the number of dike sections increases. This is caused by the higher influence of the decrease of the length effect factor. The influence is higher for inner slope stability than for piping, as inner slope stability has a lower spatial correlation. The total dike trajectory failure probability remains fairly constant with respect to the number of dike sections. This is in line with the expectation, as the different dike trajectories with a varying number of dike sections schematize the same dike trajectory.

When the trajectory contains one dominant dike section, the statement that the different dike trajectories schematize the same dike trajectory does not hold anymore. As the number of dike sections decreases, the length of the dike sections increases. This implies that the length of the dominant dike section also increases. The part of the dike trajectory with weaker parameters becomes longer, altering the dike trajectory. So, for a lower number of dike sections, the dike trajectory is weaker, which implies that the trajectory failure probability is expected to be higher. This can be seen in Figure 4.16. In this figure, the length of the dike trajectory has a fixed value of 5 kilometres.

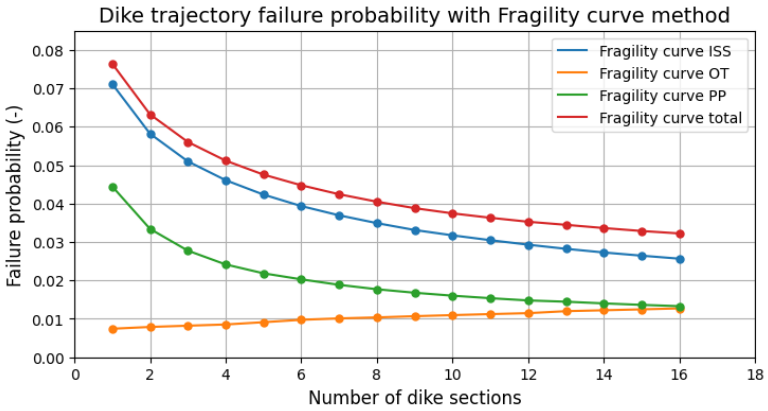

Figure 4.16: Dike trajectory failure probability computed with the fragility curve method in case of one dominant dike section

For the dike trajectories with a dominant dike section, the correlation between the dike sections slightly increases for overtopping as the number of dike sections increases and it slightly decreases for inner slope stability and piping. Due to the fact that the upper and the lower bound get further apart, the net effect for overtopping is that the dike trajectory failure probability for overtopping increases for more dike sections.

The dike trajectory failure probabilities for inner slope stability and piping lie very close to the corresponding maximum dike section failure probability (the lower bound). The maximum dike section failure probability decreases as the number of dike sections increases due to the decreased length effect factor. Therefore, the dike trajectory failure probabilities for inner slope stability and piping decrease as the number of dike sections. The total dike trajectory failure probability also decreases as a result of this. This is in line with the expectation. For a smaller number of dike sections, the weak part of the trajectory is larger, which should result in a higher failure probability.

The dike trajectory failure probabilities of inner slope stability and piping resulting from the fragility curve method match with the expectations. For the dike trajectories with approximately equal dike section failure probabilities, the combined effect from the length effect factor and the divergence of the upper and lower bound causes the dike trajectory failure probabilities to be more or less constant with respect to the number of dike sections. For the dike trajectories with a dominant dike section, especially the length effect makes sure the dike trajectory failure probability of inner slope stability and piping reduces for a higher number of dike sections.

Due to the absence of a length effect factor for overtopping, the dike trajectory failure probability for overtopping increase as the number of dike sections increase. However, if the spatial correlation of a failure mechanism is not equal to 100%, this means that some parameters are not fully correlated. Then, due to the changing length of the dike sections, a length effect factor should be applied to account for the spatial uncertainty of the parameters that are not fully correlated. In the fragility curve method, the spatial correlation of overtopping is approximately 60%. This implies that a length effect factor is required to stop the dike trajectory failure probability for overtopping to increase with an increasing number of dike sections. However, the application of a length effect factor to overtopping is not logical as the parameters of overtopping all have a high spatial correlation. Therefore, it is better to assume overtopping is fully correlated in combination with a safety factor to account for irregularities in the dike trajectory.

4.5.2 Comparison with the combination protocol

Dike trajectory failure probability per failure mechanism

According to the combination protocol, cross section failure probabilities are scaled up to dike trajectory failure probabilities per failure mechanism by choosing the minimum from the following options:

1. First compute the dike section failure probabilities by multiplying the cross section failure probabilities with the dike section length effect factor. Then, compute the dike trajectory failure probabilities per failure mechanism by assuming the dike section failure probabilities are independent.
2. Multiply the maximum cross section failure probability per failure mechanism with the dike trajectory length effect factor.

Figures 4.17 until 4.19 compare the results of the combination protocol with the results of the fragility curve method on the dike trajectory level per failure mechanism. In these graphs, the length of the dike trajectory has a fixed value of 5 kilometers. The left side of the figures presents the results in case the dike sections only contain small natural variations and the right side presents the results in case the dike trajectory contains one dominant dike section.

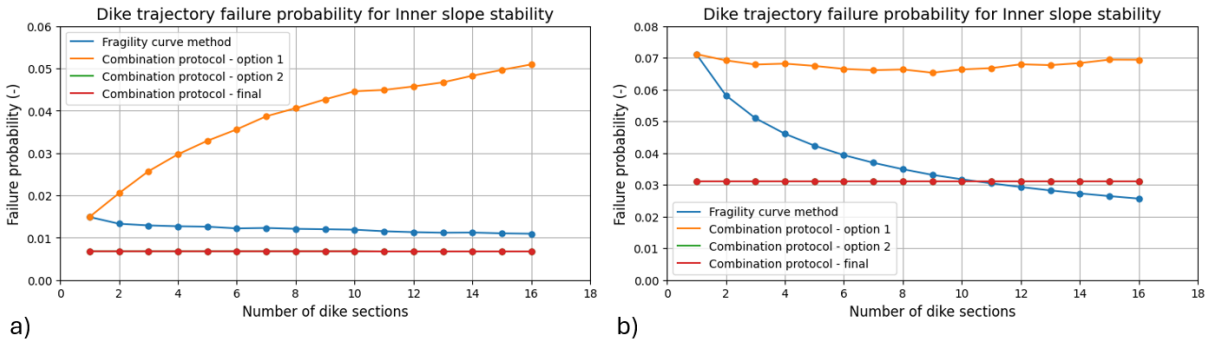

Figure 4.17: Dike trajectory failure probability for inner slope stability for a) dike sections with approximately equal failure probabilities and for b) one dominant dike section

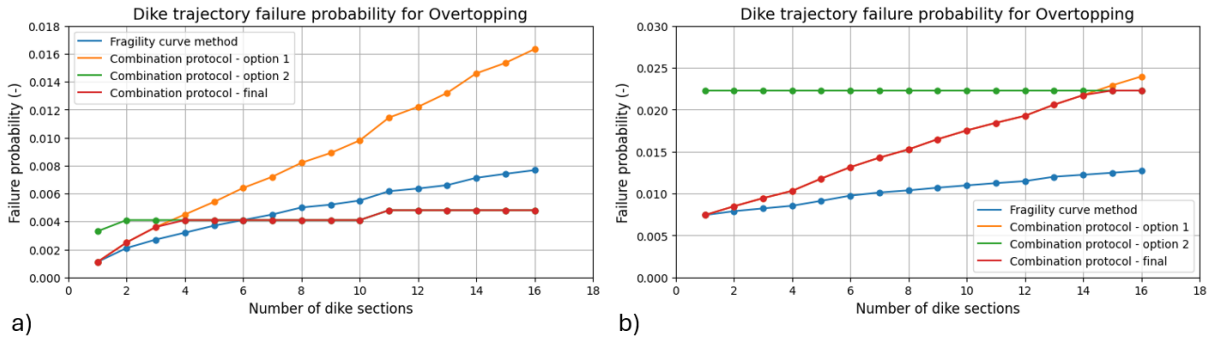

Figure 4.18: Dike trajectory failure probability for overtopping for a) dike sections with approximately equal failure probabilities and for b) one dominant dike section

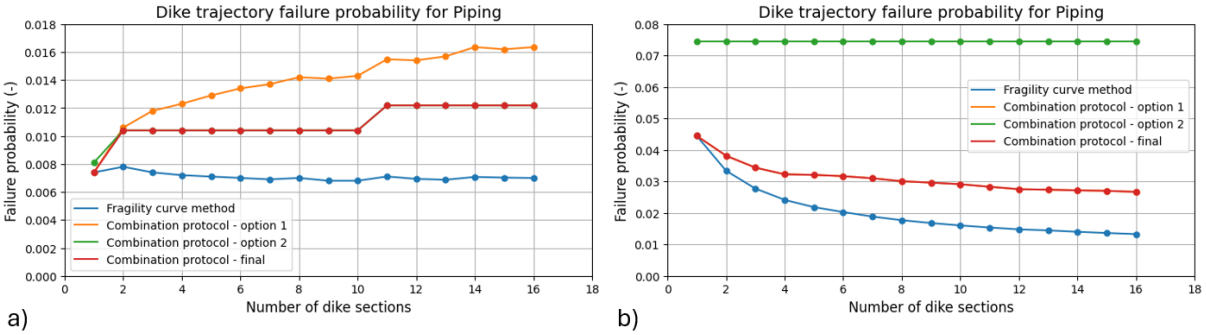

Figure 4.19: Dike trajectory failure probability for piping for a) dike sections with approximately equal failure probabilities and for b) one dominant dike section

For the rather uniform dike trajectories, the combination protocol computes the dike trajectory failure probabilities for all failure mechanisms by multiplying the maximum cross section failure probability with the dike trajectory length effect factor. The other option of the combination protocol assumes the dike sections are independent. To a good approximation, the dike trajectory failure probabilities per failure mechanism are then equal to the sum of the dike section failure probabilities. For the uniform dike trajectories, all dike sections have a comparable failure probability. Therefore, the sum of these probabilities is relatively high and the combination protocol chooses the option with the maximum cross section failure probability. In this option, the dike trajectory length effect factor of equation (2.1) is used. This length effect factor contains the variable a_l, which represents the fraction of the dike trajectory which is sensitive for the failure mechanism.

For inner slope stability, the a_l-factor has a value of $a_l = 0.033$. In other words, the combination protocol assumes that only 3.3% of the dike trajectory contributes to inner slope stability failure. When all dike sections have comparable failure probabilities, this assumption is too low. Due to the small value of the a_l-factor, the dike trajectory length effect factor for inner slope stability used by the combination protocol is only $N_{CP} = 4.3$. Because of this, the dike trajectory failure probability for inner slope stability of the combination protocol is lower than the one from the fragility curve method. Further analysis has shown that the combination protocol exceeds the fragility curve method from a contributing fraction of 8.5% onward ($a_l \geq 0.085$), which corresponds with a trajectory length effect factor of $N_{CP} \geq 9.5$. For piping, the dike trajectory failure probability from the combination protocol is higher than the one from the fragility curve method for the trajectories without a dominant section. This is due to the relatively high trajectory length effect factor for piping of the combination protocol with a value of $N_{CP} = 7.67$. For overtopping, the dike trajectory failure probability of the fragility curve method exceeds the one from the combination protocol if the number of dike sections is greater than five.

For the dike trajectories with a dominant dike section, the combination protocol computes the dike trajectory failure probability of piping by assuming the dike sections are independent. Due to the presence of the dominant dike section, the assumption of independence leads to a lower dike trajectory failure probability than the product of the maximum cross section failure probability and the dike trajectory length effect factor. As a result of the assumption of independence, the computed dike trajectory failure probability is in approximation equal to the theoretical upper bound, i.e. the sum of the dike section failure probabilities. For piping, the correlation scale computed with the fragility curve method varies around a value of 85%. This is a considerable amount of correlation, which means that the dike trajectory failure probability for piping lies close to the theoretical lower bound, i.e. the maximum section failure probability. Therefore, considering the dike sections to be independent with respect to piping leads to an overestimation of the dike trajectory failure probability for piping.

For inner slope stability, the dike trajectory failure probabilty is still computed by multiplying the maximum cross section failure probability with the dike trajectory length effect factor in case of a dominant dike section. Due to the relatively small trajectory length effect factor of inner slope stability, the product of te length effect factor and the largest cross section failure probability is smaller than the sum of all dike section failure probabilities.

Total dike trajectory failure probability

To convert the dike trajectory failure probabilities per failure mechanism into the total dike trajectory failure probability, the combination protocol assumes the failure mechanisms are independent with respect to each other. Figure 4.20 compares the total dike trajectory failure probability of the combination protocol with the results of the fragility curve method. The combination protocol is applied twice: with the dike trajectory failure probabilities per failure mechanism from the fragility curve method and with the dike trajectory failure probabilities per failure mechanism from the combination protocol. In the graphs of Figure 4.20, the length of the dike trajectory has a fixed value of 5 kilometers. The left side of the figures presents the results in case the dike sections only contain small natural variations and the right side present the results in case the dike trajectory contains one dominant dike section.

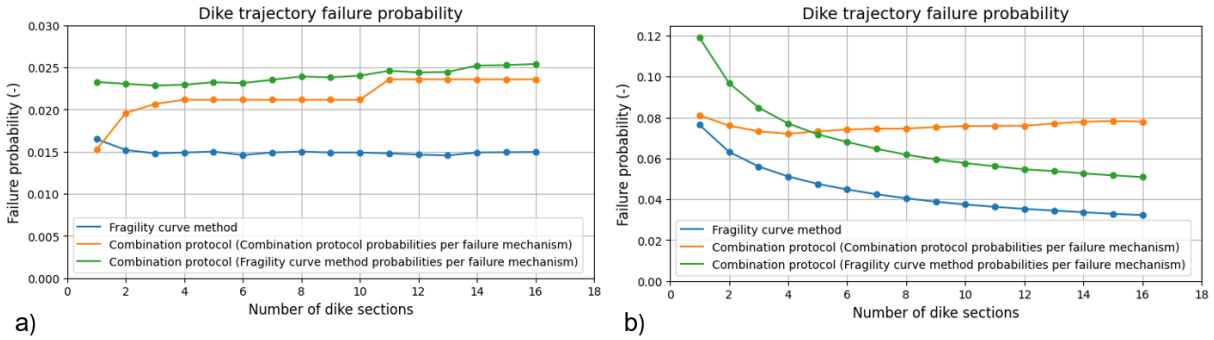

Figure 4.20: Total dike trajectory failure probability for a) dike sections with approximately equal failure probabilities and for b) one dominant dike section

As can be seen from the figure above, the total dike trajectory failure probability computed with the fragility curve method is lower than the one computed with the combination protocol. This is due to the fact that the fragility curve method considers the correlation in the water level between the failure mechanisms. The correlation scale between the failure mechanisms varies around a value of 75% for the different dike trajectories. Therefore, the computed dike trajectory failure probability lies closer to the lower bound than to the upper bound. The combination protocol assumes the failure mechanisms are independent. This results in a dike trajectory failure probability which is almost exactly equal to the upper bound. The upper and the lower bound lie relatively far apart, as the three failure mechanisms all have dike trajectory failure probabilities of the same order of magnitude. Therefore, the dike trajectory failure probability of the fragility curve method is significantly lower than the one from the combination protocol.

5. Discussion

Chapter 5 provides a discussion of the limitations and assumptions of this research. First of all, the duration and probability distribution of the water level are discussed in section 5.1. Then, the assumptions and limitations of the failure mechanism models are discussed in section 5.2. Finally, the assumptions of the fragility curve method are discussed in section 5.3.

5.1 Water level

Duration

The fragility curve method allows one load variable to be separated from the other variables. In this research, the outside water level forms the separated load variable. To be able to combine the fragility curves of different failure mechanisms, the outside water level on the x-axis of the fragility curves should be defined in exactly the same way. For example, if the water level of overtopping does not include the wind set-up, the water levels of inner slope stability and piping also may not include the wind set-up.

However, a discrepancy exists between the duration of the water level for the different failure mechanisms. To model overtopping failure, the critical overtopping rate is used. Failure occurs when the actual overtopping rate exceeds the critical overtopping rate. The critical overtopping rate does not take into account the duration of the water level and can better be regarded as a snapshot analysis. On the contrary, inner slope stability and piping are time dependent. When the high outside water level lasts long enough to infiltrate into the dike body, the phreatic line of the dike body increases. This results in lower effective soil stresses, which consequently leads to a reduction in the sliding resistance and therefore to an increase in the failure probability of inner slope stability (Jonkman et al., 2021).

The infiltration of the water level into the dike body takes time. To limit the infiltration time, the dike body in this research consists of sand. Furthermore, the outside water level is assumed to be not fully infiltrated, see Figure 3.5. This figure shows that the phreatic line of the dike body starts with a steep drop at the outer slope. Therefore, the infiltration time is assumed to be almost zero. In other words, it is assumed that the phreatic line of the dike body occurs instantaneously. The time dependence of piping is neglected. This is explained in more detail in section 5.2.

Because of these assumptions, the water level for the three failure mechanisms used in this research is exactly the same. This implies that the correlation between the water level of the different failure mechanisms is 100%. Without the assumptions, the correlation between the failure mechanisms would have been lower. A lower correlation means the dike trajectory failure probability moves away from the lower bound and towards the upper bound. This results in a higher failure probability. Therefore, the assumption that the water level is fully positively correlated between the failure mechanisms is too optimistic.

Probability distribution

The probability distribution of the water level is required to compute a failure probability from a fragility curve. To obtain the yearly failure probability, the yearly maxima of the water level are modelled with a Gumbel distribution. The parameters of the Gumbel distribution are based on the water level data of the Dutch city Vlissingen. The yearly maximum water levels at Vlissingen belong to the highest water levels of all Dutch coastal cities. For more extreme

water level distributions, with a higher standard deviation, the influence from the water level on the failure probability increases. The correlation in the water level is the only correlation that is considered in the fragility curve method. Therefore, an increase in the influence of the water level on the limit state function also increases the correlation between limit state functions. Tests have shown that the total correlation between dike sections and between failure mechanisms is very sensitive to changes in the Gumbel parameters of the water level. If a less extreme water level distribution would have been used, the computed correlations would have been smaller.

5.2 Failure mechanism models

The failure mechanism models are designed to create cross section fragility curves. For every point of the fragility curve, a full probabilistic analysis is performed for a certain fixed value of the outside water level. Even though the inner slope stability model uses a full probabilistic method, it is important to include a caveat.

The inner slope stability model of D-Stability assesses a slip plane by performing a FORM analysis, which is a full probabilistic method. However, the slip plane is determined through a semi-probabilistic slip plane analysis with the design values of the soil parameters. D-Stability does provide a method to perform a fully probabilistic slip plane analysis. Monte Carlo Importance Sampling is combined with a search algorithm to assess a large quantity of slip planes. However, this method has a run time in the order of hours whereas the combination of the predefined slip plane with the FORM analysis has a run time in the order of minutes. Therefore, the FORM analysis was chosen (Deltares, 2023).

Piping is a time dependent process (Pol et al., 2024). The pipe formation beneath the dike occurs gradually through backward erosion. However, in this research the time dependence of piping is neglected. Piping is modelled as a parallel system of uplift, heave and backward erosion. Time is not reflected in the models of the submechanisms. It is assumed that piping failure occurs if all submodels fail. There is no extra requirement for failure with respect to the duration of the water level.

The overtopping model is simplified as only one wind direction is considered. In reality, the wind speed and the corresponding wind set up are dependent on the wind direction. In a full probabilistic analysis, the probability distributions of the stochastic variables have to be determined for every wind direction.

5.3 Fragility curve method

The fragility curve method assumes that all parameters are independent, except for the separated load variable. The load variable, which is the outer water level in this research, is assumed to be fully correlated in space and between the different failure mechanisms.

If the dike sections are large enough, the assumption of independence can be justified for the failure mechanisms inner slope stability and piping. In the sensitivity study of section 4.5, the dike trajectories are schematized 16 times, every time with a different number of dike sections. The greatest number of dike sections is 16. In that case, the length of the dike sections is the smallest and has a value of $312.5\ m$.

The factor b_l of equation (3.26) is a measure of the correlation length of the failure mechanism. The correlation length represents the distance after which the spatial correlation is significantly reduced. Therefore, to a good approximation, the factor b_l describes the

distance over which a failure mechanism can be regarded as independent. For inner slope stability the factor b_l has a value of $b_{l,ISS} = 50\,m$ and for piping $b_{l,PP} = 300\,m$. For both failure mechanisms, the smallest dike section length of the sensitivity study is larger than the b_l-factors of the failure mechanisms. Therefore, the assumption that all parameters are independent except for the water level can be justified for the failure mechanisms inner slope stability and piping (Deltares, 2021).

Next to the water level, the model for overtopping contains several other parameters which have a very high spatial correlation. For example the wind speed, which is also a load variable, and the crest height, which is a strength parameter, both have a very high spatial correlation. The fragility curve method assumes these parameters are independent between dike sections. By doing so, the spatial correlation of overtopping is underestimated.

6. Conclusions & recommendations

The aim of this research was to develop a probabilistic method for dike safety assessment based on fragility curves and to compare it to the current Dutch standards for dike safety assessment. The current Dutch standards are prescribed by the combination protocol, which is part of the statutory Assessment and Design Framework (BOI). To accomplish the objective, four subquestions are answered in section 6.1. The research can be divided into three main parts. First, a literature study was done to learn about the combination protocol and the fundamentals of fragility curves. Then, a fragility-based method for dike assessment was developed, hereafter referred to as the fragility curve method. Finally, the combination protocol and the fragility curve method were both applied to hypothetical sea dike trajectories to make a comparison between the methods. The results of this application are used to answer the subquestions and consequently to answer the main research question. Section 6.2 presents recommendations for future research.

6.1 Conclusions

The answer to the main research question follows from the answers to the subquestions.

RQ1. How is dike safety assessed according to the current Dutch standards, known as the combination protocol?

Dike safety assessment knows different scale levels. The Dutch primary water defense structures are divided into dike trajectories with an average length of 15 kilometers. The maximum allowable failure probability is established by law at the dike trajectory level, which makes the dike trajectory the largest length scale of dike assessment. Dike trajectories are subdivided into dike sections with a length scale of hundreds of meters. Dike sections consist of a chain of cross sections. A cross section forms the smallest length scale with a width of zero meters.

The starting point of the combination protocol consists of the failure probabilities of the representative cross sections. Every dike section of the trajectory contains one representative cross section.

The combination protocol applies the following steps to convert the cross section failure probabilities into the dike trajectory failure probabilities per failure mechanism.

1. The first option first computes the dike section failure probabilities by multiplying the cross section failure probabilities with the dike section length effect factor. Then, the dike trajectory failure probabilities per failure mechanism are computed by assuming the dike section failure probabilities are independent.
2. Multiply the maximum cross section failure probability per failure mechanism with the dike trajectory length effect factor.
3. Take the minimum dike trajectory failure probability per failure mechanism resulting from the two options presented above.

To compute the total dike trajectory failure probability, the combination protocol assumes the failure mechanisms are independent. The total trajectory failure probability can therefore be calculated with the equation for the system failure probability of an independent series system.

RQ2. How can fragility curves be applied to combine dike failure probabilities in a probabilistic way?

Fragility-based assessment allows one of the loads to be separated from the other parameters. The advantage of the separation is that the correlation of the separated load variable can also be separated from the correlation of the other variables. This is the main principle of the fragility curve method. The outer water level, which is the separated load variable, is fully positively correlated in space and between failure mechanisms and the remaining parameters are assumed to be independent. Because of this, the system failure probability of components that are combined with the fragility curve method lies in between the theoretical lower and upper bound. The correlation scale indicates how close the result of the fragility curve method lies to the lower bound with respect to the upper bound, see Figure 6.1. A high value of the correlation scale means the system failure probability lies close to the lower bound, which implies that the components are highly correlated. The quantitative reduction of the failure probability depends on the distance between the upper and lower bound.

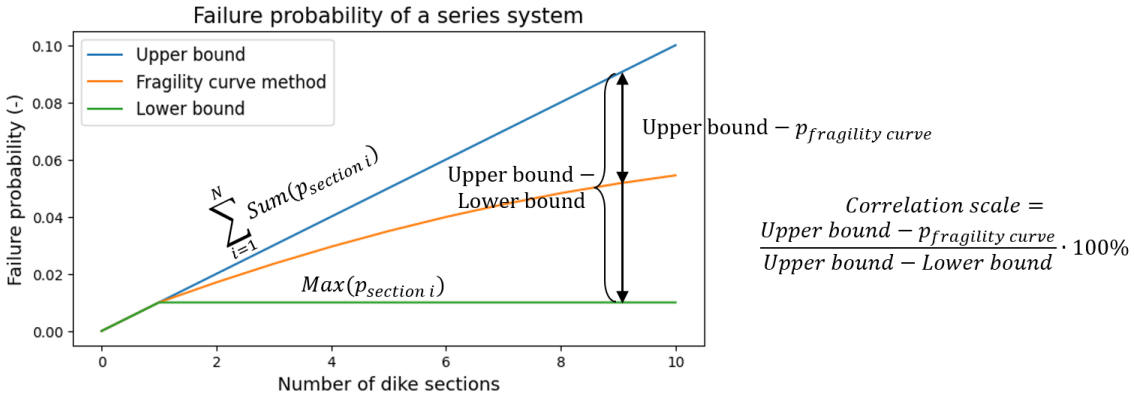

Figure 6.1: Visualization of the correlation scale

The starting point of the fragility curve method consists of the fragility curves of the representative cross sections. These fragility curves are scaled up to the dike section fragility curves by applying the dike section length effect factor to every point of the fragility curves. The length effect factor is applied to account for the spatial variation of all parameters aside from the water level. The dike section fragility curves are consequently scaled up to the dike trajectory fragility curves per failure mechanism. For every point on the fragility curves, the conditional dike trajectory failure probability per failure mechanism is computed by assuming the conditional dike section failure probabilities are independent. Then, the dike trajectory fragility curves per failure mechanism are scaled up to the total dike trajectory fragility curve. To do this, the conditional dike trajectory failure probabilities per failure mechanism are assumed to be independent as well. Finally, the total dike trajectory failure probability is computed by integrating the product of the trajectory fragility curve and the probability distribution of the water level.

The main difference between the combination protocol and the fragility curve method is that the combination protocol scales up failure probabilities to go from the cross section level to the dike trajectory level and that the fragility curve method scales up fragility curves. The combination protocol immediately converts the cross section fragility curves into cross section failure probabilities, which are then scaled up to the trajectory failure probability. Conversely, the fragility curve method first scales up the cross section fragility curves into the trajectory fragility curve and only afterwards converts this trajectory fragility curve into the trajectory failure probability. In the fragility curve method, the conversion from fragility curve to failure

probability occurs as the final step, unlike in the combination protocol, where it is the initial step.

RQ3. What is the difference between the assessment of the combination protocol and the fragility-based assessment on the scale of the dike trajectory failure probabilities per failure mechanism and which method is recommended?

To be able to compare the fragility curve method and the combination protocol, both methods are applied to two hypothetical dike trajectories. The dike trajectories are representative of a Dutch sea dike and have a length of 5 kilometers. The first dike trajectory is rather uniform and consists of dike sections that only vary slightly from each other due to natural variability. Therefore, the dike sections of the first trajectory have comparable failure probabilities. The second dike trajectory contains one dominant dike section. The failure probability of the dominant dike section is one order of magnitude higher than the failure probabilities of the other dike sections. Both dike trajectories are modelled for various numbers of dike sections.

For both dike trajectories, the combination protocol computes the dike trajectory failure probability of inner slope stability by multiplying the maximum cross section failure probability with the dike trajectory length effect factor. The resulting dike trajectory failure probability is lower than the dike trajectory failure probability from the fragility curve method. However, the geotechnical variables of inner slope stability have an extremely low spatial correlation. Yet, the approach from the combination protocol only applies a small dike trajectory length effect factor. The small length effect factor is due to the assumption of the combination protocol that only a very small portion (3.3%) of the dike trajectory contributes to inner slope stability failure. Especially for the rather uniform dike trajectory, this value is too optimistic.

As the fragility curve method assumes all parameters are independent except for the water level, it is logically consistent with probability theory. In contrast, the methodology of the combination protocol for inner slope stability lacks the same level of consistency. It relies heavily on a length effect factor, which is highly sensitive to assumptions regarding the fraction of the trajectory contributing to failure. Furthermore, considering the spatial correlation of the water level significantly reduces the trajectory failure probability for inner slope stability with respect to the theoretical upper bound. The average correlation scale found in this research is 90%. Therefore, the fragility curve method is recommended to compute the trajectory failure probability for inner slope stability.

For the rather uniform dike trajectory, the combination protocol computes the dike trajectory failure probability for piping in the same way as it does for inner slope stability. Just like inner slope stability, piping also is a failure mechanism with a low spatial correlation. Therefore, using the same rationale as for inner slope stability, the fragility curve method is recommended to compute the dike trajectory failure probability of piping in case of a uniform dike trajectory.

In case the dike trajectories of this research contain a dominant dike section, the combination protocol computes the dike trajectory failure probability for piping by assuming the dike section failure probabilities are independent. To a good approximation, the resulting dike trajectory failure probability for piping is then equal to the theoretical upper bound. The dike trajectory failure probability for piping from the fragility curve method is considerably lower than the upper bound. With an average correlation scale of 86%, the dike trajectory failure probability lies close to the lower bound. What this means for the quantitative reduction of the failure probability, depends on the gap between the upper and lower bound. The greater the number of dike sections, the larger this gap. Furthermore, the gap also increases as the failure probabilities of the dike sections become higher. So, the number of dike sections and the value of the dike section failure probabilities determine if the extra computation time of the fragility

curve method is worth the reduction in the dike trajectory failure probability for piping. However, with an average value of 86% the correlation scale is so high that, in general, the fragility curve method is recommended to compute the dike trajectory failure probability for piping in case of a trajectory with a dominant dike section.

The fragility curve method underestimates the spatial correlation of the overtopping failure mechanism. In this research, the dike trajectory contains multiple different orientations. Therefore, the dike trajectory length effect factor for overtopping is equal to $N = 3$. Because of this length effect factor, the dike trajectory failure probability for overtopping from the combination protocol and the fragility curve method only slightly deviate from each other. The underestimated correlation of the fragility curve method is compensated by the high length effect factor of the combination protocol. When the dike trajectory would have been fully straight, the dike trajectory length effect factor would have been equal to $N = 1$. In that case, the fragility curve method would have overestimated the dike trajectory failure probability for overtopping by a factor of three. It is more true to reality to assume a fully positive spatial correlation for overtopping in combination with a length effect factor to account for irregularities in the dike trajectory. This means that it is recommended to use the combination protocol to compute the dike trajectory failure probability of overtopping. Another option also exists. The fragility curve method for overtopping can also be adjusted so that it assumes all parameters are fully correlated.

RQ4. How does the dike safety assessment of the fragility curve method compare to the assessment of the combination protocol on the scale of the total dike trajectory failure probability and which method is preferred?

In case of a uniform dike trajectory, the total dike trajectory failure probability of the fragility curve method has an average correlation scale of 75%. In case of a dike trajectory with one dominant dike section, this correlation scale has an average value of 79%. Therefore, the dike trajectory failure probability of the fragility curve method lies close to the theoretical lower bound. The combination protocol assumes the failure mechanisms are independent. This means the total dike trajectory failure probability of the combination protocol is approximately equal to the theoretical upper bound. So, the dike trajectory failure probability can be reduced by applying the fragility curve method. The exact amount of reduction depends on the difference between the upper and lower bound. This results in the following recommendations:

- If the failure mechanisms have comparable dike trajectory failure probabilities, the difference between the upper and the lower bound is approximately a factor 3. In that case, the reduction of the dike trajectory failure probability is relatively high. Hence, it is recommended to apply the fragility curve method for the computation of the total dike trajectory failure probability.
- If one failure mechanism is clearly dominant over the others, the upper and lower bound lie close together. In that case, the extra computation time of the fragility curve method only causes an insignificant reduction of the dike trajectory failure probability. Therefore, the combination protocol suffices in case one failure mechanism is clearly dominant over the others.

With all subquestions addressed, the main research question can now be answered.

How do the current Dutch standards for dike safety assessment compare to a probabilistic method based on fragility curves?

In conclusion, the fragility curve method is an accessible method with potential to be used in the daily practice of dike assessors. The fragility curve method is recommended over the combination protocol for the computation of the dike trajectory failure probability of the geotechnical failure mechanisms. Furthermore, if the failure mechanisms have comparable dike trajectory failure probabilities, the fragility curve method is also recommended for the computation of the total dike trajectory failure probability. The combination protocol is recommended for the computation of the dike trajectory failure probability of overtopping. Table 6.1 provides an overview of the above conclusions.

Table 6.1: Recommended dike safety assessment method

Level of scaling up	**Recommended method**	**Highest reduction failure probability in case of:**
Dike sections to trajectory for inner slope stability	Fragility curve method	High section failure probabilities and/or large number of sections
Dike sections to trajectory for piping	Fragility curve method	High section failure probabilities and/or large number of sections
Dike sections to trajectory for overtopping	Combination protocol	-
Failure mechanisms on the trajectory level to total trajectory failure probability	Fragility curve method	Failure mechanisms same order of magnitude

6.2 Recommendations

Failure mechanism models

It is recommended to use more detailed failure mechanism models to compute the cross section fragility curves, which are the starting point of the fragility curve method. Research by Pol et al. (2024) has shown that including time dependence can significantly reduce the computed failure probability for piping. Therefore, it is recommended to incorporate time dependence in the piping model. Furthermore, it is recommended to consider all wind directions in the overtopping model. The different wind directions should be scaled with the corresponding probability of occurrence for a more accurate representation of reality.

The water level in the fragility curve method

Furthermore, it is recommended to eliminate the discrepancy in the time duration of the water levels of the different failure mechanisms. A possible way to do this would be by decreasing the correlation between the water levels of the different failure mechanisms. By decreasing the correlation, the water levels are not assumed to be exactly the same anymore, which takes away the necessity to eliminate the time discrepancy. However, this complicates the process of combining fragility curves for upscaling. Another possibility to look into would be to filter the probability distribution of the water level for water levels with a certain minimal duration. This way, the discrepancy in the time duration can be eliminated. However, this results in new problems. Now, high water levels with a short duration that lead to failure are not included in the computation. Therefore, it is recommended to carefully look into the options to deal with the time discrepancy in the water level of the different failure mechanisms.

In this research, the spatial correlation between the dike sections is relatively high for all failure mechanisms. Part of this can be attributed to the high water level distribution that is used. One of the highest sets of water level data has been used along the entire Dutch coast. It is recommended to also investigate the applicability of the fragility curve method for river and lake dikes. For these dikes, the water level data is much lower. This means that the influence of the fully positive correlation of the water level on the total correlation between dike sections and failure mechanisms will also be lower. Consequently, the reduction of the failure probability will be smaller as well. It is recommended to examine whether the application of the fragility curve method to river and lake dikes reduces the failure probability with respect to the combination protocol, and if so, whether the reduction justifies the additional computation time.

Modifications of the fragility curve method

It is also recommended to recode the fragility curve method so that, for overtopping, it aligns with the methodology used in the combination protocol. This way, if the fragility curve method is to be further developed and applied in practice, it is not required anymore to switch between different assessment methods. This means that for overtopping, the cross section fragility curves should be immediately converted into the cross section failure probabilities. Then, these probabilities should be scaled up to the trajectory failure probability by multiplying the maximum cross section failure probability with the trajectory length effect factor. The trajectory length effect factor should be carefully chosen, based on irregularities within the trajectory.

As mentioned before, less extreme water level data results in less correlation. The correlation can be increased by using multi-dimensional fragility curves (Cimellaro et al., 2006). The goal of this is not just to increase the correlation, but to be provide a more accurate representation of reality. The additional variables to condition the fragility curves should be the variables with the highest spatial correlation after the water level. Generally speaking, load variables have a higher spatial correlation than resistance variables. For example, the wind speed could be

added as a conditional load variable. The wind speed has a high spatial correlation and a great influence on the wave height.

Follow-up mechanisms

The Dutch statutory Assessment and Design Framework (BOI) wants to refine the computation of the trajectory failure probability (Rijkswaterstaat, 2023). This report looked into two refinement options that are presented by the BOI, namely the consideration of spatial correlation between dike sections and the consideration of correlation between failure mechanisms. Another refinement option of the BOI is to consider follow-up mechanisms in the computation of the failure probability. It is recommended to investigate the applicability of the fragility curve method with respect to the follow-up mechanisms. The fragility curve method might offer an accessible solution to take into account the correlation in the complex processes of the follow-up mechanisms.

Prospects of the fragility curve method in Dutch dike safety assessment

The failure mechanism models that are applied in this research are not complex enough to be applied in practice. For instance, the failure mechanism model for overtopping only considers one wind direction. However, the fragility curve method can be considered independently from the failure mechanism models. The function of the fragility curve method is to scale up from the cross section level to the trajectory level. The failure mechanism models that are used in the current Dutch dike assessment procedure could also be used as input for the fragility curve method. The only condition is that these models should be able to create fragility curves.

At present, only a select number of failure mechanisms allow for a full probabilistic calculation, which is required to create fragility curves. Therefore, to apply the fragility curve method across the entire scope of dike assessment, all failure mechanism models must first be made fully probabilistic.

Furthermore, as previously mentioned, before applying the fragility curve method in practice, it is essential to investigate the discrepancy in the duration of the water levels of the different failure mechanisms. A solution should either be developed to eliminate this time discrepancy, or it should be verified that neglecting the time discrepancy has negligible consequences.

References

Bretschneider, C. L. (1957). REVISIONS IN WAVE FORECASTING: DEEP AND SHALLOW WATER. *Coastal Engineering Proceedings*, *6*, 3. https://doi.org/10.9753/icce.v6.3

Cimellaro, G. P., Reinhorn, A. M., Bruneau, M., & Rutenberg, A. (2006). *Multi-Dimensional Fragility of Structures: Formulation and Evaluation*. Multidisciplinary Center for Earthquake Engineering Research. https://www.buffalo.edu/mceer/catalog.host.html/content/shared/www/mceer/publications/MCEER-06-0002.detail.html

De Vree, J. (n.d.). *k-waarde*. Joostdevree.nl. https://joostdevree.nl/shtmls/k-waarde.shtml

Deltares. (2016). *WBI - Onzekerheden: Overzicht van belasting- en sterkteonzekerheden in het wettelijk beoordelingsinstrumentarium* (No. 1220080-001-ZWS-0004).

Deltares. (2018). *Basisrapport WBI 2017* (No. 11202225-012–0001).

Deltares. (2021). *Assemblageprotocol WBI2017* (No. 12205758-005-GEO-0001).

Deltares. (2022). *Faalpaden combineren rekening houdend met afhankelijkheden* (No. 11206817-005-GEO-0001).

Deltares. (2023). *D-Stability: Slope stability software for soft soil engineering*. https://www.deltares.nl/en/software-and-data/products/d-stability

DU, X. (2005). *Probabilistic Engineering Design*. University of Missouri.

Hasofer, A. M., & Lind, N. C. (1974). Exact and invariant Second-Moment code format. *Journal of the Engineering Mechanics Division*, *100*(1), 111–121. https://doi.org/10.1061/jmcea3.0001848

Informatiepunt Leefomgeving. (n.d.). *Eerste landelijke beoordelingsronde (LBO-1)*. https://iplo.nl/thema/water/waterveiligheid/primaire-waterkeringen/boi-portaal/eerste-landelijke-beoordelingsronde-lbo-1/

Jonkman, S. N., Jorissen, R. E., Schweckendiek, T., & Van Den Bos, J. P. (2021). *Flood Defences: Lecture Notes CIE5314* (4th ed.). Delft University of Technology.

Jonkman, S. N., Steenbergen, R. D. J. M., Morales-Nápoles, O., Vrouwenvelder, A. C. W. M., & Vrijling, J. K. (2017). *Probabilistic Design: Risk and Reliability Analysis in Civil Engineering: Lecture notes CIE4130* (4th ed.). Delft University of Technology.

Kanning, W. (2023). *Review en verbeteropties assemblage* (No. 11208057-024-GEO-0002). Deltares.

Ministerie van Infrastructuur en Waterstaat. (2023). Regeling veiligheid primaire waterkeringen 2023. In *Staatscourant* (No. 11307). Het Koninkrijk der Nederlanden.

Pol, J., Kanning, W., Jonkman, S. N., & Kok, M. (2024). Time-dependent reliability analysis of flood defenses under cumulative internal erosion. *Structure and Infrastructure Engineering*, 1–17. https://doi.org/10.1080/15732479.2024.2416434

Remmerswaal, G. (2023). *The Random Material Point Method for assessment of residual dyke resistance: Investigating the influence of soil heterogeneity on slope failure processes*. [Dissertation (TU Delft), Delft University of Technology]. https://doi.org/10.4233/uuid:5f32c08d-bc3d-452d-9e38-91d93a3e3499

Rijkswaterstaat. (n.d.). *Waterwet*. https://www.infomil.nl/onderwerpen/lucht-water/handboek-water/wetgeving/waterwet/

Rijkswaterstaat. (2014). *De veiligheid van Nederland in kaart*. Rijkswaterstaat Projectbureau VNK.

Rijkswaterstaat. (2022). Schematiseringshandleiding grasbekleding. In *IPLO*. Ministerie van Infrastructuur en Waterstaat. https://iplo.nl/@205746/schematiseringshandleiding-grasbekleding/

Rijkswaterstaat. (2023). Handleiding Overstromingskansanalyse - Algemeen. In *Informatiepunt Leefomgeving*.

Rijkswaterstaat. (2024). *Watersnoodramp 1953*. https://www.rijkswaterstaat.nl/water/waterbeheer/bescherming-tegen-het-water/watersnoodramp-1953

Roscoe, K., Diermanse, F., & Vrouwenvelder, T. (2015). System reliability with correlated components: Accuracy of the Equivalent Planes method. *Structural Safety*, *57*, 53–64. https://doi.org/10.1016/j.strusafe.2015.07.006

Rosenblatt, M. (1952). Remarks on a multivariate transformation. *The Annals of Mathematical Statistics*, *23*(3), 470–472. https://doi.org/10.1214/aoms/1177729394

Schneider, J., & Vrouwenvelder, A. C. W. M. (2017). *Introduction to Safety and Reliability of Structures* (3rd ed.). IABSE. http://ci.nii.ac.jp/ncid/BA75383120

Schweckendiek, T., Van Der Krogt, M. G., Teixeira, A., Kanning, W., Brinkman, R., & Rippi, K. (2017). Reliability Updating with Survival Information for Dike Slope Stability Using Fragility Curves. *Geo-Risk 2017*. https://doi.org/10.1061/9780784480700.047

Sellmeijer, H., De La Cruz, J. L., Van Beek, V. M., & Knoeff, H. (2011). Fine-tuning of the backward erosion piping model through small-scale, medium-scale and IJkdijk experiments. *European Journal of Environmental and Civil Engineering*, *15*(8), 1139–1154. https://doi.org/10.1080/19648189.2011.9714845

Slomp, R. (2016). *Implementing risk based flood defence standards*. Rijkswaterstaat.

Slootjes, N., & Van der Most, H. (2016). *Achtergronden bij de normering van de primaire waterkeringen in Nederland*. Ministerie van Infrastructuur en Milieu. https://open.rijkswaterstaat.nl/open-overheid/onderzoeksrapporten/@190410/achtergronden-normering-primaire/

Smale, A. J. (2017). *Vergelijking WBI2017 met OI2014* (No. 11200575-009-GEO-0001). Deltares.

TAW. (2002). *Technisch Rapport Golfoploop en Golfoverslag bij Dijken*. Technische Adviescommissie voor de Waterkeringen. https://tl.iplo.nl/@192512/technisch-rapport-1/

TAW. (2004). *Technisch Rapport Waterspanningen bij dijken* (ISBN-90-369-5565-3). Technische Adviescommissie voor de Waterkeringen. https://tl.iplo.nl/@192510/technisch-rapport-0/

Van Eyck, B. & Rijkswaterstaat. (1995, February 2). *Hoogwater bij Ophemert 1995*. Archieven.nl. https://www.archieven.nl/nl/zoeken?mivast=0&mizig=269&miadt=2606&miview=gal&milang=nl&mistart=25&mibj=1995&miej=1995&mif4=Digitale+foto

A Parameters cross sections

In this appendix the notation is as follows:

- CS Base = the base cross section
- CS Nat. Var. = the cross section with small natural variability
- CS Dominant = the dominant cross section
- SD = standard deviation
- PD = probability distribution
- D = deterministic
- N = normal
- L = lognormal
- W = Weibull

Table A1: Geometry of the cross sections of section 3.4

Parameter	Unit	CS Base	CS Nat. Var.	CS Dominant
Crest height	$mNAP$	9.0	9.0	8.2
Width levee	m	19	19	9
Length foreshore	m	10	0	0
Thickness cover layer	m	1.5	1.5	1.5
Inner slope gradient	-	1/4	1/4	1/4
Outer slope gradient	-	1/4	1/4	1/4
Inner berm length	m	16	15	16
Inner berm height	m	4	4	4
Thickness aquitard	m	5	6	5
Thickness aquifer	m	8	7	8
Thickness deep clay layer	m	5	5	5
Thickness deep sand layer	m	>10	>10	>10

Inner slope stability

Table A2: Soil parameters of the cross sections of section 3.4

		CS Base		CS Nat. Var.		CS Dominant	
Parameter	**Unit**	**Mean**	**SD**	**Mean**	**SD**	**Mean**	**SD**
Organic clay							
Unit weight above phreatic level	kn/m^3	13.9	-	13.9	-	13.9	-
Unit weight below phreatic level	kn/m^3	13.9	-	13.9	-	13.9	-
Shear strength ratio	-	0.24	0.025	0.24	0.025	0.24	0.025
Strength increase exponent	-	0.85	0.05	0.85	0.05	0.85	0.05
Shallow clay							
Unit weight above phreatic level	kn/m^3	14.8	-	14.8	-	14.8	-
Unit weight below phreatic level	kn/m^3	14.8	-	14.8	-	14.8	-
Shear strength ratio	-	0.24	0.01	0.25	0.01	0.23	0.01
Strength increase exponent	-	0.9	0.04	0.9	0.05	0.9	0.05
Deep clay							
Unit weight above phreatic level	kn/m^3	15.6	-	15.6	-	15.6	-
Unit weight below phreatic level	kn/m^3	15.6	-	15.6	-	15.6	-
Shear strength ratio	-	0.23	0.025	0.23	0.025	0.23	0.025
Strength increase exponent	-	0.9	0.05	0.9	0.05	0.9	0.05
Sand							
Unit weight above phreatic level	kn/m^3	18	-	18	-	18	-
Unit weight below phreatic level	kn/m^3	20	-	20	-	20	-
Cohesion	kn/m^2	0	-	0	-	0	-
Frictional angle	deg	30	2	30	2	30	3
Dilatancy angle	deg	0	-	0	-	0	-

Overtopping

Table A3: Overtopping parameters of the cross sections of section 3.4

Parameter	Unit	Symbol	Distribution	Mean	SD
Foreshore water depth CS Base	m	d_1	Normal	5.3	0.2
Foreshore water depth CS Nat. Var.	m	d_2	Normal	5.5	0.2
Foreshore water depth CS Dominant	m	d_2	Normal	6.5	0.3
Fetch CS Base	km	F_1	Normal	75	3
Fetch CS Nat. Var.	km	F_2	Normal	73	3
Fetch CS Dominant	km	F_2	Normal	110	5
Wind speed 10 $\boldsymbol{m}$ above surface	m/s	u_{10}	Weibull	25	5
Gravitational constant	m/s^2	g	Deterministic	9.81	-
Empirical parameter	-	A	Deterministic	0.067	-
Empirical parameter	-	B	Normal	4.75	0.5
Empirical parameter	-	C	Deterministic	0.2	-
Empirical parameter	-	D	Normal	2.6	0.35
Critical overtopping rate	m^2/s	q_c	Lognormal	0.040	0.050

Piping

Table A4: Piping parameters of the cross sections of section 3.4

				CS Base		CS Nat. Var.	
Parameter	**Unit**	**Symbol**	**PD**	**Mean**	**SD**	**Mean**	**SD**
Hydraulic conductivity aquifer	m/s	k	L	0.0012	$6{\cdot}10^{-4}$	0.001	$5{\cdot}10^{-4}$
Hydraulic conductivity aquitard	m/s	k_h	L	$2.4{\cdot}10^{-6}$	$1.2{\cdot}10^{-6}$	$2{\cdot}10^{-6}$	$1{\cdot}10^{-6}$
Exit location (w.r.t. center of levee)	m	x_{exit}	D	2	-	2	-
Volumetric weight water	kn/m^3	γ_w	D	10	-	10	-
Saturated volumetric weight aquitard	kn/m^3	$\gamma_{sat,a}$	D	14.8	-	14.8	-
Model factor uplift	-	m_u	L	1.0	0.1	1.0	0.1
Critical heave gradient	-	$i_{c,h}$	L	0.5	0.1	0.5	0.1
Phreatic level exit point	$mNAP$	h_p	N	0	0.1	0	0.1
Seepage length	m	$L_{seepage}$	D	55	-	65	-
Volumetric weight sand grains	kn/m^3	γ_s	D	26.5	-	26.5	-
Bedding angle	°	θ	D	37	-	37	-
Drag factor coefficient	-	η	D	0.25	-	0.25	-
Kinematic viscosity water	m^2/s	ν	D	$1.33{\cdot}10^{-6}$	-	$1.33{*}10^{-6}$	-
70%-fractile grain size distribution aquifer	u	d_{70}	L	$1.5{\cdot}10^{-4}$	$1.8{\cdot}10^{-5}$	$1.5{\cdot}10^{-4}$	$1.8{\cdot}10^{-5}$
Reference value d70	m	d_{70m}	D	$2.08{\cdot}10^{-4}$	-	$2.08{\cdot}10^{-4}$	-
Model factor piping	-	m_p	L	1.0	0.12	1.0	0.12

				CS Dominant	
Parameter	**Unit**	**Symbol**	**PD**	**Mean**	**SD**
Hydraulic conductivity aquifer	m/s	k	L	0.002	0.001
Hydraulic conductivity aquitard	m/s	k_h	L	$4{\cdot}10^{-6}$	$2{\cdot}10^{-6}$
Exit location (w.r.t. center of levee)	m	x_{exit}	D	2	-
Volumetric weight water	kn/m^3	γ_w	D	10	-
Saturated volumetric weight aquitard	kn/m^3	$\gamma_{sat,a}$	D	14.8	-
Model factor uplift	-	m_u	L	1.0	0.1
Critical heave gradient	-	$i_{c,h}$	L	0.5	0.1
Phreatic level exit point	$mNAP$	h_p	N	0	0.1
Seepage length	m	$L_{seepage}$	D	50	-
Volumetric weight sand grains	kn/m^3	γ_s	D	26.5	-
Bedding angle	°	θ	D	37	-
Drag factor coefficient	-	η	D	0.25	-
Kinematic viscosity water	m^2/s	ν	D	$1.33{\cdot}10^{-6}$	-
70%-fractile grain size distribution aquifer	u	d_{70}	L	$1.5{\cdot}10^{-4}$	$1.8{\cdot}10^{-5}$
Reference value d70	m	d_{70m}	D	$2.08{\cdot}10^{-4}$	-
Model factor piping	-	m_p	L	1.0	0.12

B Fragility curves cross sections of section 3.4

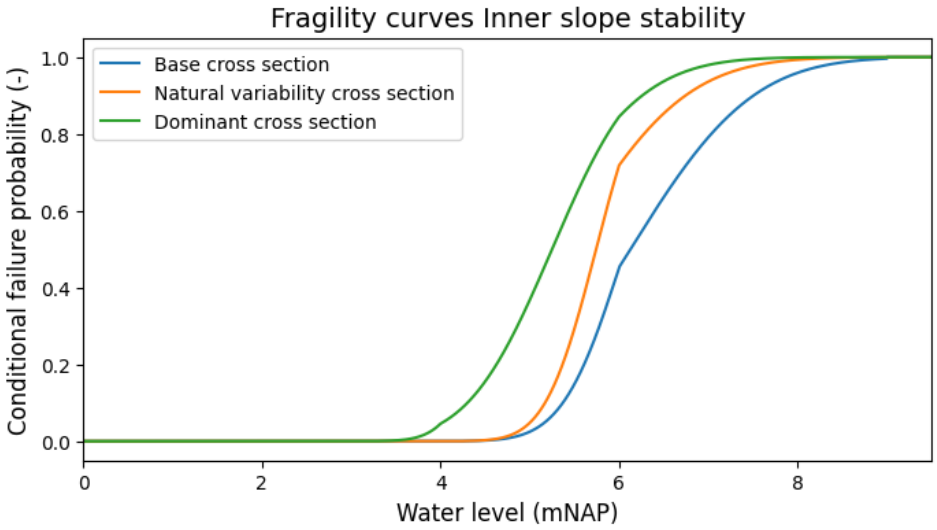

Figure B1: Fragility curves inner slope stability

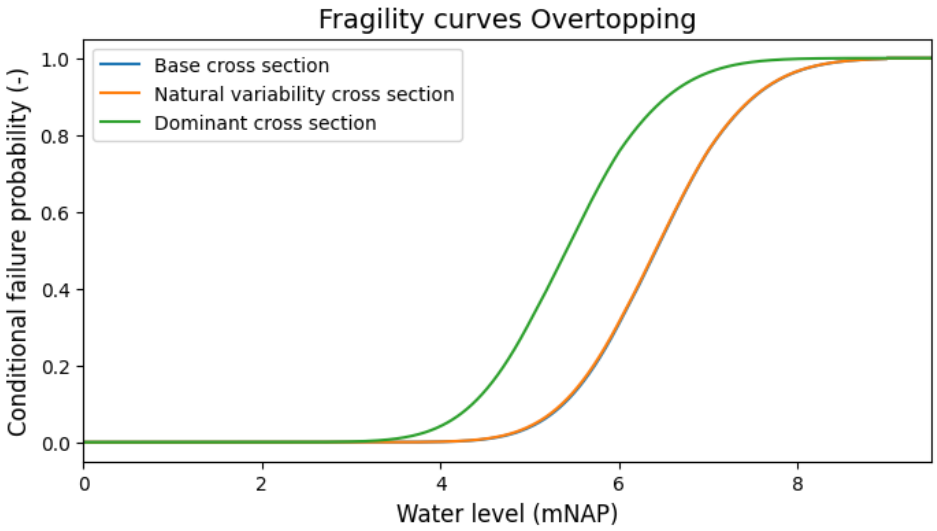

Figure B2: Fragility curves overtopping

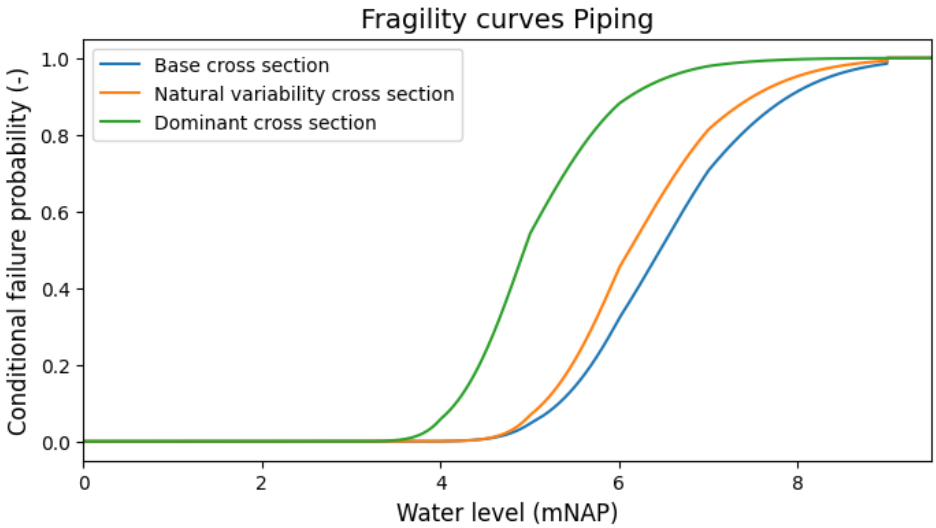

Figure B3: Fragility curves piping

C Fragility curves

Table C1 provides an overview of the different dike trajectories in this appendix.

Table C1: Description of the dike trajectories

	Dike sections	Number of dike sections
Trajectory 1.1	Small natural variability	5
Trajectory 1.2	Small natural variability	10
Trajectory 1.3	Small natural variability	15
Trajectory 2.1	One dominant section	5
Trajectory 2.2	One dominant section	10
Trajectory 2.3	One dominant section	15

Trajectory 1.1

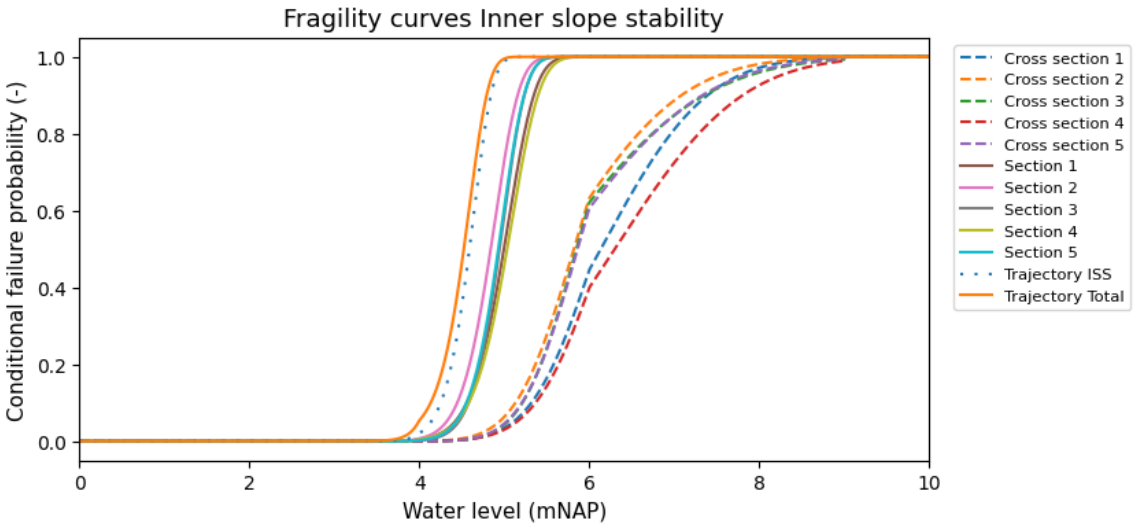

Figure C1: Fragility curves inner slope stability

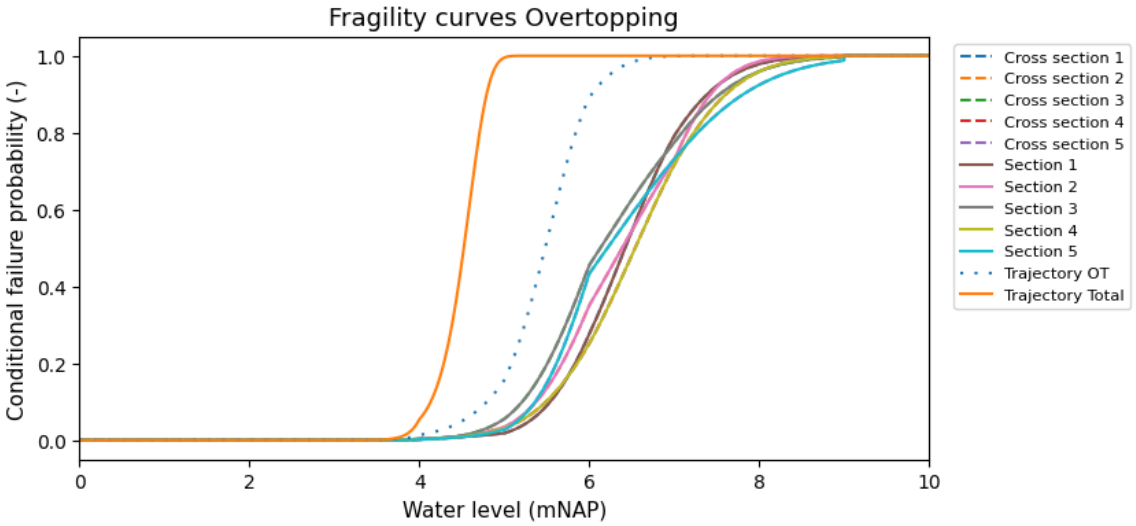

Figure C2: Fragility curves overtopping

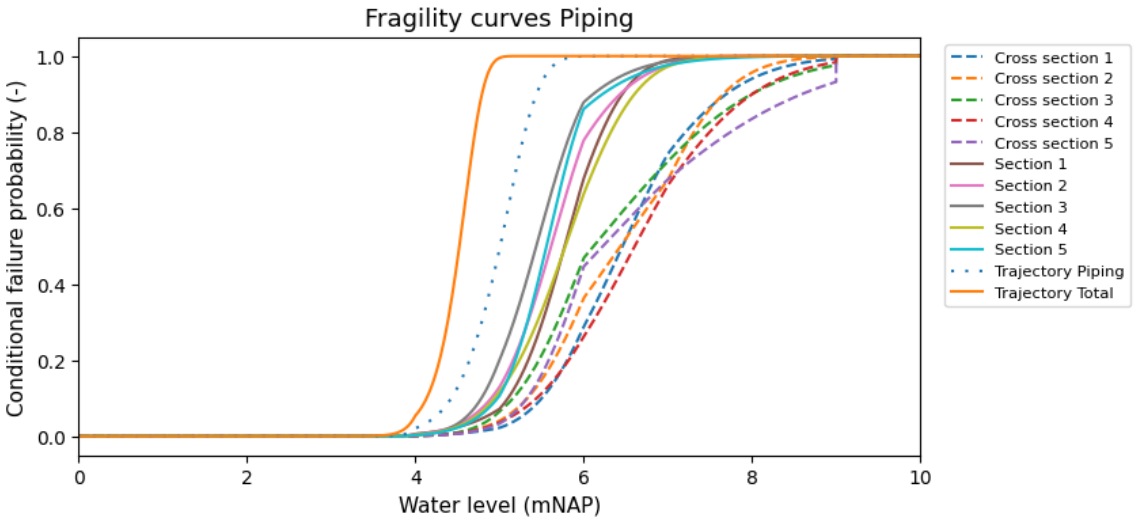

Figure C3: Fragility curves piping

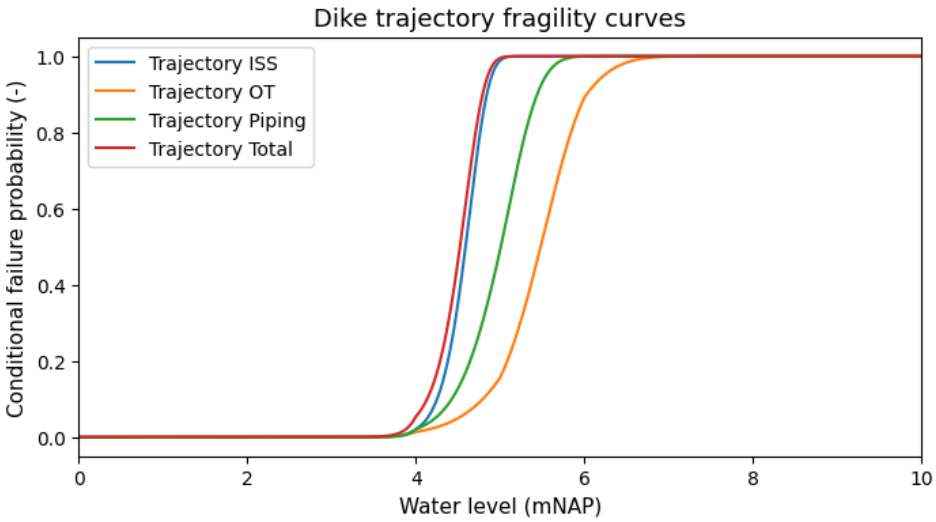

Figure C4: Dike trajectory fragility curves

Trajectory 1.2

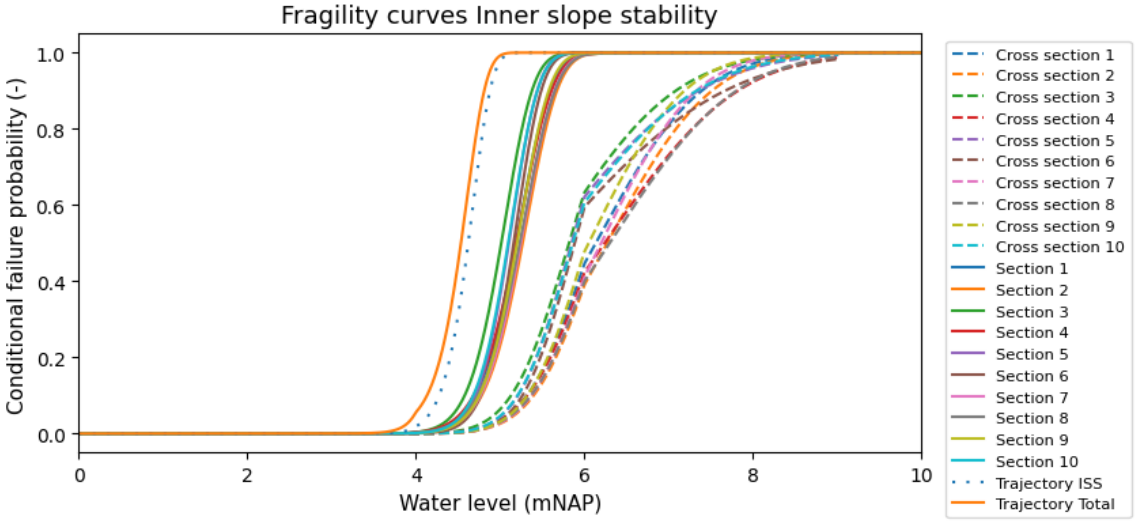

Figure C5: Fragility curves inner slope stability

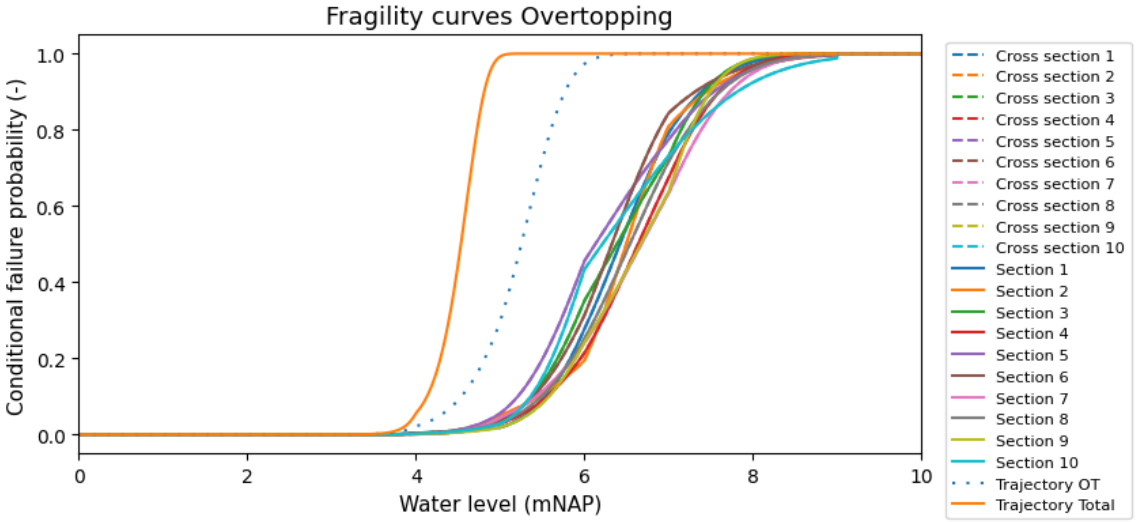

Figure C6: Fragility curves overtopping

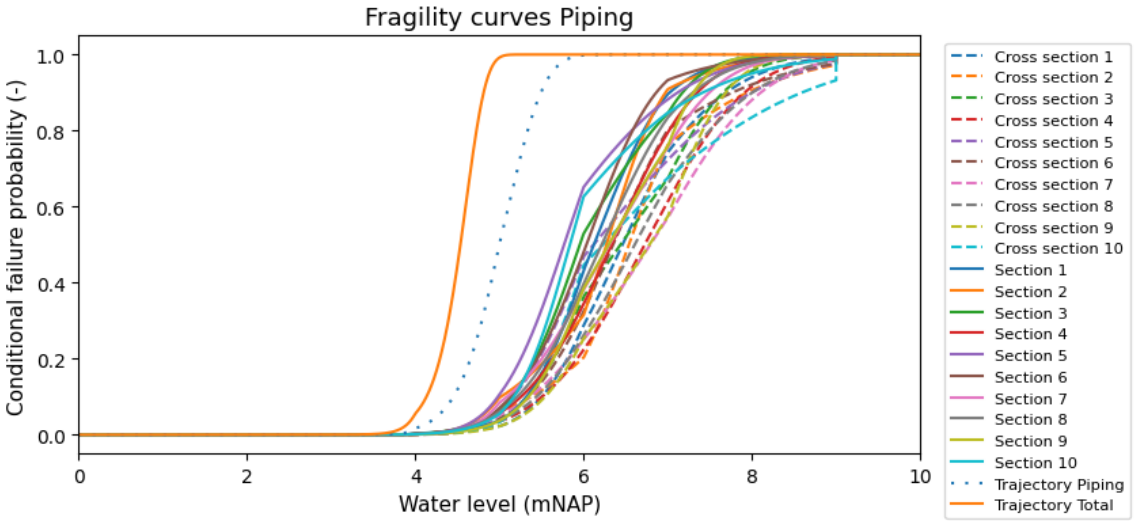

Figure C7: Fragility curves piping

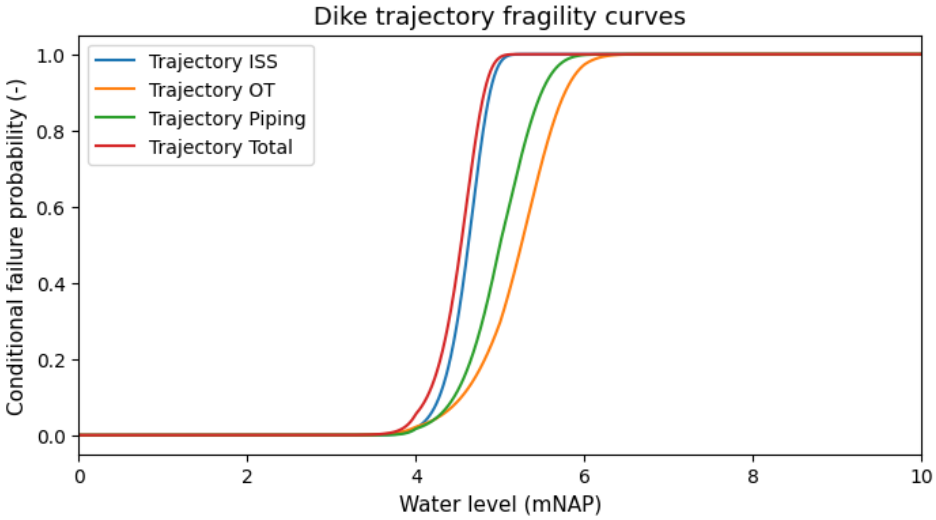

Figure C8: Dike trajectory fragility curves

Trajectory 1.3

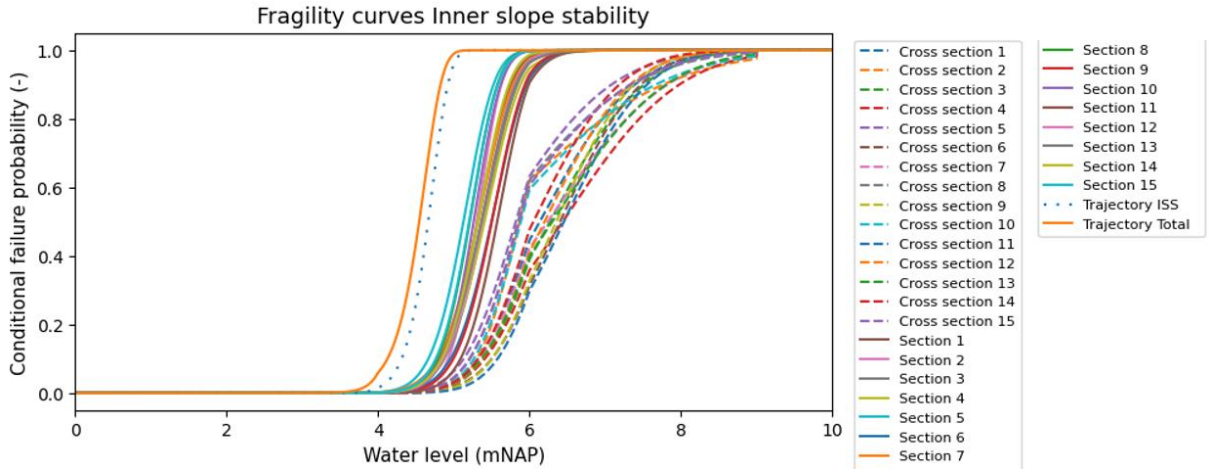

Figure C9: Fragility curves inner slope stability

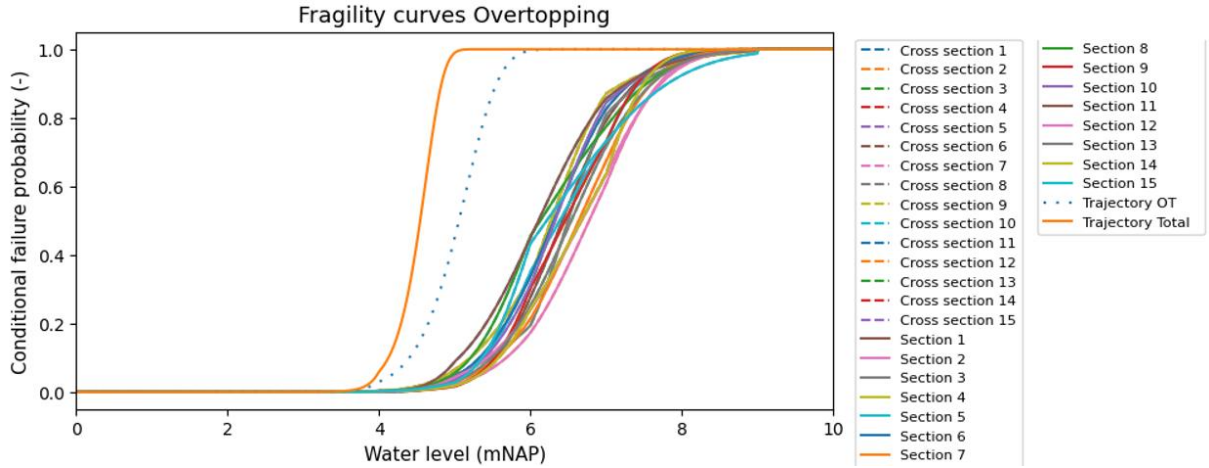

Figure C10: Fragility curves overtopping

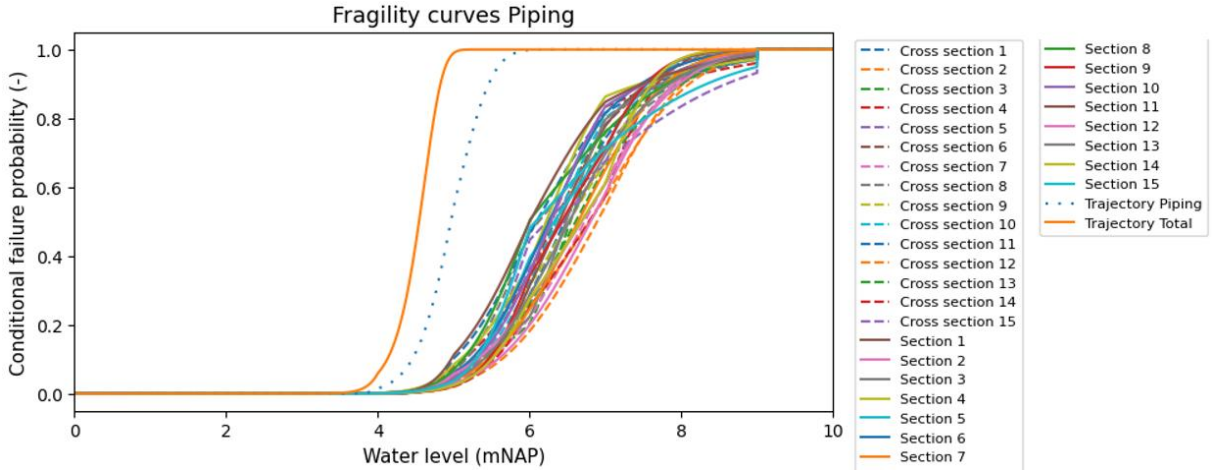

Figure C11: Fragility curves piping

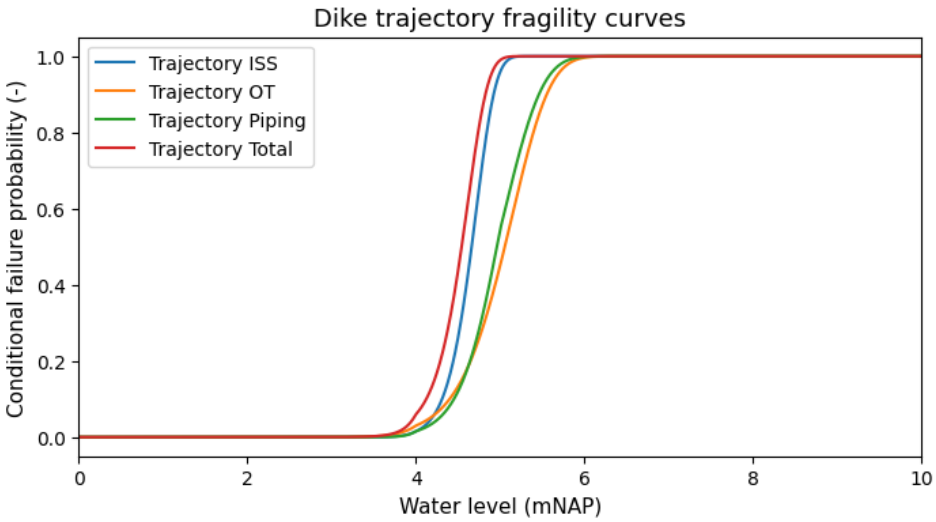

Figure C12: Dike trajectory fragility curves

Trajectory 2.1

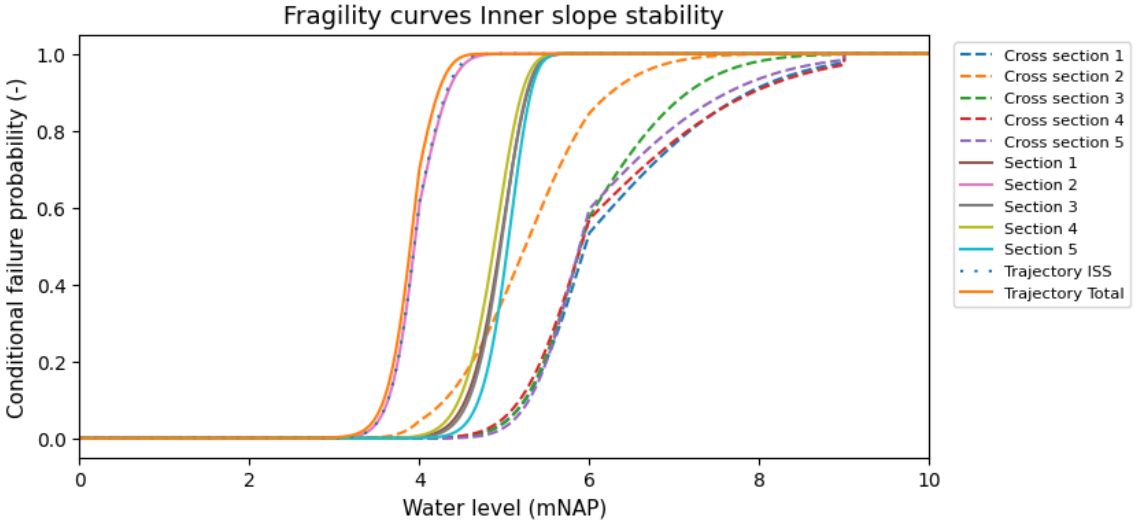

Figure C13: Fragility curves inner slope stability

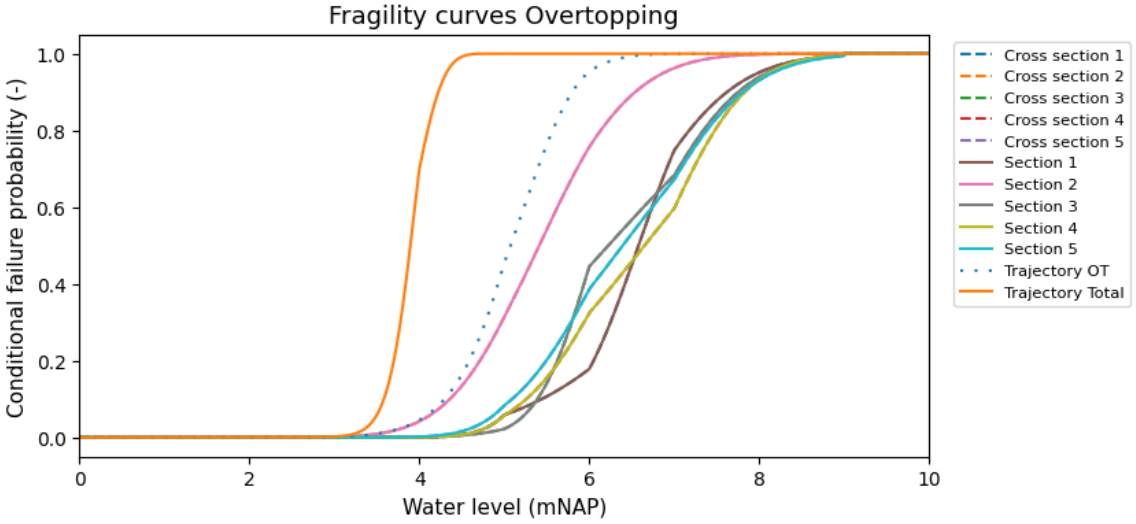

Figure C14: Fragility curves overtopping

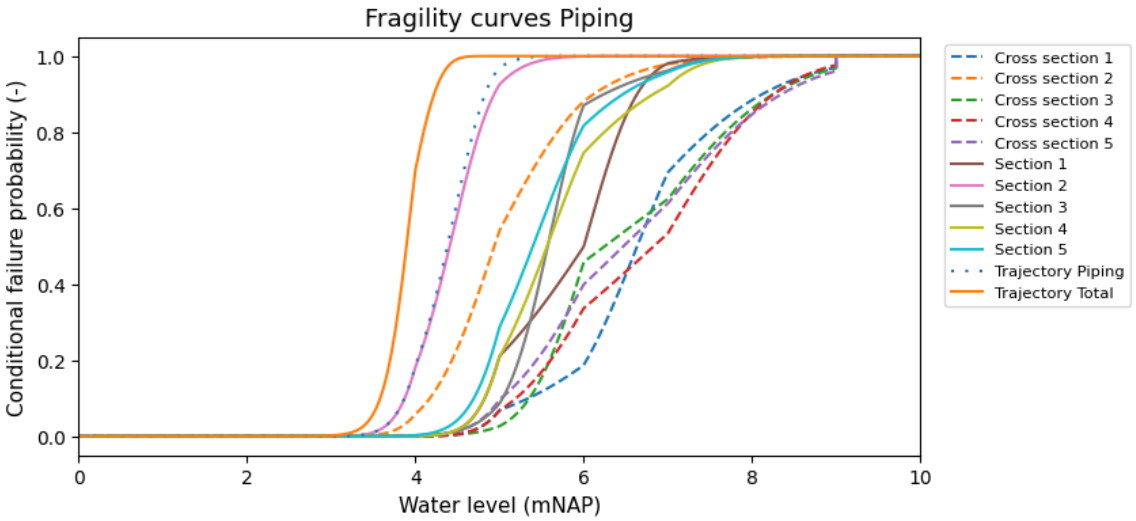

Figure C15: Fragility curves piping

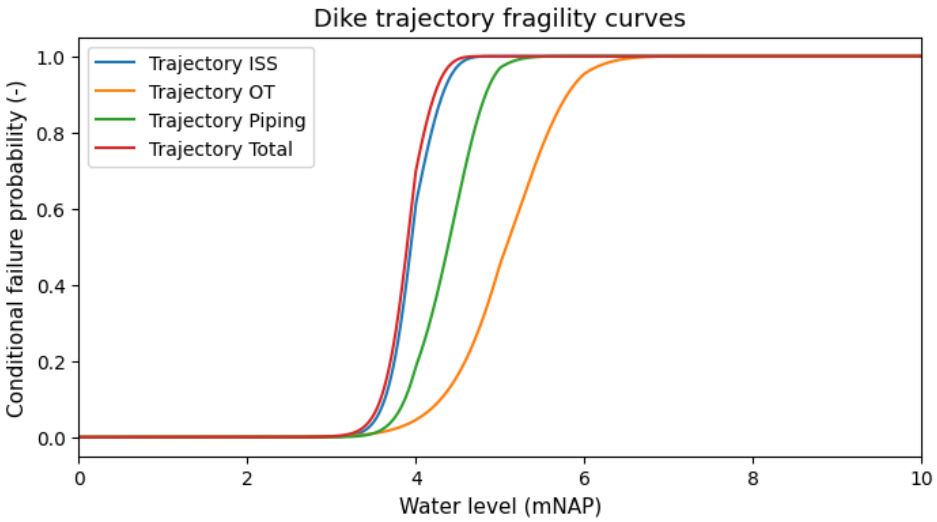

Figure C16: Dike trajectory fragility curves

Trajectory 2.2

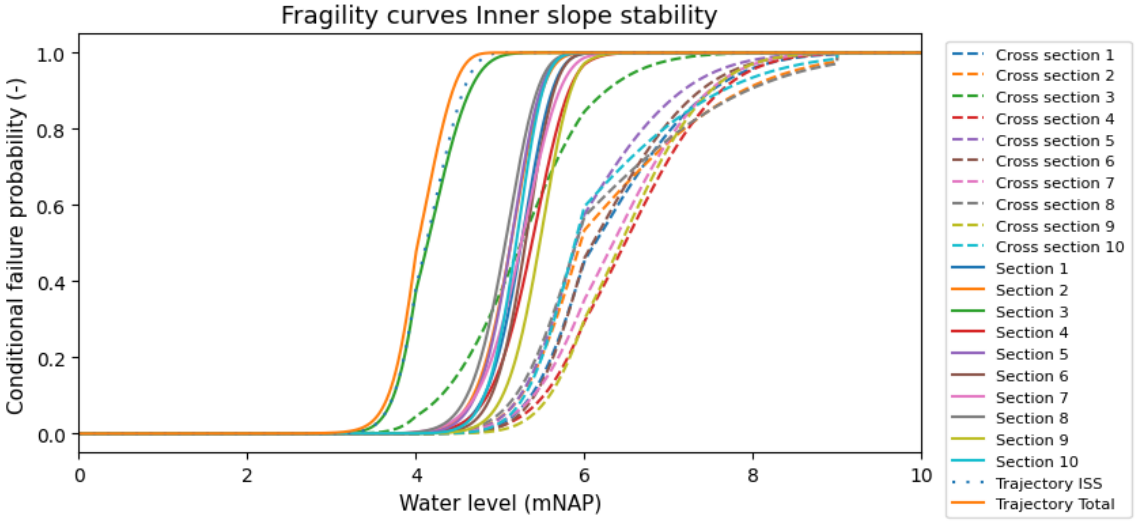

Figure C17: Fragility curves inner slope stability

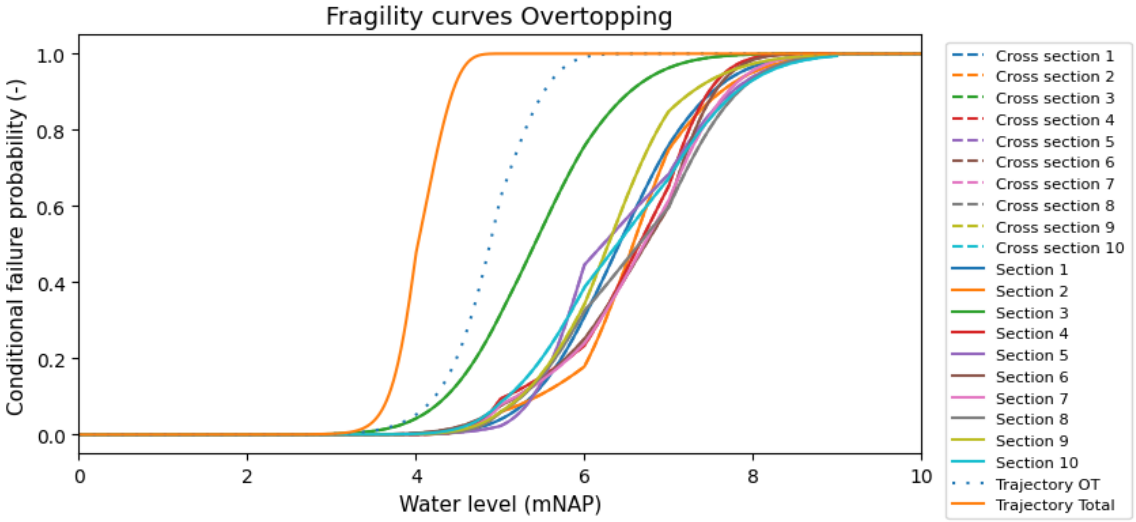

Figure C18: Fragility curves overtopping

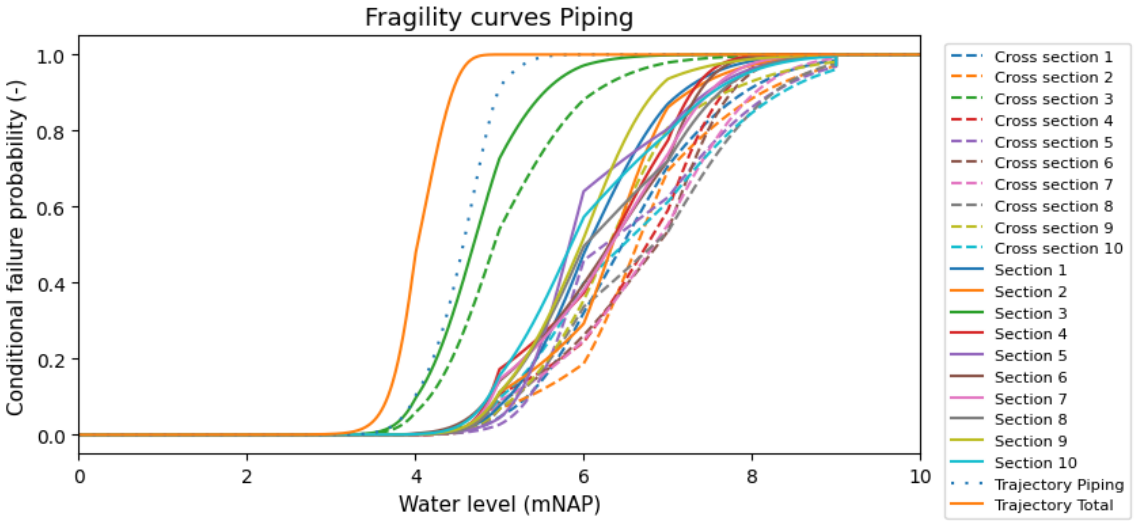

Figure C19: Fragility curves piping

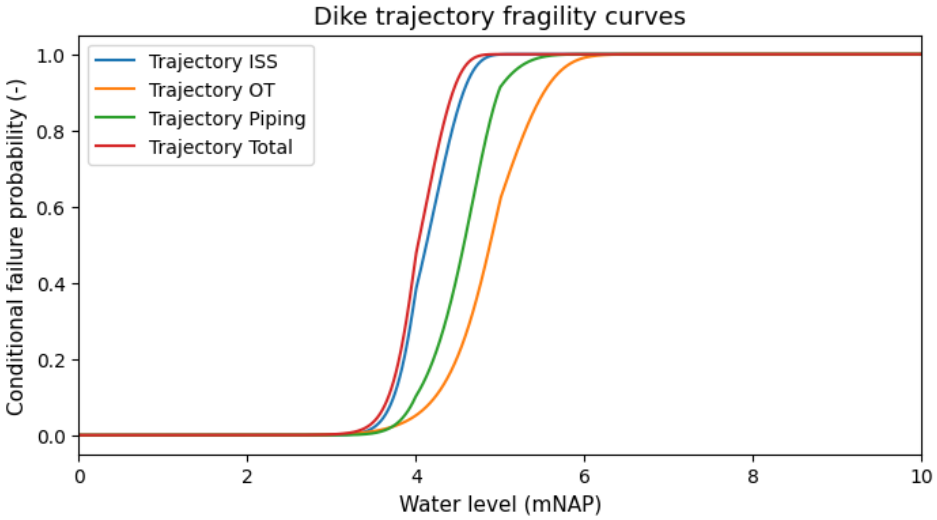

Figure C20: Dike trajectory fragility curves

Trajectory 2.3

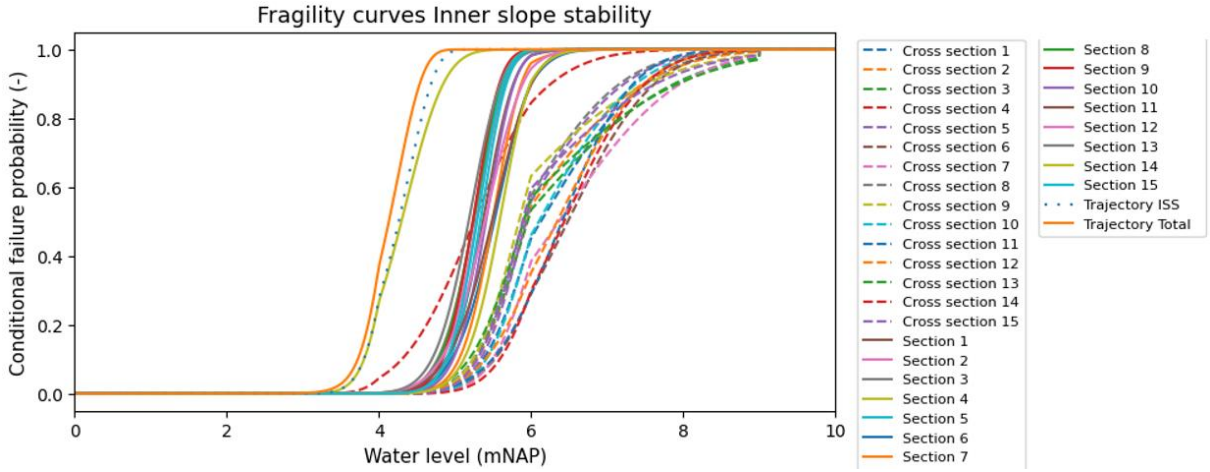

Figure C21: Fragility curves inner slope stability

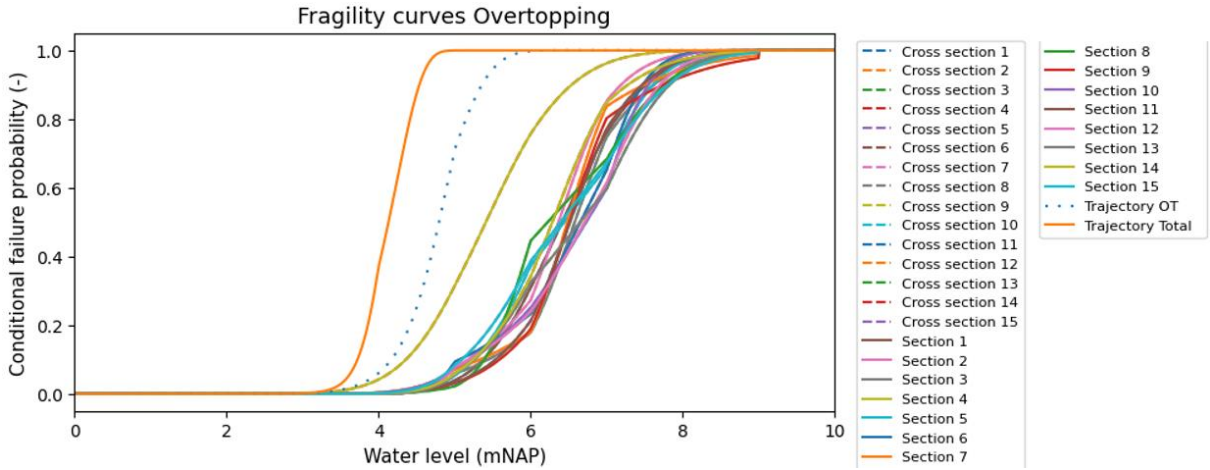

Figure C22: Fragility curves overtopping

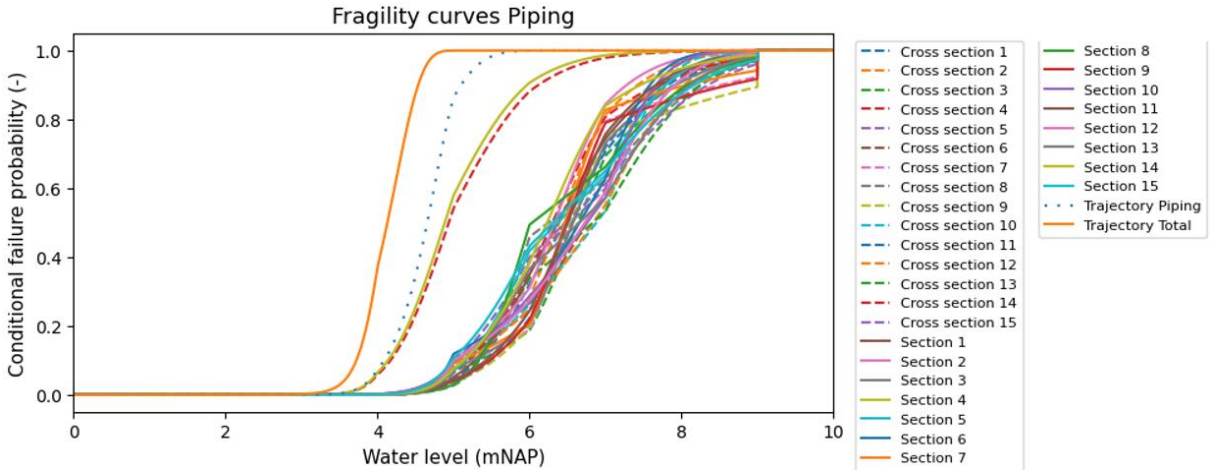

Figure C23: Fragility curves piping

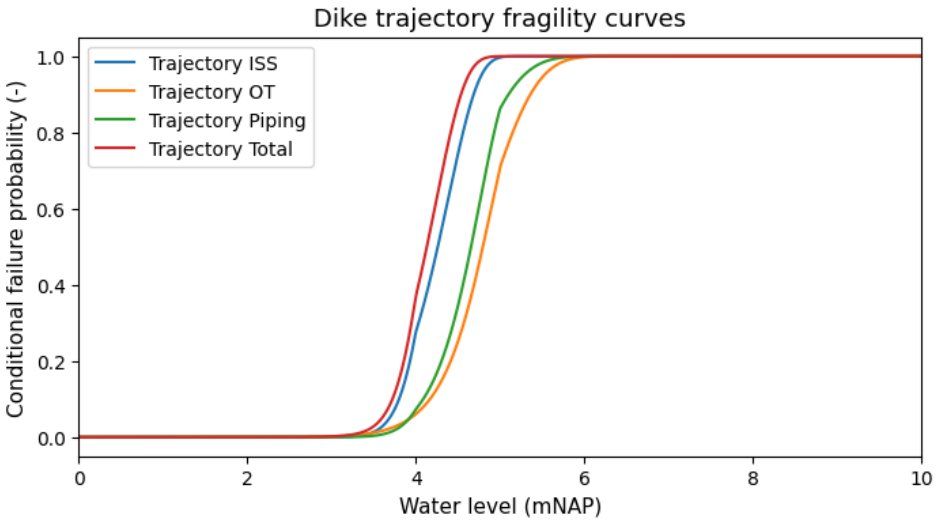

Figure C24: Dike trajectory fragility curves

D Cross section failure probabilities

Trajectory 1.1

Table D1: Cross section failure probabilities trajectory 1.1

	Inner slope stability	Overtopping	Piping
Cross section 1	0.00105	0.00090	0.00083
Cross section 2	0.00157	0.00110	0.00105
Cross section 3	0.00134	0.00137	0.00135
Cross section 4	0.00093	0.00094	0.00087
Cross section 5	0.00135	0.00108	0.00106

Trajectory 1.2

Table D2: Cross section failure probabilities trajectory 1.2

	Inner slope stability	Overtopping	Piping
Cross section 1	0.00105	0.00090	0.00083
Cross section 2	0.00088	0.00099	0.00096
Cross section 3	0.00157	0.00110	0.00105
Cross section 4	0.00101	0.00087	0.00080
Cross section 5	0.00134	0.00137	0.00135
Cross section 6	0.00120	0.00098	0.00097
Cross section 7	0.00094	0.00090	0.00088
Cross section 8	0.00093	0.00094	0.00087
Cross section 9	0.00106	0.00070	0.00068
Cross section 10	0.00135	0.00108	0.00106

Trajectory 1.3

Table D3: Cross section failure probabilities trajectory 1.3

	Inner slope stability	Overtopping	Piping
Cross section 1	0.00105	0.00090	0.00083
Cross section 2	0.00113	0.00075	0.00068
Cross section 3	0.00088	0.00099	0.00096
Cross section 4	0.00084	0.00140	0.00136
Cross section 5	0.00157	0.00110	0.00105
Cross section 6	0.00072	0.00100	0.00102
Cross section 7	0.00101	0.00087	0.00080
Cross section 8	0.00134	0.00137	0.00135
Cross section 9	0.00072	0.00077	0.00074
Cross section 10	0.00120	0.00098	0.00097
Cross section 11	0.00061	0.00160	0.00159
Cross section 12	0.00094	0.00090	0.00088
Cross section 13	0.00093	0.00094	0.00087
Cross section 14	0.00106	0.00070	0.00068
Cross section 15	0.00135	0.00108	0.00106

Trajectory 2.1

Table D4: Cross section failure probabilities trajectory 2.1

	Inner slope stability	Overtopping	Piping
Cross section 1	0.00120	0.00086	0.00088
Cross section 2	0.00723	0.00743	0.00970
Cross section 3	0.00126	0.00098	0.00096
Cross section 4	0.00137	0.00104	0.00105
Cross section 5	0.00114	0.00147	0.00145

Trajectory 2.2

Table D5: Cross section failure probabilities trajectory 2.2

	Inner slope stability	Overtopping	Piping
Cross section 1	0.00094	0.00099	0.00098
Cross section 2	0.00120	0.00086	0.00088
Cross section 3	0.00723	0.00743	0.00970
Cross section 4	0.00069	0.00113	0.00115
Cross section 5	0.00126	0.00098	0.00096
Cross section 6	0.00088	0.00136	0.00127
Cross section 7	0.00090	0.00105	0.00107
Cross section 8	0.00137	0.00104	0.00105
Cross section 9	0.00060	0.00121	0.00121
Cross section 10	0.00114	0.00147	0.00145

Trajectory 2.3

Table D6: Cross section failure probabilities trajectory 2.3

	Inner slope stability	Overtopping	Piping
Cross section 1	0.00094	0.00099	0.00098
Cross section 2	0.00114	0.00117	0.00119
Cross section 3	0.00120	0.00086	0.00088
Cross section 4	0.00723	0.00743	0.00970
Cross section 5	0.00106	0.00114	0.00113
Cross section 6	0.00069	0.00113	0.00115
Cross section 7	0.00070	0.00132	0.00120
Cross section 8	0.00126	0.00098	0.00096
Cross section 9	0.00129	0.00085	0.00079
Cross section 10	0.00088	0.00136	0.00127
Cross section 11	0.00077	0.00090	0.00084
Cross section 12	0.00090	0.00105	0.00107
Cross section 13	0.00137	0.00104	0.00105
Cross section 14	0.00060	0.00121	0.00121
Cross section 15	0.00114	0.00147	0.00145

E Dike section failure probabilities

To compute the dike trajectory failure probability per failure mechanism, the combination protocol applies the following steps:

1. The first option first computes the dike section failure probabilities by multiplying the cross section failure probabilities with the dike section length effect factor. Then, the dike trajectory failure probabilities per failure mechanism are computed by assuming the dike section failure probabilities are independent.
2. Multiply the maximum cross section failure probability per failure mechanism with the dike trajectory length effect factor.
3. Take the minimum dike trajectory failure probability per failure mechanism resulting from the two options presented above.

The row ‘Combination protocol - option 1’ refers to the first step. The row 'Combination protocol - option 2’ refers to the second step. The row ‘Combination protocol - final’ refers to the third step, which provides the definitive dike trajectory failure probabilities per failure mechanism of the combination protocol.

Trajectory 1.1

Table E1: Combination of dike section failure probabilities for trajectory 1.1

	Inner slope stability	Overtopping	Piping
Section 1	0.0062	0.0009	0.0021
Section 2	0.0080	0.0011	0.0027
Section 3	0.0063	0.0014	0.0033
Section 4	0.0058	0.0009	0.0023
Section 5	0.0066	0.0011	0.0025
Dike trajectory - Fragility curve method	0.0126	0.0037	0.0071
Upper bound (Sum)	0.0329	0.0054	0.0129
Lower bound (Max)	0.0080	0.0014	0.0033
Correlation scale	81.69	42.66	60.24
Trajectory length effect factor	4.30	3.00	7.67
Combination protocol - option 1	0.0329	0.0054	0.0129
Combination protocol - option 2	0.0068	0.0041	0.0104
Combination protocol - final	0.0068	0.0041	0.0104

Trajectory 1.2

Table E2: Combination of dike section failure probabilities for trajectory 1.2

	Inner slope stability	Overtopping	Piping
Section 1	0.0044	0.0009	0.0013
Section 2	0.0038	0.0010	0.0015
Section 3	0.0059	0.0011	0.0016
Section 4	0.0045	0.0009	0.0012
Section 5	0.0047	0.0014	0.0020
Section 6	0.0042	0.0010	0.0014
Section 7	0.0039	0.0009	0.0014
Section 8	0.0041	0.0009	0.0013
Section 9	0.0041	0.0007	0.0010
Section 10	0.0049	0.0011	0.0016
Dike trajectory - Fragility curve method	0.0119	0.0055	0.0068
Upper bound (Sum)	0.0446	0.0098	0.0143
Lower bound (Max)	0.0059	0.0014	0.0020
Correlation scale	84.53	50.68	60.90
Trajectory length effect factor	4.30	3.00	7.667
Combination protocol - option 1	0.0446	0.0098	0.0143
Combination protocol - option 2	0.0068	0.0041	0.0104
Combination protocol - final	0.0068	0.0041	0.0104

Trajectory 1.3

Table E3: Combination of dike section failure probabilities for trajectory 1.3

	Inner slope stability	Overtopping	Piping
Section 1	0.0036	0.0009	0.0009
Section 2	0.0031	0.0007	0.0007
Section 3	0.0031	0.0010	0.0011
Section 4	0.0031	0.0014	0.0015
Section 5	0.0048	0.0011	0.0011
Section 6	0.0026	0.0010	0.0011
Section 7	0.0036	0.0009	0.0009
Section 8	0.0040	0.0014	0.0015
Section 9	0.0024	0.0008	0.0008
Section 10	0.0035	0.0010	0.0011
Section 11	0.0020	0.0016	0.0017
Section 12	0.0032	0.0009	0.0010
Section 13	0.0033	0.0009	0.0009
Section 14	0.0034	0.0007	0.0007
Section 15	0.0041	0.0011	0.0011
Dike trajectory - Fragility curve method	0.0110	0.0074	0.0070
Upper bound (Sum)	0.0497	0.0154	0.0162
Lower bound (Max)	0.0048	0.0016	0.0017
Correlation scale	86.17	57.77	63.39
Trajectory length effect factor	4.30	3.00	7.67
Combination protocol - option 1	0.0497	0.0154	0.0162
Combination protocol - option 2	0.0068	0.0048	0.0122
Combination protocol - final	0.0068	0.0048	0.0122

Trajectory 2.1

Table E4: Combination of dike section failure probabilities for trajectory 2.1

	Inner slope stability	Overtopping	Piping
Section 1	0.0065	0.0009	0.0023
Section 2	0.0420	0.0074	0.0210
Section 3	0.0062	0.0010	0.0023
Section 4	0.0076	0.0010	0.0027
Section 5	0.0051	0.0015	0.0037
Dike trajectory - Fragility curve method	0.0423	0.0091	0.0219
Upper bound (Sum)	0.0675	0.0118	0.0321
Lower bound (Max)	0.0420	0.0074	0.0210
Correlation scale	98.76	60.96	92.46
Trajectory length effect factor	4.30	3.00	7.67
Combination protocol - option 1	0.0675	0.0118	0.0321
Combination protocol - option 2	0.0311	0.0223	0.0744
Combination protocol - final	0.0311	0.0118	0.0321

Trajectory 2.2

Table E5: Combination of dike section failure probabilities for trajectory 2.2

	Inner slope stability	Overtopping	Piping
Section 1	0.0037	0.0010	0.0015
Section 2	0.0048	0.0009	0.0014
Section 3	0.0309	0.0074	0.0138
Section 4	0.0032	0.0011	0.0018
Section 5	0.0046	0.0010	0.0014
Section 6	0.0032	0.0014	0.0020
Section 7	0.0042	0.0011	0.0017
Section 8	0.0055	0.0010	0.0016
Section 9	0.0024	0.0012	0.0018
Section 10	0.0039	0.0015	0.0022
Dike trajectory - Fragility curve method	0.0317	0.0110	0.0160
Upper bound (Sum)	0.0664	0.0175	0.0291
Lower bound (Max)	0.0309	0.0074	0.0138
Correlation scale	97.65	64.93	85.58
Trajectory length effect factor	4.30	3.00	7.67
Combination protocol - option 1	0.0664	0.0175	0.0291
Combination protocol - option 2	0.0311	0.0223	0.0744
Combination protocol - final	0.0311	0.0175	0.0291

Trajectory 2.3

Table E6: Combination of dike section failure probabilities for trajectory 2.3

	Inner slope stability	Overtopping	Piping
Section 1	0.0030	0.0010	0.0011
Section 2	0.0035	0.0012	0.0013
Section 3	0.0039	0.0009	0.0010
Section 4	0.0251	0.0074	0.0105
Section 5	0.0030	0.0011	0.0012
Section 6	0.0025	0.0011	0.0013
Section 7	0.0023	0.0013	0.0013
Section 8	0.0038	0.0010	0.0010
Section 9	0.0037	0.0008	0.0009
Section 10	0.0027	0.0014	0.0014
Section 11	0.0029	0.0009	0.0009
Section 12	0.0033	0.0011	0.0012
Section 13	0.0045	0.0010	0.0011
Section 14	0.0020	0.0012	0.0013
Section 15	0.0033	0.0015	0.0016
Dike trajectory - Fragility curve method	0.0264	0.0125	0.0136
Upper bound (Sum)	0.0694	0.0229	0.0270
Lower bound (Max)	0.0251	0.0074	0.0105
Correlation scale	96.94	67.41	80.83
Trajectory length effect factor	4.30	3.00	7.67
Combination protocol - option 1	0.0694	0.0229	0.0270
Combination protocol - option 2	0.0311	0.0223	0.0744
Combination protocol - final	0.0311	0.0223	0.0270

F Dike trajectory failure probabilities

Trajectory 1.1

Table F1: Combination of dike trajectory failure probabilities per failure mechanism for trajectory 1.1

	Failure probability
Trajectory failure probability for inner slope stability	0.0126
Trajectory failure probability for overtopping	0.0037
Trajectory failure probability for piping	0.0071
Total trajectory failure probability - Fragility curve method	0.0150
Upper bound (Sum)	0.0233
Lower bound (Max)	0.0126
Correlation scale	77.66
Total trajectory failure probability - Combination protocol (Combination protocol probabilities per failure mechanism)	0.0213
Total trajectory failure probability- Combination protocol (Fragility curve method probabilities per failure mechanism)	0.0233

Trajectory 1.2

Table F2: Combination of dike trajectory failure probabilities per failure mechanism for trajectory 1.2

	Failure probability
Trajectory failure probability for inner slope stability	0.0119
Trajectory failure probability for overtopping	0.0055
Trajectory failure probability for piping	0.0068
Total trajectory failure probability - Fragility curve method	0.0149
Upper bound (Sum)	0.0242
Lower bound (Max)	0.0119
Correlation scale	75.83
Total trajectory failure probability - Combination protocol (Combination protocol probabilities per failure mechanism)	0.0213
Total trajectory failure probability- Combination protocol (Fragility curve method probabilities per failure mechanism)	0.0242

Trajectory 1.3

Table F3: Combination of dike trajectory failure probabilities per failure mechanism for trajectory 1.3

	Failure probability
Trajectory failure probability for inner slope stability	0.0110
Trajectory failure probability for overtopping	0.0074
Trajectory failure probability for piping	0.0070
Total trajectory failure probability - Fragility curve method	0.0149
Upper bound (Sum)	0.0255
Lower bound (Max)	0.0110
Correlation scale	73.00
Total trajectory failure probability - Combination protocol (Combination protocol probabilities per failure mechanism)	0.0238
Total trajectory failure probability- Combination protocol (Fragility curve method probabilities per failure mechanism)	0.0255

Trajectory 2.1

Table F4: Combination of dike trajectory failure probabilities per failure mechanism for trajectory 2.1

	Failure probability
Trajectory failure probability for inner slope stability	0.0423
Trajectory failure probability for overtopping	0.0091
Trajectory failure probability for piping	0.0219
Total trajectory failure probability - Fragility curve method	0.0475
Upper bound (Sum)	0.0733
Lower bound (Max)	0.0423
Correlation scale	83.21
Total trajectory failure probability - Combination protocol (Combination protocol probabilities per failure mechanism)	0.0750
Total trajectory failure probability- Combination protocol (Fragility curve method probabilities per failure mechanism)	0.0733

Trajectory 2.2

Table F5: Combination of dike trajectory failure probabilities per failure mechanism for trajectory 2.2

	Failure probability
Trajectory failure probability for inner slope stability	0.0317
Trajectory failure probability for overtopping	0.0110
Trajectory failure probability for piping	0.0160
Total trajectory failure probability - Fragility curve method	0.0374
Upper bound (Sum)	0.0587
Lower bound (Max)	0.0317
Correlation scale	78.82
Total trajectory failure probability - Combination protocol (Combination protocol probabilities per failure mechanism)	0.0777
Total trajectory failure probability- Combination protocol (Fragility curve method probabilities per failure mechanism)	0.0587

Trajectory 2.3

Table F6: Combination of dike trajectory failure probabilities per failure mechanism for trajectory 2.3

	Failure probability
Trajectory failure probability for inner slope stability	0.0264
Trajectory failure probability for overtopping	0.0125
Trajectory failure probability for piping	0.0136
Total trajectory failure probability - Fragility curve method	0.0329
Upper bound (Sum)	0.0525
Lower bound (Max)	0.0264
Correlation scale	75.39
Total trajectory failure probability - Combination protocol (Combination protocol probabilities per failure mechanism)	0.0804
Total trajectory failure probability- Combination protocol (Fragility curve method probabilities per failure mechanism)	0.0525

G Python code

Functions

```python
# Packages to import
import numpy as np
import matplotlib.pyplot as plt
import scipy as sp
from scipy.stats import norm
from scipy.stats import lognorm
from scipy.stats import gumbel_r
import random
import pandas as pd

# Variables that can be adjusted
N = 5000
crest_h = 9
loc = 2.32
scale = 0.5
Nsections = 16
Ltrack = 5000
Lsection = int(Ltrack/Nsections)
# Length weak dike section is 312.5 m or 1250 m
Lsection_weak = 312.5
corr_length_iss = 50
corr_length_pp = 300
N_ass_iss = 1 + Ltrack * 0.033 / 50
N_ass_ot = 3
N_ass_pp = 1 + Ltrack * 0.4 / 300

# Create water level array (No function needed as is the same for all fragility curves)
h1 = np.linspace(0, 8, N)
h2 = np.linspace(8, crest_h, int(0.25*N))
h = np.zeros(int(2.25*N-2))
h[0:N] = h1
h[N-1:int(1.25*N-1)] = h2
h[int(1.25*N-2):int(2.25*N-2)] = np.linspace(crest_h, 100, N)

# Gumbel distribution
def Gumbel(x, loc, scale):
    z = (x - loc) / scale
    y = gumbel_r.pdf(z) / scale
    return y

# PDF of water level
prob_h = np.zeros(int(2.25*N-2))
for i in np.arange(0, int(2.25*N-2), 1):
    prob_h[i] = Gumbel(h[i], loc, scale)

# Inter- and extrapolate beta array (fragility curve)
def interpolate_beta(beta_data):
    if len(beta_data) == 5:
        h_data = np.array([0, 2, 4, 6, 8])
    else:
        h_data = np.array([0, 1, 2, 3, 4, 5, 6, 7, 8])
    beta1 = np.interp(h1, h_data, beta_data)
    coeff = np.polyfit([h_data[-2], h_data[-1]], [beta_data[-2], beta_data[-1]], 1)
    a,b = coeff[0], coeff[1]
    beta2 = a * h2 + b
    beta = np.zeros(int(2.25*N-2))
    beta[0:N] = beta1
    beta[N-1:int(1.25*N-1)] = beta2
    beta[int(1.25*N-2):int(2.25*N-2)] = -100*np.ones(N)
    return beta

# Probability of failure from beta array (fragility curve)
def prob_f(beta):
    cond_f = norm.cdf(-beta, 0, 1)
    prob_f = 0
    for i in range(int(2.25*N-3)):
        prob_f += cond_f[i] * prob_h[i] * (h[i+1] - h[i])
    return prob_f

# Create new cross sections from the difference between the base cross section and the one with natural variability
def section(beta, N):
    random.seed(10)
    sections = np.zeros((N, len(beta)))
    for i in range(N):
        for j in range(len(beta)):
            sections[i, j] = beta[j] + random.uniform(-2*u, 2*u)
    sections[0] = beta
    return sections

# beta in the next function is an array consisting of all fragility curves one wants to scale up
# This function is used to combine fragility curves
def scale_up(beta):
```

```
    Pf = norm.cdf(-beta, 0, 1)
    series = 1 - Pf
    product = np.ones(beta.shape[1])
    for i in range(beta.shape[1]):
        for j in series[:, i]:
            product[i] = product[i] * j
    Pf_new = 1 - product
    beta_new = -norm.ppf(Pf_new)
    return beta_new

# This function scales up the fragility curves from the cross section level to the section level
# To do this, this functions multiplies the cross section fragility curves with the section length effect factor
def beta_le(beta_cs, fm):
    if fm == 'iss':
        power = Lsection/corr_length_iss
    elif fm == 'pp':
        power = Lsection/corr_length_pp
    else:
        power = 1
    Pf_cs = norm.cdf(-beta_cs, 0, 1)
    Pf_section = 1 - (1 - Pf_cs)**power
    beta_section = -norm.ppf(Pf_section)
    return beta_section
```

Cross section fragility curves from failure mechanism models

```
# The data from the failure mechanism models
# Fragility curves base cross sections
beta_base_iss_data = np.array([10.925, 7.867, 3.810, 0.118, -1.742])
beta_base_ot_data = np.array([8.2, 6.96, 5.68, 4.33, 3.06, 1.76, 0.498, -0.704, -1.82])
beta_base_pp_data = np.array([40, 40, 9.8, 5.76, 3.3, 1.68, 0.465, -0.543, -1.36])

# Fragility curves design cross sections
beta_design_iss_data = np.array([9.732, 6.437, 1.689, -1.015, -3.075])
beta_design_ot_data = np.array([6.85, 5.56, 4.26, 2.99, 1.73, 0.485, -0.696, -1.78, -2.88])
beta_design_pp_data = np.array([40, 40, 7.67, 3.92, 1.57, -0.102, -1.18, -2.03, -2.7])

# Fragility curves cross sections with natural variability
beta_smallvar_iss_data = np.array([10.811, 7.724, 3.905, -0.578, -2.471])
beta_smallvar_ot_data = np.array([8.07, 6.85, 5.62, 4.3, 3.01, 1.73, 0.486, -0.708, -1.83])
beta_smallvar_pp_data = np.array([40, 40, 11, 6.3, 3.44, 1.49, 0.119, -0.89, -1.67])

# Average difference between the fragility curves of the base and the natural variability cross section
# u is the average of the uniform distribution that is used to sample multiple new cross section fragility curves
a = beta_base_iss_data - beta_smallvar_iss_data
b = beta_base_ot_data - beta_smallvar_ot_data
c = beta_base_pp_data - beta_smallvar_pp_data
d = np.sum(np.abs(a))+np.sum(np.abs(b))+np.sum(np.abs(c))
u = d/(len(a)+len(b)+len(c))
```

Compute all cross section fragility curves

Rather uniform dike trajectory with comparable dike sections

```
beta_csections_all_iss = section(beta_base_iss_data, 16)
beta_csections_all_iss = beta_csections_all_iss.tolist()
beta_csections_all_ot = section(beta_base_ot_data, 16)
beta_csections_all_ot = beta_csections_all_ot.tolist()
beta_csections_all_pp = section(beta_base_pp_data, 16)
beta_csections_all_pp = beta_csections_all_pp.tolist()

# The code below ensures that the right cross sections are assigned to the dike sections
if Nsections == 1:
    for i in [0, 0, 0, 0, 0, 1, 1, 1, 1, 1, 1, 1, 1, 1]:
        beta_csections_all_iss.pop(i)
        beta_csections_all_ot.pop(i)
        beta_csections_all_pp.pop(i)
if Nsections == 2:
    for i in [0, 0, 0, 0, 0, 1, 1, 2, 2, 2, 2, 2, 2]:
        beta_csections_all_iss.pop(i)
        beta_csections_all_ot.pop(i)
        beta_csections_all_pp.pop(i)
if Nsections == 3:
    for i in [0, 0, 0, 0, 0, 1, 1, 2, 2, 2, 2, 2]:
        beta_csections_all_iss.pop(i)
        beta_csections_all_ot.pop(i)
        beta_csections_all_pp.pop(i)
if Nsections == 4:
    for i in [0, 1, 1, 1, 2, 2, 3, 3, 3, 3, 3]:
        beta_csections_all_iss.pop(i)
        beta_csections_all_ot.pop(i)
        beta_csections_all_pp.pop(i)
if Nsections == 5:
    for i in [0, 1, 1, 1, 2, 2, 3, 3, 3, 4]:
        beta_csections_all_iss.pop(i)
        beta_csections_all_ot.pop(i)
        beta_csections_all_pp.pop(i)
```

```
if Nsections == 6:
    for i in [0, 1, 1, 1, 2, 2, 3, 4, 4, 5]:
        beta_csections_all_iss.pop(i)
        beta_csections_all_ot.pop(i)
        beta_csections_all_pp.pop(i)
if Nsections == 7:
    for i in [0, 1, 1, 1, 2, 4, 5, 5, 6]:
        beta_csections_all_iss.pop(i)
        beta_csections_all_ot.pop(i)
        beta_csections_all_pp.pop(i)
if Nsections == 8:
    for i in [0, 1, 2, 3, 5, 6, 6, 7]:
        beta_csections_all_iss.pop(i)
        beta_csections_all_ot.pop(i)
        beta_csections_all_pp.pop(i)
if Nsections == 9:
    for i in [0, 1, 2, 3, 5, 6, 6]:
        beta_csections_all_iss.pop(i)
        beta_csections_all_ot.pop(i)
        beta_csections_all_pp.pop(i)
if Nsections == 10:
    for i in [0, 1, 2, 3, 5, 6]:
        beta_csections_all_iss.pop(i)
        beta_csections_all_ot.pop(i)
        beta_csections_all_pp.pop(i)
if Nsections == 11:
    for i in [0, 1, 2, 3, 5]:
        beta_csections_all_iss.pop(i)
        beta_csections_all_ot.pop(i)
        beta_csections_all_pp.pop(i)
if Nsections == 12:
    for i in [0, 1, 2, 3]:
        beta_csections_all_iss.pop(i)
        beta_csections_all_ot.pop(i)
        beta_csections_all_pp.pop(i)
if Nsections == 13:
    for i in [0, 1, 2]:
        beta_csections_all_iss.pop(i)
        beta_csections_all_ot.pop(i)
        beta_csections_all_pp.pop(i)
if Nsections == 14:
    for i in [0, 1]:
        beta_csections_all_iss.pop(i)
        beta_csections_all_ot.pop(i)
        beta_csections_all_pp.pop(i)
if Nsections == 15:
    beta_csections_all_iss.pop(0)
    beta_csections_all_ot.pop(0)
    beta_csections_all_pp.pop(0)
beta_csections_data_iss = np.array(beta_csections_all_iss)
beta_csections_data_ot = np.array(beta_csections_all_ot)
beta_csections_data_pp = np.array(beta_csections_all_pp)
```

Dike trajectory with one dominant dike section

```
beta_csections_all_iss = section(beta_base_iss_data, 16)
beta_csections_all_iss = beta_csections_all_iss.tolist()
beta_csections_all_ot = section(beta_base_ot_data, 16)
beta_csections_all_ot = beta_csections_all_ot.tolist()
beta_csections_all_pp = section(beta_base_pp_data, 16)
beta_csections_all_pp = beta_csections_all_pp.tolist()

# The length of dike part with weak parameters is equal to 312.5 m = 1 dike sections when Nsections = 16
beta_csections_all_iss = section(beta_base_iss_data, 16).tolist()
beta_csections_all_iss.pop(4)
beta_csections_all_iss = np.insert(beta_csections_all_iss, 4, beta_design_iss_data, axis=0).tolist()
beta_csections_all_ot = section(beta_base_ot_data, 16).tolist()
beta_csections_all_ot.pop(4)
beta_csections_all_ot = np.insert(beta_csections_all_ot, 4, beta_design_ot_data, axis=0).tolist()
beta_csections_all_pp = section(beta_base_pp_data, 16).tolist()
beta_csections_all_pp.pop(4)
beta_csections_all_pp = np.insert(beta_csections_all_pp, 4, beta_design_pp_data, axis=0).tolist()

if Nsections == 1:
    for i in [0, 0, 0, 0, 1, 1, 1, 1, 1, 1, 1, 1, 1, 1]:
        beta_csections_all_iss.pop(i)
        beta_csections_all_ot.pop(i)
        beta_csections_all_pp.pop(i)
if Nsections == 2:
    for i in [0, 0, 0, 0, 1, 1, 1, 1, 1, 1, 1, 2, 2]:
        beta_csections_all_iss.pop(i)
        beta_csections_all_ot.pop(i)
        beta_csections_all_pp.pop(i)
if Nsections == 3:
    for i in [0, 0, 0, 0, 1, 1, 1, 2, 2, 2, 2, 3, 3]:
        beta_csections_all_iss.pop(i)
        beta_csections_all_ot.pop(i)
        beta_csections_all_pp.pop(i)
if Nsections == 4:
    for i in [0, 0, 0, 2, 2, 2, 3, 3, 3, 4, 4]:
        beta_csections_all_iss.pop(i)
        beta_csections_all_ot.pop(i)
        beta_csections_all_pp.pop(i)
```

```
if Nsections == 5:
    for i in [0, 0, 0, 2, 2, 2, 3, 3, 3, 4]:
        beta_csections_all_iss.pop(i)
        beta_csections_all_ot.pop(i)
        beta_csections_all_pp.pop(i)
if Nsections == 6:
    for i in [0, 0, 0, 2, 2, 2, 3, 4, 4, 5]:
        beta_csections_all_iss.pop(i)
        beta_csections_all_ot.pop(i)
        beta_csections_all_pp.pop(i)
if Nsections == 7:
    for i in [0, 0, 0, 2, 3, 4, 5, 5, 6]:
        beta_csections_all_iss.pop(i)
        beta_csections_all_ot.pop(i)
        beta_csections_all_pp.pop(i)
if Nsections == 8:
    for i in [1, 1, 3, 4, 5, 6, 6, 7]:
        beta_csections_all_iss.pop(i)
        beta_csections_all_ot.pop(i)
        beta_csections_all_pp.pop(i)
if Nsections == 9:
    for i in [1, 1, 3, 4, 5, 6, 6]:
        beta_csections_all_iss.pop(i)
        beta_csections_all_ot.pop(i)
        beta_csections_all_pp.pop(i)
if Nsections == 10:
    for i in [1, 1, 3, 4, 5, 6]:
        beta_csections_all_iss.pop(i)
        beta_csections_all_ot.pop(i)
        beta_csections_all_pp.pop(i)
if Nsections == 11:
    for i in [1, 1, 3, 4, 5]:
        beta_csections_all_iss.pop(i)
        beta_csections_all_ot.pop(i)
        beta_csections_all_pp.pop(i)
if Nsections == 12:
    for i in [1, 1, 3, 4]:
        beta_csections_all_iss.pop(i)
        beta_csections_all_ot.pop(i)
        beta_csections_all_pp.pop(i)
```

```
if Nsections == 13:
    for i in [1, 1, 3]:
        beta_csections_all_iss.pop(i)
        beta_csections_all_ot.pop(i)
        beta_csections_all_pp.pop(i)
if Nsections == 14:
    for i in [1, 1]:
        beta_csections_all_iss.pop(i)
        beta_csections_all_ot.pop(i)
        beta_csections_all_pp.pop(i)
if Nsections == 15:
    beta_csections_all_iss.pop(1)
    beta_csections_all_ot.pop(1)
    beta_csections_all_pp.pop(1)
```

Scale up fragility curves and compute failure probabilities

```
# The cross section fragility curves are computed now
# The next step is to scale up the fragilty curves and compute the corresponding failure probabilities along the way
# Internal slope stability
a = []
for i in range(beta_csections_data_iss.shape[0]):
    a.append(interpolate_beta(beta_csections_data_iss[i]))
beta_csections_iss = np.array(a)
b = []
for i in range(beta_csections_iss.shape[0]):
    b.append(prob_f(beta_csections_iss[i]))
Pf_csections_iss = np.array(b)
beta_sections_iss = beta_le(beta_csections_iss, 'iss')
c = []
for i in range(beta_sections_iss.shape[0]):
    c.append(prob_f(beta_sections_iss[i]))
Pf_sections_iss = np.array(c)
beta_track_iss = scale_up(beta_sections_iss)
Pf_track_iss = prob_f(beta_track_iss)
Cond_failure_csections_iss = norm.cdf(-beta_csections_iss, 0, 1)
Cond_failure_sections_iss = norm.cdf(-beta_sections_iss, 0, 1)
Cond_failure_track_iss = norm.cdf(-beta_track_iss, 0, 1)

# Overtopping
a = []
for i in range(beta_csections_data_ot.shape[0]):
    a.append(interpolate_beta(beta_csections_data_ot[i]))
beta_csections_ot = np.array(a)
b = []
for i in range(beta_csections_ot.shape[0]):
    b.append(prob_f(beta_csections_ot[i]))
Pf_csections_ot = np.array(b)
beta_sections_ot = beta_le(beta_csections_ot, 'ot')
c = []
```

```
for i in range(beta_sections_ot.shape[0]):
    c.append(prob_f(beta_sections_ot[i]))
Pf_sections_ot = np.array(c)
beta_track_ot = scale_up(beta_sections_ot)
Pf_track_ot = prob_f(beta_track_ot)
Cond_failure_csections_ot = norm.cdf(-beta_csections_ot, 0, 1)
Cond_failure_sections_ot = norm.cdf(-beta_sections_ot, 0, 1)
Cond_failure_track_ot = norm.cdf(-beta_track_ot, 0, 1)

# Piping
a = []
for i in range(beta_csections_data_pp.shape[0]):
    a.append(interpolate_beta(beta_csections_data_pp[i]))
beta_csections_pp = np.array(a)
b = []
for i in range(beta_csections_pp.shape[0]):
    b.append(prob_f(beta_csections_pp[i]))
Pf_csections_pp = np.array(b)
beta_sections_pp = beta_le(beta_csections_pp, 'pp')
c = []
for i in range(beta_sections_pp.shape[0]):
    c.append(prob_f(beta_sections_pp[i]))
Pf_sections_pp = np.array(c)
beta_track_pp = scale_up(beta_sections_pp)
Pf_track_pp = prob_f(beta_track_pp)
Cond_failure_csections_pp = norm.cdf(-beta_csections_pp, 0, 1)
Cond_failure_sections_pp = norm.cdf(-beta_sections_pp, 0, 1)
Cond_failure_track_pp = norm.cdf(-beta_track_pp, 0, 1)

# Total trajectory failure probability
beta_track_failmechs = np.array((beta_track_iss, beta_track_ot, beta_track_pp))
beta_track_total = scale_up(beta_track_failmechs)
Pf_track_total = prob_f(beta_track_total)
Cond_failure_track_total = norm.cdf(-beta_track_total, 0, 1)
```

Organize results in tables

```
# Cross section failure probabilities
data = {'Slope stability': Pf_csections_iss, 'Overtopping': Pf_csections_ot, 'Piping': Pf_csections_pp}
indices = []
for i in range(len(Pf_csections_iss)):
    indices.append(f'Cross section {i+1}')
table_pf_csections = pd.DataFrame(data, index=indices)
table_pf_csections = table_pf_csections.round(5)
display(table_pf_csections)

# Dike section to trajectory per failure mechanism
data = {'Slope stability': Pf_sections_iss, 'Overtopping': Pf_sections_ot, 'Piping': Pf_sections_pp}
indices = []
for i in range(len(Pf_sections_iss)):
    indices.append(f'Section {i+1}')
table_pf_sections = pd.DataFrame(data, index=indices)
a = np.array(([Pf_track_iss, Pf_track_ot, Pf_track_pp], [np.sum(Pf_sections_iss), np.sum(Pf_sections_ot), np.sum(Pf_sections_pp)], \
    [np.max(Pf_sections_iss), np.max(Pf_sections_ot), np.max(Pf_sections_pp)], \
    [100*(np.sum(Pf_sections_iss)-Pf_track_iss)/(np.sum(Pf_sections_iss)-np.max(Pf_sections_iss)), \
    100*(np.sum(Pf_sections_ot)-Pf_track_ot)/(np.sum(Pf_sections_ot)-np.max(Pf_sections_ot)), \
    100*(np.sum(Pf_sections_pp)-Pf_track_pp)/(np.sum(Pf_sections_pp)-np.max(Pf_sections_pp))], [N_ass_iss, N_ass_ot, N_ass_pp], \
    [np.sum(Pf_sections_iss), np.sum(Pf_sections_ot), np.sum(Pf_sections_pp)], \
    [N_ass_iss*np.max(Pf_csections_iss), N_ass_ot*np.max(Pf_csections_ot), N_ass_pp*np.max(Pf_csections_pp)], \
    [np.min((np.sum(Pf_sections_iss), N_ass_iss*np.max(Pf_csections_iss))), np.min((np.sum(Pf_sections_ot), N_ass_ot*np.max(Pf_csections_ot))), \
    np.min((np.sum(Pf_sections_pp), N_ass_pp*np.max(Pf_csections_pp)))]))
for row in a:
    table_pf_sections.loc[len(table_pf_sections.index)] = row
table_pf_sections.rename(index={len(table_pf_sections)-8: 'Frag curve', len(table_pf_sections)-7: 'Sum', len(table_pf_sections)-6: 'Max', \
        len(table_pf_sections)-5: 'Correlation scale', len(table_pf_sections)-4: 'N_comb.pr.', \
        len(table_pf_sections)-3: 'Combination protocol  - a)', len(table_pf_sections)-2: 'Combination protocol - b)', \
        len(table_pf_sections)-1: 'Combination protocol - final'}, inplace=True)
table_pf_sections = table_pf_sections.round(4)
display(table_pf_sections)

# Trajectory per failure mechanism to total trajectory
data2 = np.array((Pf_track_iss, Pf_track_ot, Pf_track_pp, Pf_track_total, Pf_track_iss+Pf_track_ot+Pf_track_pp, \
                  np.max((Pf_track_iss, Pf_track_ot, Pf_track_pp)), \
                  100*(Pf_track_iss+Pf_track_ot+Pf_track_pp-Pf_track_total)/(Pf_track_iss+Pf_track_ot+Pf_track_pp- \
                  np.max((Pf_track_iss, Pf_track_ot, Pf_track_pp))), table_pf_sections.iloc[-1].sum(), Pf_track_iss+Pf_track_ot+Pf_track_pp))
data2_table = {'Failure probability': data2}
table_pf_track = pd.DataFrame(data2_table, index=['Track internal slope stability', 'Track overtopping', 'Track piping', \
                                                  'Total track - Fragility curve method', 'Sum', 'Max', 'Correlation scale', \
                                                  'Total track - Combination protocol (Combination protocol probabilities)', \
                                                  'Total track - Combination protocol (Fragility curve method probabilities)'])
table_pf_track = table_pf_track.round(4)
display(table_pf_track)
```

Create fragility curves

```python
# Labels for the legends
label_csections = []
for i in range(len(Pf_csections_iss)):
    label_csections.append(f'Cross section {i+1}')
label_sections = []
for i in range(len(Pf_sections_iss)):
    label_sections.append(f'Section {i+1}')

# Fragility curves inner slope stability
plt.figure(figsize=(8, 4))
for i in range(len(Cond_failure_csections_iss)):
    plt.plot(h, Cond_failure_csections_iss[i], label=label_csections[i], linestyle='--')
for i in range(len(Cond_failure_csections_iss)):
    plt.plot(h, Cond_failure_sections_iss[i], label=label_sections[i])
plt.plot(h, Cond_failure_track_iss, label='Trajectory ISS', linestyle=(0, (1, 4)))
plt.plot(h, Cond_failure_track_total, label='Trajectory Total')
plt.xlim([0, 10])
plt.legend(bbox_to_anchor=(1.02, 1), loc='upper left', fontsize=8.25)
# plt.tight_layout()
plt.xlabel('Water level (mNAP)', fontsize=11)
plt.ylabel('Conditional failure probability (-)', fontsize=11)
plt.title('Fragility curves Internal slope stability', fontsize=13)

# Fragility curves Overtopping
plt.figure(figsize=(8, 4))
for i in range(len(Cond_failure_csections_ot)):
    plt.plot(h, Cond_failure_csections_ot[i], label=label_csections[i], linestyle='--')
for i in range(len(Cond_failure_csections_iss)):
    plt.plot(h, Cond_failure_sections_ot[i], label=label_sections[i])
plt.plot(h, Cond_failure_track_ot, label='Trajectory OT', linestyle=(0, (1, 4)))
plt.plot(h, Cond_failure_track_total, label='Trajectory Total')
plt.xlim([0, 10])
plt.legend(bbox_to_anchor=(1.02, 1), loc='upper left', fontsize=8.25)
# plt.tight_layout()
plt.xlabel('Water level (mNAP)', fontsize=11)
plt.ylabel('Conditional failure probability (-)', fontsize=11)
plt.title('Fragility curves Overtopping', fontsize=13)

# Fragility curves piping
plt.figure(figsize=(8, 4))
for i in range(len(Cond_failure_csections_pp)):
    plt.plot(h, Cond_failure_csections_pp[i], label=label_csections[i], linestyle='--')
for i in range(len(Cond_failure_csections_iss)):
    plt.plot(h, Cond_failure_sections_pp[i], label=label_sections[i])
plt.plot(h, Cond_failure_track_pp, label='Trajectory Piping', linestyle=(0, (1, 4)))
plt.plot(h, Cond_failure_track_total, label='Trajectory Total')
plt.xlim([0, 10])
plt.legend(bbox_to_anchor=(1.02, 1), loc='upper left', fontsize=8.25)
# plt.tight_layout()
plt.xlabel('Water level (mNAP)', fontsize=11)
plt.ylabel('Conditional failure probability (-)', fontsize=11)
plt.title('Fragility curves Piping', fontsize=13)

# Dike trajectory fragiliyt curves
plt.figure(figsize=(8, 4))
cond_fail = [Cond_failure_track_iss, Cond_failure_track_ot, Cond_failure_track_pp, Cond_failure_track_total]
Label = ['Trajectory ISS', 'Trajectory OT', 'Trajectory Piping', 'Trajectory Total']
for i in range(4):
    plt.plot(h, cond_fail[i], label=Label[i])
plt.xlim([0, 10])
plt.legend(loc='best')
plt.xlabel('Water level (mNAP)', fontsize=11)
plt.ylabel('Conditional failure probability (-)', fontsize=11)
plt.title('Dike trajectory fragility curves', fontsize=13);
```

Sensitivity study

```python
# Put Nsections to 16
# Create Figure 4.11 for Inner slope stability
beta_track_iss_array = np.zeros((np.shape(beta_sections_iss)[0], np.shape(beta_sections_iss)[1]))
beta_track_iss_array[0] = beta_sections_iss[0]
for i in range(np.shape(beta_sections_iss)[0]-1):
    beta_track_iss_array[i+1] = scale_up(beta_sections_iss[0:i+2, :])
c = []
for i in range(beta_track_iss_array.shape[0]):
    c.append(prob_f(beta_track_iss_array[i]))
Pf_track_iss_array = np.array(c)

max_iss = np.zeros(len(Pf_sections_iss))
sum_iss = np.zeros(len(Pf_sections_iss))
correlation_scale_iss = np.zeros(len(Pf_sections_iss))
for i in range(len(Pf_sections_iss)):
    max_iss[i] = np.max(Pf_sections_iss[0:i+1])
    sum_iss[i] = np.sum(Pf_sections_iss[0:i+1])
    if i == 0:
        correlation_scale_iss[i] = 0
    else:
        correlation_scale_iss[i] = 100 * (sum_iss[i] - Pf_track_iss_array[i]) / (sum_iss[i] - max_iss[i])

```

```
plt.figure(figsize=(8, 4))
plt.xlim((0, 18))
plt.grid()
plt.plot(np.arange(1, len(max_iss)+1), Pf_track_iss_array, label='Fragility curve method', color='tab:blue')
plt.plot(np.arange(1, len(max_iss)+1), Pf_track_iss_array, 'o', ms='5')
plt.plot(np.arange(1, len(max_iss)+1), max_iss, label='Lower bound - Max', color='tab:orange')
plt.plot(np.arange(1, len(max_iss)+1), max_iss, 'o', ms='5')
plt.plot(np.arange(1, len(max_iss)+1), sum_iss, label='Upper bound - Sum', color='tab:green')
plt.plot(np.arange(1, len(max_iss)+1), sum_iss, 'o', ms='5')
plt.legend(loc='best', fontsize=10)
plt.xlabel('Number of dike sections', fontsize=12)
plt.ylabel('Failure probability (-)', fontsize=12)
plt.title('Dike trajectory failure probability for inner slope stability', fontsize=14);

# Create Figure 4.12 for Overtopping
beta_track_ot_array = np.zeros((np.shape(beta_sections_ot)[0], np.shape(beta_sections_ot)[1]))
beta_track_ot_array[0] = beta_sections_ot[0]
for i in range(np.shape(beta_sections_ot)[0]-1):
    beta_track_ot_array[i+1] = scale_up(beta_sections_ot[0:i+2, :])
c = []
for i in range(beta_track_ot_array.shape[0]):
    c.append(prob_f(beta_track_ot_array[i]))
Pf_track_ot_array = np.array(c)

max_ot = np.zeros(len(Pf_sections_ot))
sum_ot = np.zeros(len(Pf_sections_ot))
for i in range(len(Pf_sections_ot)):
    max_ot[i] = np.max(Pf_sections_ot[0:i+1])
    sum_ot[i] = np.sum(Pf_sections_ot[0:i+1])

plt.figure(figsize=(8, 4))
plt.xlim((0, 18))
plt.grid()
plt.plot(np.arange(1, len(max_iss)+1), Pf_track_ot_array, label='Fragility curve method', color='tab:blue')
plt.plot(np.arange(1, len(max_iss)+1), Pf_track_ot_array, 'o', ms='5')
plt.plot(np.arange(1, len(max_iss)+1), max_ot, label='Lower bound - Max', color='tab:orange')
plt.plot(np.arange(1, len(max_iss)+1), max_ot, 'o', ms='5')
plt.plot(np.arange(1, len(max_iss)+1), sum_ot, label='Upper bound - Sum', color='tab:green')
plt.plot(np.arange(1, len(max_iss)+1), sum_ot, 'o', ms='5')
plt.legend(loc='best', fontsize=10)
plt.xlabel('Number of dike sections', fontsize=12)
plt.ylabel('Failure probability (-)', fontsize=12)
plt.title('Dike trajectory failure probability for overtopping', fontsize=14);

# Create Figure 4.13 for Piping
beta_track_pp_array = np.zeros((np.shape(beta_sections_pp)[0], np.shape(beta_sections_pp)[1]))
beta_track_pp_array[0] = beta_sections_pp[0]
for i in range(np.shape(beta_sections_pp)[0]-1):
    beta_track_pp_array[i+1] = scale_up(beta_sections_pp[0:i+2, :])
c = []
for i in range(beta_track_pp_array.shape[0]):
    c.append(prob_f(beta_track_pp_array[i]))
Pf_track_pp_array = np.array(c)

max_pp = np.zeros(len(Pf_sections_pp))
sum_pp = np.zeros(len(Pf_sections_pp))
for i in range(len(Pf_sections_pp)):
    max_pp[i] = np.max(Pf_sections_pp[0:i+1])
    sum_pp[i] = np.sum(Pf_sections_pp[0:i+1])

plt.figure(figsize=(8, 4))
plt.xlim((0, 18))
plt.grid()
plt.plot(np.arange(1, len(max_pp)+1), Pf_track_pp_array, label='Fragility curve method', color='tab:blue')
plt.plot(np.arange(1, len(max_pp)+1), Pf_track_pp_array, 'o', ms='5')
plt.plot(np.arange(1, len(max_pp)+1), max_pp, label='Lower bound - Max', color='tab:orange')
plt.plot(np.arange(1, len(max_pp)+1), max_pp, 'o', ms='5')
plt.plot(np.arange(1, len(max_pp)+1), sum_pp, label='Upper bound - Sum', color='tab:green')
plt.plot(np.arange(1, len(max_pp)+1), sum_pp, 'o', ms='5')
plt.legend(loc='best', fontsize=10)
plt.xlabel('Number of dike sections', fontsize=12)
plt.ylabel('Failure probability (-)', fontsize=12)
plt.title('Dike trajectory failure probability for piping', fontsize=14);

# Create Figure 4.14 for Total dike trajectory
beta_track_array = np.zeros((np.shape(beta_sections_iss)[0], np.shape(beta_sections_iss)[1]))
beta_section_combined = np.zeros((np.shape(beta_sections_iss)[0], np.shape(beta_sections_iss)[1]))
for i in range(np.shape(beta_sections_iss)[0]):
    beta_track_array[i] = scale_up(np.array((beta_track_iss_array[i], beta_track_ot_array[i], beta_track_pp_array[i])))
    beta_section_combined[i] = scale_up(np.array((beta_sections_iss[i], beta_sections_ot[i], beta_sections_pp[i])))
c = []
d = []
for i in range(beta_track_array.shape[0]):
    c.append(prob_f(beta_track_array[i]))
    d.append(prob_f(beta_section_combined[i]))
Pf_track_array = np.array(c)
Pf_section_combined = np.array(d)

max_combined = np.zeros(len(Pf_section_combined))
sum_combined = np.zeros(len(Pf_section_combined))
for i in range(len(Pf_section_combined)):
    max_combined[i] = np.max(Pf_section_combined[0:i+1])
    sum_combined[i] = np.sum(Pf_section_combined[0:i+1])

```

```
plt.figure(figsize=(8, 4))
plt.xlim((0, 18))
plt.grid()
plt.plot(np.arange(1, len(max_iss)+1), Pf_track_array, label='Fragility curve method', color='tab:blue')
plt.plot(np.arange(1, len(max_iss)+1), Pf_track_array, 'o', ms='5')
plt.plot(np.arange(1, len(max_iss)+1), max_combined, label='Lower bound - Max', color='tab:orange')
plt.plot(np.arange(1, len(max_iss)+1), max_combined, 'o', ms='5')
plt.plot(np.arange(1, len(max_iss)+1), sum_combined, label='Upper bound - Sum', color='tab:green')
plt.plot(np.arange(1, len(max_iss)+1), sum_combined, 'o', ms='5')
plt.legend(loc='best', fontsize=10)
plt.xlabel('Number of dike sections', fontsize=12)
plt.ylabel('Failure probability (-)', fontsize=12)
plt.title('Total dike trajectory failure probability', fontsize=14);
```